

LOWER LIMB ACTIVITY AND MOBILITY PATTERNS IN MEDIEVAL NUBIA: A
BIOMECHANICAL APPROACH OF FEMORAL AND TIBIAL CROSS-SECTIONAL
GEOMETRY FROM MIS ISLAND

By

Elena O. Watson

A THESIS

Submitted to
Michigan State University
in partial fulfillment of the requirements
for the degree of

Forensic Science—Master of Science

2018

ABSTRACT

LOWER LIMB ACTIVITY AND MOBILITY PATTERNS IN MEDIEVAL NUBIA: A BIOMECHANICAL APPROACH OF FEMORAL AND TIBIAL CROSS-SECTIONAL GEOMETRY FROM MIS ISLAND

By

Elena O. Watson

This study analyzed femoral and tibial cross-sectional properties in a medieval Nubian skeletal sample to explore patterns of lower limb activity and mobility. The sample of skeletal remains was excavated from two cemeteries on Mis Island—cemetery 3-J-10 (AD 1100 – AD 1400) and cemetery 3-J-11 (AD 300 – AD 1400). Two research questions were investigated within the Mis Island sample. The first set of comparisons were conducted between the two cemetery groups that comprise the sample, to evaluate potential temporal and spatial differences between the communities. Biomechanical data between adult males and females were also compared to infer the degree of sexual division of activity and mobility in this society.

The cross-sectional properties between the two cemetery sub-samples were not significantly different, suggesting that both groups of individuals shared similar levels of physical activity concerning the lower limbs during this period. Results of the comparison between male and female groups demonstrated significantly higher measures of diaphyseal robusticity in males compared to females. This finding indicates that male individuals in this society were generally involved in more physically demanding activity concerning the lower limbs. However, results of diaphyseal shape suggest that males and females may have been more similar in their roles regarding logistic mobility. The outcomes from this study indicate a sexual division of activity involving the lower limb, but perhaps a relatively equal level of mobility, that may have been present in this region throughout the medieval period.

Copyright by
ELENA O. WATSON
2018

ACKNOWLEDGEMENTS

This thesis and all that it represents was made possible by the caring assistance of many people. I would like to first acknowledge the support from my committee members. Foremost, I must thank my advisor Dr. Todd Fenton, for always encouraging me to do my best and pursue my interests while providing every possible opportunity for me to grow as a scholar. His enthusiasm in this project was a valued driving force as I forged ahead. I greatly appreciated Dr. Joseph Hefner's kind patience in providing wisdom and guidance as I worked through my statistical analyses, as well as for introducing me to the wonderful world of R. My sincere thanks to Dr. April Zeoli, for her keen insight and contributions. I would also like to acknowledge the MSU School of Criminal Justice for their support in awarding a Forensic Science Summer Research Fellowship towards this project. I am grateful for the opportunity to study such a truly remarkable collection which was made possible by the generous loan from The British Museum and the hard work by Dr. Fenton and many others to bring the collection to MSU.

My many thanks to Dr. Gina Agostini and Dr. Gillian Bice for their instrumental guidance and insight they graciously imparted on me as I developed my thesis. As an MSU undergraduate, Ms. Christiana Hench provided immense help in collecting data and was a pleasure to work with. To my fellow graduate students from MSU, thank you for inspiring me every day and for cheering me on along the way. I would like to particularly acknowledge Valerie Leah and Maureen Moffit for their treasured friendship and for our copious writing sessions that were both productive and filled with laughter. Finally, I am grateful for the endless support from my family and friends. To my parents and brother, thank you for your unwavering belief in me.

TABLE OF CONTENTS

LIST OF TABLES	vii
LIST OF FIGURES	ix
CHAPTER 1: INTRODUCTION	1
CHAPTER 2: HISTORICAL BACKGROUND AND RESEARCH FROM THE REGION	4
Historical background of medieval Nubia	4
Background of research sample	8
Related research and context from the region	9
Research questions and hypotheses	15
CHAPTER 3: CROSS-SECTIONAL GEOMETRY AND THE BIOMECHANICAL APPROACH	17
Premises behind the biomechanical approach	18
Bone functional adaptation	18
Beam theory	19
Biomechanical principles	20
Cross-sectional geometric properties	22
Non-mechanical factors	26
Obtaining cross-sectional geometric properties	29
Applications of cross-sectional geometry	31
Human athlete studies	31
Bioarchaeological studies	34
CHAPTER 4: MATERIALS AND METHODS	38
Materials	38
The Mis Island skeletal collection	38
Generating the research sample	39
Methods	41
Obtaining cross-sections	41
Calculating cross-sectional geometric properties	46
Statistical analyses	50
Intra- and inter-observer error	53
CHAPTER 5: RESULTS	55
Research Question 1	55
Midshaft femur	56
Subtrochanteric region of femur	60
Midshaft tibia	63
Research Question 2	66
Midshaft femur	67

Subtrochanteric region of femur	73
Midshaft tibia	79
Comparisons within cemeteries	85
Intra- and inter-observer error	88
Intra-observer error	88
Inter-observer error	89
CHAPTER 6: DISCUSSION	91
Research Question 1	91
Research Question 2	93
Diaphyseal robusticity (<i>J</i> and <i>TA</i>)	93
Diaphyseal shape (<i>I_{max}/I_{min}</i>)	97
Intra- and inter-observer error	105
Limitations	106
CHAPTER 7: CONCLUSION	108
LITERATURE CITED	111

LIST OF TABLES

Table 4.1: Number of total individuals, separated by sex, for each cross-sectional variable at the three diaphyseal locations	41
Table 4.2: Number of males and females, separated by cemetery, for each cross-sectional variable at the three diaphyseal locations	41
Table 4.3: Cross-sectional geometric variables with descriptions	47
Table 4.4: Body mass estimation formulae derived from Ruff et al. (1997)	50
Table 5.1: <i>P</i> -values from t-tests between males from 3-J-10 and males from 3-J-11, and females from 3-J-10 and females from 3-J-11 for each cross-sectional property at the three diaphyseal locations	55
Table 5.2: Summary statistics for cross-sectional geometric properties at midshaft femur, separated by cemetery and sex	56
Table 5.3: Summary statistics for cross-sectional geometric properties at the subtrochanteric region of the femur, separated by cemetery and sex	60
Table 5.4: Summary statistics for cross-sectional geometric properties at midshaft tibia, separated by cemetery and sex	63
Table 5.5: <i>P</i> -values from comparisons between males and females for each cross-sectional property at the three diaphyseal locations	66
Table 5.6: Summary statistics for cross-sectional geometric properties at midshaft femur, separated by sex	67
Table 5.7: Summary statistics for cross-sectional geometric properties at subtrochanteric region of femur, separated by sex	73
Table 5.8: Summary statistics for cross-sectional geometric properties at midshaft tibia, separated by sex	79
Table 5.9: <i>P</i> -values from comparisons between males and females from cemetery 3-J-10 and males and females from 3-J-11 for each cross-sectional property at the three diaphyseal locations	85
Table 5.10: Summary statistics for cross-sectional geometric properties at midshaft femur (F50), subtrochanteric femur (F80), and midshaft tibia (T50) separated by sex from cemetery 3-J-10	86

Table 5.11: Summary statistics for cross-sectional geometric properties at midshaft femur (F50), subtrochanteric femur (F80), and midshaft tibia (T50) separated by sex from cemetery 3-J-11	87
Table 5.12: TEM and %TEM, and ICC consistency and agreement values for CSG intra-observer error.....	88
Table 5.13: TEM and %TEM, and ICC consistency and agreement values for intra-observer error of measurements	89
Table 5.14: TEM and %TEM, and ICC consistency and agreement values for inter-observer error of femoral measurements	90
Table 5.15: TEM and %TEM, and ICC consistency and agreement values for inter-observer error of tibial measurements	90

LIST OF FIGURES

Figure 2.1: Map of the medieval Nubian kingdoms, adapted from Hurst (2013); original image by Mark Dingemans	5
Figure 2.2: Map of Nile Valley Region, adapted from Stock et al. (2011)	12
Figure 3.1: Axes commonly used in deriving cross-sectional geometric properties	23
Figure 3.2: Lower leg mid-shaft cross sections from pQCT scans by Shaw and Stock (2009)	32
Figure 4.1: Proper orientation and reference planes of the femur (from Ruff and Hayes, 1983)	42
Figure 4.2: Proper orientation and reference planes for the tibia (from Ruff and Hayes, 1983)	43
Figure 4.3: Femur with molds at midshaft and the subtrochanteric region	45
Figure 4.4: Tibia with cast at midshaft	46
Figure 4.5: Two solid outlines process in BoneJ with principal axes	47
Figure 5.1: Boxplots for I_{max}/I_{min} at midshaft femur between cemeteries, separated by sex	57
Figure 5.2: Scatter plots between I_{max}/I_{min} and AP/ML at midshaft femur, separated by cemetery	58
Figure 5.3: Boxplots for J at midshaft femur between cemeteries, separated by sex	58
Figure 5.4: Boxplots for TA at midshaft femur between cemeteries, separated by sex	59
Figure 5.5: Boxplots for I_{max}/I_{min} at subtrochanteric femur between cemeteries, separated by sex	61
Figure 5.6: Boxplots for J at subtrochanteric femur between cemeteries, separated by sex	61
Figure 5.7: Boxplots for TA at subtrochanteric femur between cemeteries, separated by sex	62

Figure 5.8: Boxplots for I_{max}/I_{min} at midshaft tibia between cemeteries, separated by sex	64
Figure 5.9: Boxplots for J at midshaft tibia between cemeteries, separated by sex	64
Figure 5.10: Boxplots for TA at midshaft tibia between cemeteries, separated by sex	65
Figure 5.11: Violin plot of I_{max}/I_{min} values between males and females at midshaft femur	68
Figure 5.12: Density plot of I_{max}/I_{min} values between males (blue) and females (red) at midshaft femur	68
Figure 5.13: Violin plot of J (mm^4) values between males and females at midshaft femur	69
Figure 5.14: Density plot of J (mm^4) values between males (blue) and females (red) at midshaft femur	69
Figure 5.15: Violin plot of TA (mm^2) values between males and females at midshaft femur	70
Figure 5.16: Density plot of TA (mm^2) values between males (blue) and females (red) at midshaft femur	70
Figure 5.17: Scatter plot (with random jitter) of clusters after k -means cluster analysis of I_{max}/I_{min} at midshaft femur	71
Figure 5.18: Scatter plot (with random jitter) of clusters after k -means cluster analysis of J at midshaft femur	72
Figure 5.19: Scatter plot (with random jitter) of clusters after k -means cluster analysis of TA at midshaft femur	72
Figure 5.20: Violin plot of I_{max}/I_{min} values between males and females at subtrochanteric femur	74
Figure 5.21: Density plot of I_{max}/I_{min} values between males (blue) and females (red) at subtrochanteric femur	74
Figure 5.22: Violin plot of J (mm^4) values between males and females at subtrochanteric femur	75
Figure 5.23: Density plot of J (mm^4) values between males (blue) and females (red) at subtrochanteric femur	75

Figure 5.24: Violin plot of TA (mm^2) values between males and females at subtrochanteric femur	76
Figure 5.25: Density plot of TA (mm^2) values between males (blue) and females (red) at subtrochanteric femur	76
Figure 5.26: Scatter plot (with random jitter) of clusters after k -means cluster analysis of I_{max}/I_{min} at subtrochanteric femur	77
Figure 5.27: Scatter plot (with random jitter) of clusters after k -means cluster analysis of J at subtrochanteric femur	78
Figure 5.28: Scatter plot (with random jitter) of clusters after k -means cluster analysis of TA at subtrochanteric femur	78
Figure 5.29: Violin plot of I_{max}/I_{min} values between males and females at midshaft tibia	80
Figure 5.30: Density plot of I_{max}/I_{min} values between males (blue) and females (red) at midshaft tibia	80
Figure 5.31: Violin plot of J (mm^4) values between males and females at midshaft tibia	81
Figure 5.32: Density plot of J (mm^4) values between males (blue) and females (red) at midshaft tibia	81
Figure 5.33: Violin plot of TA (mm^2) values between males and females at midshaft tibia	82
Figure 5.34: Density plot of TA (mm^2) values between males (blue) and females (red) at midshaft tibia	82
Figure 5.35: Scatter plot (with random jitter) of clusters after k -means cluster analysis of I_{max}/I_{min} at midshaft tibia	83
Figure 5.36: Scatter plot (with random jitter) of clusters after k -means cluster analysis of J at midshaft tibia	84
Figure 5.37: Scatter plot (with random jitter) of clusters after k -means cluster analysis of TA at midshaft tibia	84
Figure 6.1: Two subtrochanteric cross-sections from a female (left) and male (right) from Mis Island	104

CHAPTER 1: INTRODUCTION

The biomechanical approach is based on the ability of bone to adapt and change in response to habitual mechanical stimuli that occur over an individual's life. This method utilizes engineering models in analyzing how long bones respond to mechanical forces and stress. A main premise in these models is that in order to prevent structural failure or injury, bone must be able to resist deformations and strains that occur during activity (Carlson and Marchi, 2014; Meyer et al., 2011). Bone thus adapts to mechanical loads by modeling and remodeling processes that distribute material where it is needed to reduce the stresses within the bone (Nikita et al., 2011). The accumulated responses of bone from mechanical and non-mechanical factors should then be observable in the structure of an individual's long bone diaphyses. Comparing cross-sectional properties of long bones between individuals of similar age provides a means of inferring level of habitual activity and mobility of past populations.

This thesis research applies the biomechanical approach to the medieval Nubian skeletal collection from Mis Island which is comprised of two cemeteries—cemetery 3-J-10 (AD 1100 – 1400) and cemetery 3-J-11 (AD 300 – 1400). With this approach, the study investigates patterns of cross-sectional geometric properties and mechanical loading within this collection to contribute to the efforts of uncovering what life was like for this population. Through an exploration of lower limb diaphyseal robusticity, this project places the reconstructed biomechanical profiles of these individuals within the framework of habitual activity and social structures related to distribution of labor, and infer how these cultural aspects may have organized daily life in medieval Nubian society. In doing so, non-mechanical (e.g., age and nutrition) factors are also considered in interpreting the processes that influence variation in diaphyseal morphology.

The data in this research are comprised of cross-sectional geometric properties that indicate the robusticity and mechanical loading of the individuals' remains. This project focuses on diaphyseal cross-sections at midshaft femur, the subtrochanteric region of the femur, and midshaft tibia. With these data, two research questions are explored. The first of these research objectives is a comparison of the biomechanical data between cemeteries 3-J-10 and 3-J-11 in order to determine if any spatial and temporal differences between these communities at this location existed regarding activity and mobility. The second research question is an intra-site investigation to assess whether significant patterns of mechanical loading exist within the sample, primarily between males and females, to infer distribution of labor and activity.

Supporting the biomechanical approach are two main principles that demonstrate how long bones react to mechanical loading and associated forces. The concept of bone functional adaptation asserts that bone responds to mechanical loading regimes over an individual's life (Carlson and Marchi, 2014; Davies et al., 2014; Ruff et al., 2006b). In a simplified description of these processes, a greater amount of bone is deposited in response to elevated activity and with inactivity, bone tissue may be resorbed. The quantification of these accumulated changes forms an analytical basis for inferring past mechanical loading patterns from skeletal remains. Beam theory is an engineering concept which is used in the biomechanical approach to model the ways in which skeletal tissue in long bones respond to stresses and strains imposed by externally applied forces (Carlson and Marchi, 2014; Lieberman et al., 2004; Ruff, 2008). By modeling long bones as beams, investigators estimate mechanical properties of skeletal elements by analyzing the amount and distribution of bone within a cross-section (Davies et al., 2014). The greater bone mass in a diaphyseal section lessens stress and increases resistance to externally applied loads (Pearson and Lieberman, 2004).

Given these foundational principles, researchers can generate inferences about activity levels and patterns of mobility from variation in cross-sectional robusticity and shape. In the context of skeletal remains, robusticity refers to the “strength or rigidity of a structure relative to the mechanically relevant measure of body size” (Ruff et al., 1993:25). Quantifications of skeletal robusticity therefore provides a means of inferring activity levels within and/or between populations. Diaphyseal shape appears to be more associated with mobility patterns than relative robusticity (Ruff and Larsen, 2014). Mobility is defined here as the totality of activities related to locomotion conducted with the lower limb (Pearson et al., 2014). This kind of mobility involves the “daily walking and/or running activities of an individual to move from one location to another” (Wescott, 2014:112). While there are many categories of mobility, logistic mobility is the most probable type to induce these skeletal responses and affect diaphyseal shape (Wescott, 2014). Inferences regarding robusticity and mobility shed light on habitual activity of past populations and aid in reconstructing the experiences and social structures that framed daily life.

The outcomes from this project build upon pre-existing research of this small farming community at Mis Island during the medieval period, in order to form a more complete picture of what life was like for these individuals. This project examines patterns of mechanical loading in the lower limb and interpret the cross-sectional data with regards to sub-group variation and mobility patterns. Through this approach, inferences are drawn about habitual activity and distribution of labor within the medieval Mis Island society. The comparison between the two cemeteries from Mis Island explores any emergence of communal trends in lower limb robusticity at this location. Ultimately, this research furthers our understanding of the life experience and societal frameworks that structured life in medieval Nubia.

CHAPTER 2: HISTORICAL BACKGROUND AND RESEARCH FROM THE REGION

Historical background of medieval Nubia

Medieval Nubia extended over a period of approximately one thousand years from the sixth to the sixteenth century AD. The sixth century in the middle Nile Valley was a transformative period as local tribes united into larger polities, resulting in the establishment and development of three medieval Nubian kingdoms (Figure 2.1)—Nobadia between the First and Third Cataracts, Makuria between the Third and Fifth Cataracts, and Alwa located upstream of the Fifth Cataract (Edwards, 2007; Welsby, 2002; Żurawski, 2014). Shortly following their establishment in the mid-sixth century AD, these medieval kingdoms separately converted to Christianity (Hurst, 2013). The resulting political organization within these ruling bodies was tied to the Christian religion (Edwards, 2007).

The medieval period in Nubia is characterized as a time of sedentism based on evidence of substantial, permanent settlements (Żurawski, 2014). For several centuries, medieval Nubia experienced an era of peace and prosperity and shared strong political relations with Muslim Egypt. However, as the medieval Nubian period continued, internal political conflicts coupled with external aggression and broken ties with Muslim Egypt weakened the Nubian kingdoms until their fall to Muslim control (Edwards, 2007). The medieval Nubian period can be divided into five approximate stages—Transitional, Early, Classic, Late, and Terminal (Adams, 1977; Welsby, 2002).

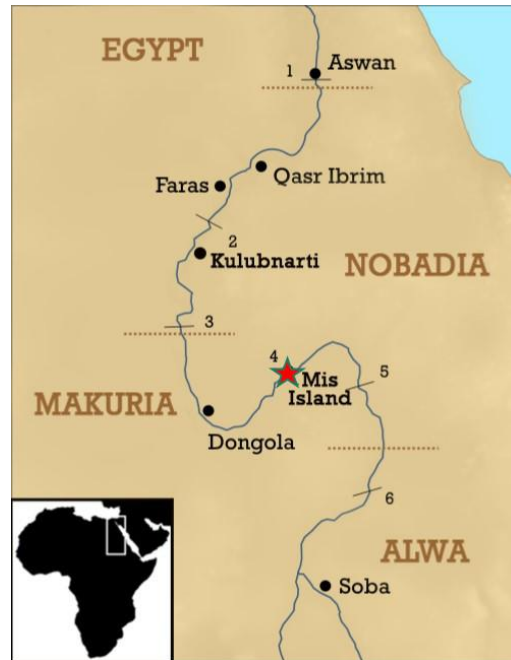


Figure 2.1: *Map of the medieval Nubian kingdoms, adapted from Hurst (2013); original image by Mark Dingemans. Red star added to mark location of Mis Island.*

Transitional Phase (AD 550 – 600)

The decline and collapse of the Kushite civilization in the fourth century resulted in an intricate political, cultural, and social transformation in the Nile Valley between the fourth and sixth centuries AD, also known as the Post-Meroitic period (Edwards 2007; Godlewski, 2014). The smaller polities that occupied the Nile Valley region prior to the medieval period are believed to have combined to form the three medieval Nubian kingdoms during the sixth century (Welsby, 2002). Much remains unknown about the origin of these groups; however, evidence suggests some degree of continuity with previous Nile Valley populations (Soler, 2012). Soon after their formation, the medieval Nubian kingdoms independently converted to Christianity, which is regarded as a critical moment in the beginning of medieval Nubia.

Early Medieval Phase (AD 600 – 850)

In the beginning of the Early Medieval Phase, the Christian kingdoms of Nobadia, Makuria, and Alwa were independent and steady political entities (Soler, 2012). As population increased in the Nile Valley, urban settlements were established (Soler, 2012). The kingdoms' power also grew and the political organizations exercised more control and protection of their people and land (Soler, 2012). To the north of Nubia in the mid-seventh century AD, impending danger threatened as Egypt was conquered by the Second Caliph's Arab Muslim forces (Soler, 2012). Not long after their conquest of Egypt, the Arab Muslim armies set out for Makuria and reached as far as Dongola in AD 652 (Soler, 2012; Trigger 1965). However, the Nubian kingdoms were formidable by this point and successfully faced the invasion, causing the Muslim armies to withdraw to Egypt (Hurst, 2013; Soler, 2012; Trigger, 1965). These confrontations led to an agreement between Egypt and Nubia to settle their disputes.

The *Baqt* Treaty of AD 652 reinstated peace between these forces and set the relationship between Muslim Egypt and the Christian kingdom of Makuria which was peaceful and profitable for centuries to come (Godlewski, 2014; Soler, 2012; Welsby, 2002). This treaty involved a trade agreement in which the Nubians provided hundreds of slaves each year and occasional material goods to the Arabs in exchange for food, drink, horses, textiles, cloth, and pottery from Egypt (Trigger, 1965; Welsby, 2002). Between the late sixth and mid-seventh centuries, the kingdoms of Makuria and Nobadia united under Makurian rule, centered at Dongola (Edwards, 2007; Godlewski, 2014; Trigger, 1965; Welsby, 2002).

Classic Medieval Phase (AD 850 – 1110)

The Classic Medieval phase is characterized as a politically, economically, and culturally prosperous era for the kingdoms with substantial urban growth and development (Soler, 2012; Trigger, 1965; Welsby, 2002). During this time, the relationship between Nubia and Egypt grew

as a mutually beneficial association with a free-trade area between the First and Second Cataracts that created a more relaxed border for immigration (Soler, 2012). The affluence of the Nile Valley was also likely facilitated by elevated river levels that resulted in more effective irrigation (Soler, 2012). Signs of highly active agriculture were found in Lower Nubia, perhaps aided by a larger population (Trigger, 1965). This period's heightened production is also evidenced by archaeological discoveries of large food storage units that surpassed those from other periods (Soler, 2012). The peace between Egypt and Nubia was occasionally disrupted by military confrontations, which were likely the result of not adhering to the treaty (Soler, 2012). While these conflicts from both sides challenged the relationship between the Nubians and Egyptians, the raids never escalated into war (Soler, 2012; Welsby, 2002). Muslims and Christians of the Classic Period continued to live together in accord (Soler, 2012).

Late Medieval Phase (AD 1100 – 1400)

Towards the end of the Classic Phase and into the Late Phase, Nubia experienced increased hostility from Egyptian Muslims and Arab tribes that had entered North Africa and conducted raids on Nubia from the desert (Soler, 2012; Trigger, 1965). Nubia was further weakened by the open economic ties it had during the Classic phase. Through these exposed relations, outside forces set their sights on Nubia's resources and Nubia was threatened by the increased presence of Arab Muslim merchants (Soler, 2012). The kingdom of Makuria was experiencing internal power struggles which depleted the government's authority and ability to protect its inhabitants (Hurst, 2013; Soler, 2012; Welsby, 2002). The people took on the responsibility of defending their communities by moving closer together and as evidenced in Lower Nubia, settlements increased their fortifications (Soler, 2012; Trigger, 1965). As Makuria weakened, Muslim Egyptians and Arabs from the desert crossed the region at an increased rate to

take control of Nubian lands (Soler, 2012). In AD 1365, the Makurian capital at Dongola was lost and the kingdom fell (Hurst, 2013; Welsby, 2002).

Terminal Medieval Phase (AD 1400 – 1500)

After the collapse of Makuria, the kingdom of Alwa continued its power and practice of Christianity until its capture by the Funj Sultanate in AD 1504 (Hurst, 2013; Soler, 2012; Welsby, 2002). The fall of Alwa marked the conclusion of the Christian age of Medieval Nubia (Hurst, 2013; Soler, 2012). The end of Nubian Christianity appears to have been a result of political turmoil, increased conversion to Islam, and economic deterioration (Soler, 2012).

Background of research sample

The medieval Nubian kingdom of Makuria spanned the region from the Third Cataract to approximately half-way between the Fifth and Sixth cataracts of the Nile. This thesis focuses on a small farming community from Mis Island, located upstream from the Fourth Cataract in Makurian territory and dating from the mid-fifth to the early fifteenth centuries AD. The landscape of the Fourth Cataract islands appears to have sustained substantial agriculture in ancient Nubia (Hurst, 2013) with thin sections of fertile alluvium that support today's labor-intensive agriculture (Näser, 2007). The Fourth Cataract's challenging accessibility and resulting isolation has been presented as an advantage for the region that provided refuge from political instability, although the continuous occupation of the numerous settlements in the area indicate the region's steady use as a home (Hurst, 2013). Craniometric analysis of the population at Mis Island performed by Vollner (2016) also suggests a relatively isolated community based on low external gene flow into the population.

Examination of the health status of individuals at Mis Island expresses a life of hardship, but also illustrates a population that could adapt and maintain stability. Soler (2012) investigated

adult health on Mis Island through analyzing paleopathological indicators of stress. This population exhibited a high incidence of skeletal indicators of stress, including porotic hyperostosis, cribra orbitalia, linear enamel hypoplasias, periostitis, and maxillary sinusitis. However, many adults demonstrated healed lesions which implied an ability to survive the stressors faced during childhood and adulthood. There were no significant differences in stress indicators through comparing sex and age cohorts and burial groups, suggesting the stressors associated with life on Mis Island equally affected the population (Soler, 2012). In an investigation of subadult health and nutritional status at Mis Island, Hurst (2013) observed the presence of scurvy, megaloblastic anemia, and tuberculosis which signified limited access to nutrients and stress that started early in life.

Comparisons between the two cemeteries that comprise the research sample, cemetery 3-J-10 and cemetery 3-J-11, demonstrated differences between the communities of these burial groups. In comparing the mortuary archaeology between the cemeteries, Soler (2012) found different organizational patterns. Burials at cemetery 3-J-10 seemed to be based on community given the lack of distinct burial groupings, whereas small burial clusters were observed in cemetery 3-J-11, possibly associated with family or other cultural groupings (Soler, 2012). While adults from both cemeteries displayed equal rates of skeletal stress, Hurst (2013) observed higher levels of cribra orbitalia in subadults from cemetery 3-J-11 than subadults from cemetery 3-J-10.

Related research and context from the region

In investigating temporal trends in lower limb strength among various samples around the world, previous researchers have observed a chronological reduction in lower limb strength. These researchers have attributed this pattern to decreasing mobility concomitant with the onset

of agricultural practices that steadily continued as food production and sedentism escalated (Macintosh et al., 2014; Ruff et al., 2015). Within the Nile Valley region, a similar pattern has been observed over the suspected transition to agricultural subsistence strategies. Stock and colleagues (2011) analyzed lower limb robusticity between samples along the Nile River in Egypt and Nubia, dating between 13,000 BCE and 1,500 BCE. This time period encompasses shifts in subsistence practices from hunting and gathering, nomadic pastoralism, and the origins of agriculture, as well as the formation and development of the Egyptian state. Over this change in subsistence strategies, there appeared to be a decrease in femoral strength in the included samples, which indicates a reduction in mechanical loading and lowered mobility with the transition to agriculture.

In medieval Nubia, subsistence was grounded in small-scale agriculture and supplemented to some degree by animal husbandry, hunting, and fishing (Adams, 1977; Welsby, 2002). The water wheel, or *saquia*, was introduced in late Roman Egypt and subsequently spread to Nubia roughly sometime between the fourth and fifth centuries AD, where it transformed subsistence patterns by enabling irrigated farming and intensifying agriculture (Edwards, 2007; Trigger, 1965; Welsby, 2002). This change in agricultural infrastructure resulted in a population increase, a growth in settlements with the dispersion of new crops, and inhabitation in areas that previously could not support agriculture (Edwards, 2007; Trigger, 1965).

At Mis Island, there is a lack of archaeological evidence to indicate subsistence practices during the medieval period (Hurst, 2013). Some signs of keeping livestock is suggested by post-holes at the settlement of 3-J-19 on Mis Island which Ginns (2007) interpreted as possible remnants of animal pens, similar to those seen today. Given the absence of information on subsistence practices at Mis Island, reference to finds from other medieval Nubian locations need

to be made (Hurst, 2013). Populations from the site of Kulubnarti appeared to live in small farming villages that engaged in agriculture with *saquia* irrigation and walls that maintained and protected fertile soil from floods (Mulhern and Van Gerven, 1997). Archaeological evidence from the region suggest crops of sorghum, millet, barley, beans, lentils, peas, dates, and wheat; as well as livestock of cattle, sheep, and pigs (Mulhern and Van Gerven, 1997).

Until relatively recently, this subsistence economy and irrigation farming had not changed substantially since the introduction of the water wheel during the Roman period (Edwards, 2007; Kilgore, 1984; Trigger, 1965). Ethnographic analogies with modern populaces in Sudan must be used with caution, particularly regarding pre-Islamic populations in Sudan (Kilgore, 1984). Despite modern technology and changes in population and lifestyle, observations of modern everyday activity and tasks associated with subsistence can provide insight because carrying out roles repeatedly over a lifetime affects skeletal robusticity.

Ethnographic observations of the people in this region today suggest continued patterns of activity that translate to biomechanical stresses. The region's modern subsistence strategy relies largely on agriculture and modern pumps for irrigation infrastructure (Mulhern and Van Gerven, 1997). While both men and women participate in physical activity in modern Nubia, recent observations describe a separation of daily tasks. Men are typically responsible for heavier labor related to clearing fields and women carry out roles that take more time, but are not as physically intense, such as maintaining fields, helping with the harvest, and caring for livestock (Kilgore, 1984; Mulhern and Van Gerven, 1997). Cross-sectional geometry studies and related research that explore questions on activity level in ancient Nubia have interpreted differences between males and females of these populations within the context of differential roles and division of labor.



Figure 2.2: *Map of Nile Valley Region, adapted from Stock et al. (2011)*. Stars added to show the location of Kerma (blue) and Kulubnarti (yellow) in relation to Mis Island (red).

Investigation of cross-sectional properties in remains from the Upper Nubian site of Kerma (~2000 BCE –1500 BCE) has demonstrated sexual dimorphism in mechanical loading values. Compared to samples from Jebel Sahaba (13,000 – 9,000 BCE), el-Badari (5,000 – 4,000 BCE), and Hierakonpolis (4,000 – 3,000 BCE), Stock and colleagues (2011) observed an increase in sexual dimorphism at Kerma in humeral and femoral strength. The researchers attributed this finding to possible changes in habitual activity and nutrition, or a higher diversity in the population from migration. Within the Kerma sample, Stock et al. found indicators of greater strength in male upper and lower limbs than female limbs. Additionally, Nikita et al. (2011) observed sexual dimorphism in femoral diaphyseal shape from Kerma, with females exhibiting a more circular morphology. These findings indicate a division of labor and higher levels of loading in males from Kerma.

Research from the medieval Nubian site of Kulubnarti has supported a sexual division of activity in this population. In a study on cross-sectional geometry of adult femora from medieval Kulubnarti, Kyle (2008) observed indications of greater strength and higher mobility in males compared to females. Further suggestion of sexual division in activity in medieval Nubia is suggested by Kilgore's (1984) research on degenerative joint disease in an adult sample from Kulubnarti. In this sample, higher frequencies of osteophyte formation were observed in males compared to females, which was consistent with males carrying out more physically demanding labor. Mulhern and Van Gerven (1997) investigated femoral remodeling patterns in an adult sample from the late medieval period at Kulubnarti and explored the association between sex and histomorphometric variables. In comparing the remodeling indicators between males and females, the researchers found that males had significantly more intact osteons than females, females had significantly more osteon fragments than males, and females had significantly larger osteons than males. Mulhern and Van Gerven attributed these differences in osteon number and size between the sexes to probable disparate mechanical strains resulting from separate physical activities, and thus support sexual division of labor in this population.

Mulhern and Van Gerven (1997) likened the trends in their research to those observed by Martin (1983) in a sample of subadult and adult femora from Wadi Halfa (350 BC – AD 1300), in which more complete osteons were present in males than females. In addition to other lines of analysis, Martin (1983) associated this pattern to greater nutritional and reproductive stress in females that negatively affected bone maintenance. Mulhern and Van Gerven (1997) however, concluded that such remodeling dynamics observed in their study were likely caused by mechanical strain rather than differential nutrition based on interpopulational comparisons.

Studies on subadults from Kulubnarti have investigated the health and nutritional status of these individuals through analyzing long bone growth and robusticity, and diaphyseal cortical bone growth. In assessing postcranial strength of a subadult sample from medieval Kulubnarti, Cowgill (2010) observed substantially low levels of long bone robusticity compared to other populations. Based on the likely consistent nutritional deficiency these subadults experienced, Cowgill attributed the low degree of strength to nutritional stress, which may have resulted in a decrease in body mass and affected cortical bone growth.

Additional indication of dietary stress in subadults from medieval Kulubnarti was suggested by Hummert (1983), who investigated the relationship between longitudinal growth of the tibial diaphysis and the percent of cortical bone at midshaft. While growth in tibial length and cortical area at midshaft was well-maintained in these subadults, the decrease in percent of cortical area exhibited during early and later childhood indicated acute endosteal resorption as the area of the medullary cavity increased. Hummert interpreted this relative decrease in bone as an expression of the nutritional stress supported by previous studies. A re-analysis of this sample, conducted by Van Gerven et al. (1985), further explored cortical bone maintenance by analyzing percent cortical area, bone mineral content, and cross-sectional geometric variables. Despite the endosteal resorption observed during the later juvenile period in this sample, the external bone dimensions and measures of bone strength were not affected and continued to increase with age—suggesting sustained mechanical integrity throughout growth and development. These results also propose that the periosteal and endosteal surfaces respond differently to nutritional stress and/or perhaps the periosteal surface deposits more bone to recompense for added mechanical stresses (Ruff et al., 2013).

Research questions and hypotheses

Research Question 1—Inter-cemetery: Is there a difference in cross-sectional geometric properties between cemeteries 3-J-10 and 3-J-11?

H₀: There will not be a difference in cross-sectional properties between cemeteries 3-J-10 and 3-J-11.

Expectation: Based on the differences in mortuary practices from both cemeteries, there is some degree of diachronic change in cultural constructs between the communities (Soler, 2012). This change may have affected habitual activity and mobility, and organization of labor, between individuals from the two cemeteries. Additionally, a group of individuals interred at 3-J-11 may have experienced low levels of the Nile River which could have affected normal agricultural yields (Hurst, 2013). This environmental disturbance might have caused these individuals to alter habitual activity to acquire resources. Therefore, there may be differences in cross-sectional properties between these two cemeteries potentially resulting from diachronic cultural changes and environmental disruption of subsistence practices.

Research Question 2—Intra-site: Are there patterns of cross-sectional geometric properties within the Mis Island collection that would suggest significantly different groups of individuals, primarily regarding males and females?

H₀: There will be no differences in cross-sectional properties between males and females.

Expectation: The Nubian sites of Kerma and Kulubnarti practiced developed agriculture in the Nile Valley. Previous observations of individuals from these sites indicated greater strength and higher mobility in males compared to females. Despite spatial and temporal

differences, there may be some underlying cultural similarities with Mis Island regarding mobility levels and sexual division of labor with an agricultural subsistence strategy. Therefore, cross-sectional properties between males and females from the farming community at Mis Island are expected to differ.

CHAPTER 3: CROSS-SECTIONAL GEOMETRY AND THE BIOMECHANICAL APPROACH

Bone is a highly dynamic tissue continuously responding to its mechanical environment and altering the distribution of material to comply with loading regimes (Meyer et al., 2011; Wescott and Cunningham, 2006). This concept of skeletal plasticity forms the basis of the biomechanical approach, which seeks to infer the accumulation of mechanical loading over the individual's life through the analysis of diaphyseal cross-sectional geometry (Bice, 2003; Carlson and Marchi, 2014). Cross-sectional properties are measures of skeletal robusticity, which describe the amount and distribution of bone in a cross-section, and therefore indicate the rigidity and strength of a bone, relative to a standardized estimate of body size (Carlson et al., 2007; Ruff, 2008). In order to prevent structural failure or injury during activity, bone must have an adequate level of robusticity to be able to resist deformations and minimize potentially harmful strain (Carlson and Marchi, 2014; Meyer et al., 2011). This optimal degree of structural integrity is achieved through modeling and remodeling processes, in which bone material is distributed to lessen internal stresses within the bone's structure (Nikita et al., 2011). Although these processes are primarily regulated by localized mechanical strain, non-mechanical factors (e.g., genes, nutrition, hormones) also influence this system (Carlson and Marchi, 2014; Maggiano et al., 2008).

The combined interaction of these factors is reflected in diaphyseal cross-sectional properties, which are analyzed in studies of past populations to gain insight into habitual activity of past populations and to attempt reconstructing the experiences and social structures that framed daily life (Davies et al., 2014). Previous bioarchaeological studies employing this approach have interpreted lower limb robusticity within the context of mobility levels, shifts in economic or subsistence strategies, and division of labor regarding sex and presumed status

(Agarwal, 2016). Mobility is defined by Pearson and colleagues (2014) as “the sum total of locomotor activities performed using the lower limb” (134). This concept of mobility refers to the movement of the individual across a landscape on a variety of temporal levels (e.g., daily, annually, seasonally), and is likely logistical mobility in these contexts (Carlson et al., 2007; Wescott, 2014). The inferences drawn from lower limb skeletal robusticity are based on the foundational principles of bone functional adaptation and the engineering concepts from beam theory.

Premises behind the biomechanical approach

Bone functional adaptation

The foundation for the biomechanical approach has been traditionally referred to as “Wolff’s law”, which was misrepresented and contested since its original form (Pearson and Lieberman, 2004; Ruff et al., 2006b). What became Wolff’s law was actually a combination of three ideas developed by 19th century anatomists, but began with Julius Wolff’s theory that trabeculae align with the directions of primary stresses that could be mathematically modeled (Pearson and Lieberman, 2004). Similar ideas for the mechanisms behind cortical bone were integrated into the subsequent form of Wolff’s law by other contemporaries (Carlson and Marchi, 2014). Although theoretical and semantic issues have arisen from the application of Wolff’s law, the general concept of the model is accepted—mechanical loading influences and modifies bone structure (Frankel and Nordin, 2012; Pearson and Lieberman, 2004; Ruff et al., 2006b; Ruff, 2008). The revised and modern version of Wolff’s law is now referred to as “bone functional adaptation” and forms the basis for cross-sectional geometric studies (Carlson and Marchi, 2014; Ruff et al., 2006b). The current model of bone functional adaptation states that bone adapts to its mechanical environment over an individual’s life course, resulting in

measurable differences in morphology for which inferences of past mechanical contexts can be made; however, it is recognized that this is a complex and nuanced model (Carlson and Marchi, 2014; Davies et al., 2014; Ruff et al., 2006b). Bone functional adaptation provides the framework to indirectly predict the mechanical profiles of individuals based on cross-sectional geometric values. The specific skeletal responses to mechanical loads are modeled by beam theory.

Beam theory

Studies that investigate the cross-sectional geometric properties of bone employ concepts from an engineering model, referred to as beam theory, to represent how a long bone behaves under mechanical loading (Carlson and Marchi, 2014; Lieberman et al., 2004; Ruff, 2008). This model demonstrates that if applied forces acting on the beam's structure surpass a critical threshold, the structure will fail and break (Ruff, 2008). Therefore, to prevent structural failure or injury, bone must be able to withstand the forces that occur during activity (Carlson and Marchi, 2014). The properties of a structure that describe its ability to tolerate mechanical loads are termed rigidity and strength. Rigidity reflects the structure's capacity to withstand deformation before the critical point of failure. The strength of a structure describes its resistance to fracturing. Both the rigidity and strength of a structure are crucial in supporting loads and not failing under the resultant stresses. Beam theory posits that the stresses produced by externally applied loads and forces can be calculated from the cross-sectional geometric properties of the structure (Ruff, 2008). The application of beam theory to modeling long bones as beams thus allows researchers to estimate mechanical properties of skeletal elements by measuring the amount and distribution of material within a diaphyseal cross-section (Davies et al., 2014). These

cross-sectional measures are then used to calculate the rigidity of a bone, and more indirectly its strength (Bice, 2003).

In applying beam theory to skeletal elements, it is assumed that bone will react to mechanical loads as engineering beams would (Davies et al., 2014; Ruff, 2008); however, given the organic shape of a diaphysis, the neutral axis does not run through the centroid area of a diaphyseal section as it would in a beam (Lieberman et al., 2004). Non-human animal studies have shown that the combined effect of bending and axial compressive forces of the diaphysis shifts the neutral axis away from the centroid toward the cortex under tension—an important consideration in cross-sectional geometric studies because properties for estimating rigidity are usually calculated around axes that pass through the section centroid (Ruff et al., 2006b).

Lieberman and colleagues (2004) found that in a sheep model, estimates for rigidity and strength using the assumed section centroid could be in error by as much as 30 – 50%. However, they concluded that traditionally calculated properties derived about centroidal axes are still valid representations of mechanical loading, and are highly correlated with true measures of rigidity and strength. These values of rigidity and strength are influenced by the combination of forces experienced by the structure.

Biomechanical principles

Forces can be applied to the lower limbs in various directions, creating axial compression and tension, bending, torsion, and combined loading (Frankel and Nordin, 2012; Pearson and Lieberman, 2004; Ruff, 2008). Through the long axis of the bone, axial compression and tension forces act to compress or pull apart the bone's structure. As a bone experiences bending loads, there is both compression and tension forces on opposite sides of a cross-section. Torsion loads are the result of the bone being twisted about its long axis, creating diagonal/shearing stress. The

primary types of stress experienced by long bones are bending and torsion (Ruff, 2008), and are reflected in cross-sectional geometric properties. The subsequent stresses from these forces result from muscles pulling at origin or insertion regions, and from outside loads acting through a joint or the external environment (Pearson and Lieberman, 2004).

In response to loading, bone experiences two main factors—stress and strain (Pearson and Lieberman, 2004). Stress is the intensity of the load/force per unit of area that is generated within a structure by externally applied loads. Strain is the change in dimension and deformation of bone produced within a structure from an external load (Frankel and Nordin, 2012), and is seemingly the main stimulus for bone modeling and remodeling (Pearson and Lieberman, 2004; Ruff et al., 2006b). Mechanical loading initiates mechanotransduction within skeletal tissue, which is the process of cells sensing the surrounding mechanical stimuli and relaying that information to other cells to initiate a response (Pearson and Lieberman, 2004). One of these reactions is modeling, which entails bone formation and resorption along the periosteum or endosteum (Gosman et al., 2011). The process of remodeling involves the coordinated and sequenced actions of osteoclasts and osteoblasts along the same surface (Gosman et al., 2011; Pearson and Lieberman, 2004).

The biological pathways that respond to loading operate through feedback loops to lessen strain to an optimum level (Ruff et al., 2006b). As strain increases (e.g., elevated activity), a greater amount of bone is deposited and with inactivity, bone tissue may be resorbed. In order to reduce strain, bone is deposited along the diaphysis in areas where it is subjected to the greatest load, and therefore indicates the direction of higher loads (Davies et al., 2014). For example, walking or running places greater anterior-posterior bending forces on the lower limbs, resulting in distribution of bone material more anteriorly and posteriorly (Davies et al., 2014). The cross-

section from this constant motion may produce a more elongated and elliptical shape (Davies et al., 2014). Depositing bone during modeling strengthens the bone's structure in two ways (Pearson and Lieberman, 2004). Through enlarging the cross-sectional area, compressive forces are distributed over a greater area, thus reducing stress. The increased deposition of bone also elevates resistance to bending and torsion through the placement of bone mass in areas to counteract those forces. Therefore, the further the bone is distributed about the centroid axis, the stronger the structure is and the greater its resistance to bending and torsion (Stock and Shaw, 2007). A skeletal element's bending and torsional rigidity are proportional to cross-sectional properties referred to second moments of area, with reference to a defined plane (Davies et al., 2014; Maggiano et al., 2008; Ruff, 2008).

Cross-sectional geometric properties

Second moments of area, or moments of inertia (denoted by I), are measures of the distribution and distance of bone material from a defined axis, and are a reflection of bending rigidity with reference to a defined plane (Davies et al., 2014; Macdonald et al., 2009; Maggiano et al., 2008; Marchi et al., 2006). Under bending forces, a bone's mechanical behavior is affected by both the area and distribution of bone tissue around a neutral axis (Frankel and Nordin, 2012). Therefore, second moments of area, which account for these two factors, are significant cross-sectional measures. Moments of inertia are the product of small units of the material's area that are multiplied by the squared distances of these areas to a particular axis (Ruff, 2008). They are calculated about an axis parallel with the cross-section and relative to the section's centroid to measure bending rigidity perpendicular to that axis (Davies et al., 2014; Lieberman et al., 2004; Macdonald et al., 2009).

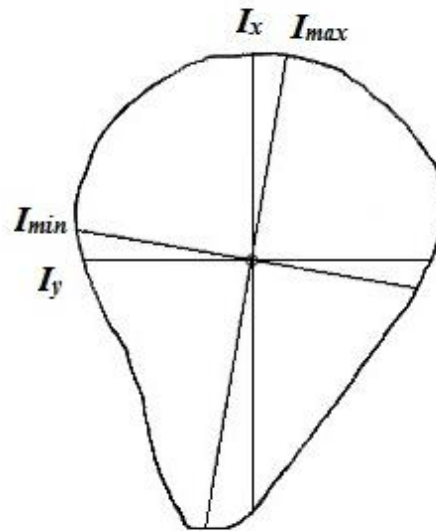


Figure 3.1: Axes commonly used in deriving cross-sectional geometric properties.

For each cross-section of bone, second moments of area can be calculated from as many reference axes that can be made; however, studies taking a biomechanical approach typically focus on four of these axes, as shown in Figure 3.1 (Bice, 2003). Moments of inertia are typically first based on orthogonal axes determined by anatomical planes of a long bone—the antero-posterior (AP) and medio-lateral (ML) axes, which are designated as I_x and I_y , respectively (Davies et al., 2014; Lieberman et al., 2004; Ruff, 2008). These measures represent the distribution of bone material relative to the AP and ML axes of the cross-section (Bice, 2003). For example, a larger ML diameter would result in a greater value of I_y , because there is more bone distributed around the y-axis of the cross-section. The other two commonly employed axes are known as the principal second moments of area, and are notated as I_{max} and I_{min} (Bice, 2003). These two measures reflect maximum and minimum bending rigidity with respect to two empirically determined orthogonal planes, or more simply, two axes where it is hardest and easiest to bend the bone (Bice, 2003; Macdonald et al., 2009). Second moments of area based on

these two sets of planes are proportional to bending rigidities in the antero-posterior and medio-lateral directions, and maximum and minimum resistance to bending (Ruff, 2008). A larger second moment of inertia occurs when there is greater mass of bone further from the centroid axis, and indicates greater strength and rigidity to bending and torsional forces (Frankel and Nordin, 2012; Noldner, 2013).

To infer torsional rigidity of a long bone, a second moment of area is calculated about the cross-section's centroid axis, and is referred to as the polar second moment of area, or J (Macdonald et al., 2009). The polar second moment of area for a cross-section is the sum of any two perpendicular second moments of area (Lieberman et al., 2004). This measure reflects the strength of the bone in torsion (Macdonald et al., 2009), as well as the average bending rigidity of any two perpendicular planes (Ruff, 2008). Therefore, the value of J is often interpreted as a reflection of overall levels of loading and a long bone's strength (Davies et al., 2014; Ruff, 2008). Based on in-vivo research, the polar second moment of area for a bone's cross-section has been posited as the most accurate and biomechanically relevant measure in the absence of experimental data on loading for the bone, and is not as susceptible to positional error (Lieberman et al., 2004).

In addition to these properties of bending and torsional rigidity, the relative distribution of bone within a cross-section is measured by the section's total subperiosteal area (TA), which is the area within the boundaries of a section's outer perimeter (Bice, 2003; Ruff, 2008). The total subperiosteal area estimates compressional strength (Macintosh et al., 2014) and is assessed as an indicator of overall bone robusticity (Noldner, 2013). A larger total subperiosteal area is more effective at resisting deformation from pure axial loads because the distribution of forces over more mass reduces strains and stresses (Bice, 2003).

The shape of a long-bone's cross-section can be quantified and assessed using the ratio of two second moments of area in axes perpendicular to one another, such as I_x/I_y and I_{max}/I_{min} (Davies et al., 2014). These ratios reflect the amount and distribution of cortical bone at a diaphyseal location, and when applied to the lower limb, are often interpreted in terms of mobility (Stock et al., 2011). The I_x/I_y property is the ratio of anteroposterior to mediolateral bending rigidity and describes the relative distribution of bone material in the AP and ML planes of a cross-section (Maggiaro et al., 2008; Macintosh et al., 2014). The ratio between I_{max} and I_{min} is a measure of overall circularity and indicates cortical allocation about the major and minor axes at a diaphyseal location (Maggiaro et al., 2008; Macintosh et al., 2014). The ratio of diaphyseal AP and ML diameters can also be used to analyze cross-sectional shape, and is an effective estimate of the ratio between two second moments of area (Wescott, 2001). Additionally, these ratios can inform researchers on the type of load a bone sustained based on how its shape adapted (Macdonald et al., 2009). For example, the main direction of bending at the tibial midshaft is in the antero-posterior plane, and thus the ideal cross-sectional shape at the midshaft is one in which the greatest moment of area is in line with the AP bending shape.

After calculating these cross-sectional measures, it is important to consider how variation in body size can bias the data and control for those differences among individuals. An individual's body mass creates mechanical loads and is also associated with other effects on loading, such as muscle size (Ruff, 2008). To control for the diversity in body size, the cross-sectional geometric data are standardized using approximations of body size based on bone length and an estimate of body mass (Ruff, 2008; Stock and Shaw, 2007). Other contributing influences on cross-sectional variables are non-mechanical in nature.

Non-mechanical factors

A bone's capability to model and remodel can be impacted by non-mechanical factors such as genetics, nutrition, age, and hormonal fluctuations (Bice, 2003; Carlson and Marchi, 2014). In research on cross-sectional geometry, it is important to consider the role of genetics in morphological propensities and processes regulating diaphyseal structure (Davies et al., 2014). Cowgill (2010) studied the ontogeny of cross-sectional geometry through comparing seven geographically distinct Holocene populations, to investigate the potential influence of genetic differences on inter-population variation. The results from this research illustrated that population differences in postcranial robusticity appear early in development, suggesting that genetic predisposition may factor into the complex combination of influences that affect the expression of cortical bone distribution. However, the powerful response of bone functional adaptation to mechanical stimuli is likely to obscure any underlying genetic distinctions in many situations (Davies et al., 2014). For example, midshaft morphology seems to be independent from growth plate shape, which is under greater genetic constraint (Davies et al., 2014). Genetic components are also involved in cross-sectional shape through affecting the sensitivity of the physiological mechanisms that respond to mechanical loads (Davies et al., 2014; Gosman et al., 2011). These physiological processes facilitating cortical bone growth can additionally be affected by the nutritional status of an individual. In a subadult sample from the medieval Nubian site of Kulubnarti studied by Cowgill (2010), the young individuals exhibited significantly low levels of postcranial strength. These subadults appeared to have also experienced "severe and persistent nutritional stress" with minimal protein in their diets (32). Cowgill concluded that the lower robusticity likely reflected long-term nutritional difficulties, and the concomitant effects of

systemic distress and decreased body mass. The age at which these individuals experienced health issues is a crucial stage for diaphyseal development.

Diaphyseal morphology and the processes that alter cross-sectional properties are influenced by age, both during early growth and throughout adulthood (Davies et al., 2014). Evidence suggests, however, that cortical bone appears to be more sensitive and responsive to mechanical loads prior to sexual maturity, particularly throughout the later stages of growth, compared to after early adulthood (Carlson and Marchi, 2014; Davies et al., 2014; Sparacello et al., 2011; Wescott and Cunningham, 2006). During childhood and adolescence, mechanical loading seems to particularly affect the rates of new bone growth (modeling) and bone turnover (remodeling), making this life stage an essential developmental phase for bone mechanical properties (Jurmain et al., 2012; Meyer et al., 2011; Pearson and Lieberman, 2004). This stimulation of increased subperiosteal expansion is thought to be related to surges in growth and sex hormone levels, indicating that hormonal levels also mediate diaphyseal morphology (Gosman et al., 2011; Jurmain, 1999; Pearson and Lieberman, 2004; Ruff et al., 2006b). In older adults, there is generally less periosteal apposition and more endosteal resorption, particularly in post-menopausal women (Davies et al., 2014; Gosman et al., 2011; Jurmain, 1999). The apposition that does occur in older adults is thought to be more in response to endosteal bone loss and the consequential need to strengthen the structure, rather than predominantly induced by activity (Gosman et al., 2011). Therefore, in studies focused on cross-sectional variation from mechanical loads, samples exclude adults over the age of fifty years with the intent to control for this more age-mediated process (Davies et al., 2014).

Given the influence of age on cross-sectional properties, the cortical bone morphology observed in adult remains is largely the history of loading during adolescence, and cross-

sectional analyses performed with adult samples divulge insights from relatively early adult life (Davies et al., 2014; Pearson and Lieberman, 2004). However, it is often presumed that in most prehistoric societies, adolescents often assume adult tasks at this stage and these activities frequently parallel those carried out during early adulthood (Ruff et al., 2006b; Sparacello et al., 2011). Although remodeling rates are likely slower in adulthood, there are still observable changes in cross-sectional morphology due to activity or non-activity (Ruff et al., 2006b). Adult cross-sectional properties therefore represent the cumulative condition, created from both positive and negative changes in bone mass and structure resulting from mechanical loads experienced through activities over life (Ruff et al., 2006b).

These non-mechanical considerations are more associated with studies that compare populations that are biologically and culturally unrelated, or have substantial economic differences (Wescott and Cunningham, 2006). When a single population that occupied the same geographical region over time is studied, there is more control of biological, cultural, and economic factors. In a sample from one population, the individuals are more likely to share similar genetics and diseases. There is also a greater chance that the individuals had common cultural practices, such as age at which adult activities commenced and social constructs regulating mobility patterns, both residentially and logistically. In staying within a geographic region, the effects of physical terrain and nutritional availability presumably had some overarching response on the individuals within the sample. The accumulation of mechanical inputs, and skeletal responses mediated these non-mechanical factors, are evident in diaphyseal cross-sectional properties.

Obtaining cross-sectional geometric properties

Measures of cross-sectional geometry may be destructive or non-invasive, and are collected at certain locations along the diaphysis. A “true” cross-section of a long bone is acquired by physically cutting at the site of interest; however, this technique causes irrevocable damage to the bone and is inappropriate in most curatorial situations (Davies et al., 2014; Jurmain et al., 2012; Macintosh et al., 2013; Meyer et al., 2011; Stock 2002). Consequently, many researchers utilize methods that do not harm the skeletal elements (Davies et al., 2014; Jurmain et al., 2012; Ruff, 2008). These noninvasive methods have been tested in recent years for their validity and applicability in various research contexts. Computed tomography and biplanar radiography are accepted techniques to measure cross-sectional properties that also account for the medullary cavity (O’Neil and Ruff, 2004; Stock, 2002). However, the logistical concerns, expenses, and need for experienced operators can make these methods invariable for research (Stock and Shaw, 2007). The data derived from biplanar radiography have additionally been shown to overestimate the “true” cross-sectional quantifications and require corrective steps (Jurmain et al., 2012; O’Neil and Ruff, 2004; Ruff, 2008). Further studies demonstrated that the additional use of periosteal molding, in conjunction with biplanar radiography, increased the accuracy and produced data close to the true values (O’Neil and Ruff, 2004; Stock, 2002). Given the success of accounting for the subperiosteal contour, subsequent studies tested the accuracy of methods that measure only the external outline of a cross-section and do not include dimensions of the medullary cavity.

Techniques that provide solid outlines of a cross-section and exclude the endosteal contour have proven valid methods of attaining cross-sectional geometric properties. To determine the accuracy of a solid cross-section, Sparacello and Pearson (2010) compared two

hypothetical samples of human femoral midshaft cross-sections that had the same total subperiosteal area, but different percentages of cortical bone that were at the opposite ends of human population-level variation. Even in this unlikely situation, the population-level differences in percentage cortical area had minimal effect on calculating polar second moments of area, suggesting that the data produced by periosteal contours alone are sufficient to detect trends in bone rigidity within a population. Macintosh et al. (2013) further supported the use of techniques that exclude endosteal contour by testing the ability of solid cross-sections to accurately predict cross-sectional geometric properties of sections along the diaphysis. All cross-sectional geometric measures quantified from periosteal contours alone revealed high correspondence to those from true sections, with the exception of a few locations along the diaphysis that had lower correlation values. The results from this study illustrate that cross-sectional geometric properties generated from periosteal contours provide comparable results to true properties across the long bone's diaphysis, and are also likely to detect patterns in mechanical data within a large sample.

Methods that produce solid images of cross-sections, such as external molding, 3D laser scanning, and external measurements have been shown to generate data that are highly correlated with the true cross-sectional geometric properties (Davies et al., 2014; Jurmain et al, 2012; Wescott, 2001). In a comparison of cross-sectional measures derived from external methods, Stock and Shaw (2007) found periosteal molding to produce measures highly correlated with true values, and was associated with low prediction errors. Similar results were found in a test of 3D laser scanning by Davies et al. (2012), who found that automated analysis of diaphysis 3D scans resulted in accurate cross-sectional data. Although not as accurate as these methods, external measurements of the diaphysis have been shown to be adequately correlated with true

cross-sectional data. Strong relationships between external diameters alone and true cross-sectional geometric properties for polar second moments of area have been observed (Pearson, 2000), as well as high correlations between ratios of diaphyseal diameters (e.g., AP/ML diameters) and I_x/I_y and I_{max}/I_{min} ratios (Stock and Shaw, 2007; Wescott, 2001). The relative accuracy of external dimensions for predicting overall mechanical levels and shape agrees with the importance of accounting for periosteal contours (Stock and Shaw, 2007).

Applications of cross-sectional geometry

Human athlete studies

Studies on athlete participants provide opportunities to directly investigate how physical activity affects cross-sectional geometry of long bones, and how specific loading regimes alter diaphyseal shape. The conclusions from this research on human athletes have shown clear evidence supporting bone functional adaptation and the (re)modeling responses to mechanical loads in the lower limbs (Ruff et al., 2006b). Several recent studies on cross-sectional geometry of the tibia in humans demonstrated how increased physical activity strengthens bone and can affect diaphyseal shape with different loading directions. To examine the effects of diverse loading histories on tibial rigidity, a study by Shaw and Stock (2009) compared cross-sectional properties of tibiae belonging to male university cross-country runners, field hockey players, and control subjects (Figure 3.2). Both runners and field hockey players exhibited significantly higher cross-sectional measures of tibial rigidity than the control individuals, implying the initiation of skeletal responses to strengthen the diaphysis from amplified activity. This study also investigated how differences in directionality of repetitive forces affect tibial shape of the participants in terms of the variation in loading orientation associated with their respective

sports. The runners and hockey players had significantly different tibial shape, demonstrated by maximum and minimum second moments of area. The tibiae of the runners displayed a prominent maximum plane of rigidity, indicative of the primarily unidirectional motion of runners. The hockey players' tibial shape showed more symmetrical hypertrophy, which corresponded with the multidirectional movements in their sport.

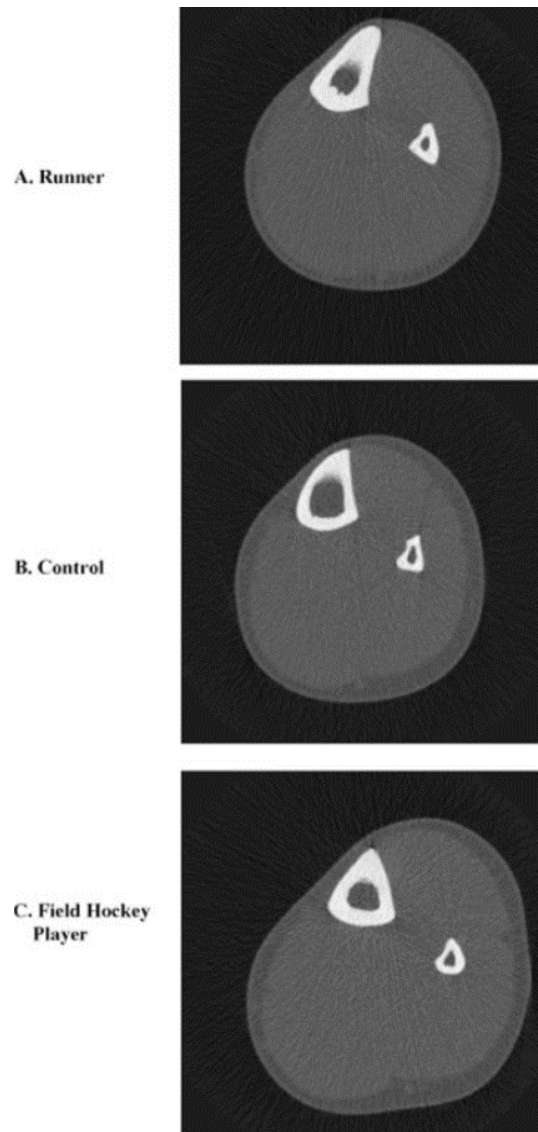


Figure 3.2: Lower leg mid-shaft cross sections from pQCT scans by Shaw and Stock (2009).

In another study, researchers found a significant increase in anteroposterior bending rigidity of the tibiae at midshaft in young boys, who were involved in a physical activity intervention program compared to those who were randomly assigned as controls (Macdonald et al., 2009). After the course of sixteen months, the boys in the intervention group presented a significant gain in maximum second moments of area compared to the boys in the control group, indicating that increased bone deposition in the tibia was induced by greater anterior-posterior bending loads enacted through the program (Macdonald et al., 2009). Similar results were also observed in a study by Nikander and colleagues (2006), who compared tibial cross-sectional properties between adult women involved in a variety of sports. Compared to individuals who were not as athletic, these female athletes exhibited significantly greater total cross-sectional area of the tibia, representing a stronger structure for weight-bearing (Nikander et al., 2006). There was additional evidence of amplified bone mass deposition where the individuals' tibiae experienced the greatest forces depending on the different loading orientations of their respective sports category. This result indicated the diaphysis adapting to optimal rigidity against torsion and bending in the structure during vigorous motion (Nikander et al., 2006).

These human athlete studies support the principles of bone functional adaptation, in that increased physical activity initiated bone depositional responses where needed. However, there are aspects of these studies to consider further, particularly with respect to the intensity of physical activity and the age of the participants. Although loading intensity is likely a primary influence on cross-sectional properties, the frequency and repetitiveness of the activity also plays a major role in bone modeling and remodeling (Davies et al., 2014; Shaw and Stock, 2009). When applied to investigations of past population mobility, these studies support the premise that increased lower limb robusticity is associated with higher levels of mobility (Shaw and Stock,

2009). Therefore, more mobile individuals likely exhibit greater lower limb long bone robusticity than those who are more sedentary. These studies also corroborate the concept that variation in diaphyseal shape corresponds with different activity patterns, in that primary directions of movement in habitual locomotion can influence cross-sectional shape (Shaw and Stock, 2009). The conclusions from these studies support generating practical interpretations of cross-sectional properties of past populations.

Bioarchaeological studies

Agricultural subsistence

Bioarchaeological studies employing a biomechanical approach have explored lower limb diaphyseal robusticity in past populations that experienced changes in agricultural subsistence strategies to better understand such cultural shifts. Ruff et al. (2015) investigated temporal trends in lower limb strength within a large sample comprised of various populations originating across Europe and spanning from the Upper Paleolithic to the 20th century. The results from this study indicate a significant decrease in antero-posterior bending strength of the femur and tibia in samples spanning the Neolithic to the Iron/Roman period. This gradual reduction in lower limb robusticity is interpreted as a decrease in mobility occurring at the onset of agricultural practices, and steadily continuing as food production and sedentism escalated. In the samples dating to the past 2,000 years however, researchers observed no significant change in relative limb strength, suggesting that the comparatively lower mobility resulted from increased sedentism associated with food production rather than subsequent industrialization. These results are carried further with a similar study conducted by Macintosh et al. (2014), who investigated diachronic changes in lower limb cross-sectional geometry over a 6,000-year period of agricultural development in Central Europe. In comparing femoral and tibial cross-sectional

properties of remains dating to the beginnings of agriculture in the region to the Early Medieval period, Macintosh and colleagues found a chronological reduction in lower limb strength, as well as increasingly more circular cross-sections. They attributed these results to decreasing mobility concomitant with the cultural changes in that region over time. In addition to research questions regarding subsistence strategies, studies have investigated patterns of cross-sectional properties related to demographic characteristics.

Patterns regarding sex and socioeconomic status

Trends of cross-sectional geometric properties among individuals within a sample are interpreted as possible indications of distribution of labor and differences in mobility. One commonly employed comparison is that of cross-sectional properties between male and female long bones to infer gendered patterns of mobility level. In an analysis of lower limb rigidity in a Garamatian sample from the Sahara, Nikita et al. (2011) found significantly higher total subperiosteal area values in male remains than females. This sign of greater lower limb strength in males was interpreted as elevated levels of mobility associated with roles of herding. Within a Neolithic sample from Italy, male femoral strength exceeded female femoral strength, perhaps as a result of the combination between higher mobility and uneven mountainous terrain traversed during highly pastoralist activities by males (Marchi et al., 2006; Marchi, 2008). Differences in femoral and tibial diaphyseal shape between males and females in this sample also suggest behavioral differences between the sexes related to activity. In a diachronic comparison of Neolithic and Medieval samples from Liguria, Italy, male femoral robusticity was elevated in the Medieval sample, demonstrating greater sexual dimorphism than the Neolithic sample (Sparacello and Marchi, 2008). Therefore, there may have been more divided gender roles in the later culture which exploited coastal resources compared to the earlier population, which likely

relied on pastoralism. Greater lower limb indicators of mobility in males were also observed in an Iron Age Samnite sample from the Alfedena necropolis in Italy (Sparacello et al., 2011). The female remains in this sample exhibited significantly lower average tibial robusticity and shape index, indicating that females may have carried out more sedentary tasks compared with most males in this society. A similar conclusion was drawn in a comparison of Mid-Holocene hunter-gatherer populations at Cis-Baikal in modern-day Siberia, in which increased sexual dimorphism over time was observed by a significant decline in tibial rigidity in females (Stock and Macintosh, 2015). This decline in tibial strength was interpreted as a shift in sexual division of labor, with females becoming less mobile.

Female mobility seemed to increase in a sample of an American Great Plains Indian tribe during an intensification of horticulture (Wescott and Cunningham, 2006). In an analysis of temporal change in long bone cross-sectional properties from three archaeological groups of the Arikara, there were significant modifications in femoral cross-sectional properties in the female remains. Wescott and Cunningham interpreted this trend as potentially reflecting increased labor roles for females to produce surplus crops. Although subsistence patterns involving high levels of mobility are often associated to greater sexual dimorphism in lower limb strength (Carlson et al., 2007; Marchi, 2008), this is not always the case. Carlson et al. (2007) compared male and female lower limb cross-sectional properties in a sample of Australian hunter-gatherers, and found relatively equivalent measures, which was supported by ethnographic evidence suggesting equally high mobility in males and females. This study demonstrated that there are no established mechanical profiles for a given subsistence strategy category.

In addition to similarities or differences relating to the sex of the individuals, patterns may appear potentially based on some form of socioeconomic status. In a biomechanical analysis

of long bones from the Mayan site of Xcambó, Maggiano et al. (2008) found that as the population experienced economic growth, overall long bone robusticity decreased. The proposed improvement in living standards may have heightened the inhabitants' statuses, while lowering their workloads—a pattern evident from other studies finding a negative relationship between physical activity and high status (Maggiano et al., 2008). The researchers point out another potential scenario involving a migration of lower status workers and the city thereafter inhabiting primarily higher status individuals. Sexual dimorphism in cross-sectional geometric properties also decreased over this time. However, long bone strength in females did not lower as much as robusticity in males, perhaps because their socioeconomic status as physical laborers was not as affected by the changes brought on by the economic growth (Maggiano et al., 2008).

In a sample from Colonial Period Tipu, comparisons in lower limb cross-sectional geometry between apparent elite and non-elite males and females revealed a trend that suggested distribution of labor based on social status, and therefore not determined strictly by gender (Noldner, 2013). While both male non-elites and elites displayed similar lower limb strength, the non-elite females displayed greater tibial robusticity compared to elite females. Additionally, a collection of remains separated from the rest of the sample by burial location exhibited more gracile lower limbs, further suggesting a group of individuals within this society's organization that may not have participated in the same amount or type of physical activity compared to the likely full-time agriculturalists comprising most the sample. Following Spanish colonization at Tipu, male and female remains showed similar cross-sectional shape and may have shared comparable habitual loads. These studies demonstrate how exploring lower limb diaphyseal robusticity may contribute to interpretations of social structure regarding distribution of labor and mobility.

CHAPTER 4: MATERIALS AND METHODS

To investigate lower limb robusticity in the Mis Island collection, adult femora and tibiae were sampled. Three diaphyseal locations were selected to sample from each individual for acquiring cross-sections—the subtrochanteric region of the femur, the midshaft of the femur, and the midshaft of the tibia. The cross-sections for these three diaphyseal sites were obtained through a non-invasive technique that generated subperiosteal outlines of the cross-sections, and thus excluded the endosteal contours of the diaphyseal sections. This method involved a putty material molded around the diaphyseal locations and hardened to create casts of the cross-sections at these sites. After documenting the subperiosteal outlines from these casts, cross-sectional geometric data were calculated from these outlines with a software application. Finally, comparisons were conducted between groups of individuals for the cross-sectional variables for each diaphyseal location.

Materials

The Mis Island skeletal collection

Mis Island, located along the Fourth Cataract of the Nile River, was a primary focus during a salvage archaeology effort that resulted in invaluable osteological and material recoveries. The Sudan Archaeological Research Society (SARS) initiated this large project on Mis Island and other locations along the Nile River in response to the planned construction of the Merowe Dam (Welsby, 2006). Mis Island was first surveyed in 1999 under the direction of Dr. Derek Welsby and fifteen archaeological sites were identified on the island, six of which were chosen for further excavation (Ginns, 2006). Much of the subsequent work focused on the medieval period and the following sites were excavated during the 2005 – 2007 seasons: a Late Christian church, medieval Christian cemeteries, a medieval settlement, an isolated

tumulus, and a cemetery from the Kerma period (Ginns, 2006; 2007). Two of these medieval Nubian cemeteries are the focus of this thesis research. Remains from Muslim burials were not excavated to comply with religious observations and therefore, the individuals in this study are from the Christian burials (Soler, 2012).

The skeletal remains studied in this research were excavated from medieval Christian burials at cemetery 3-J-10 and cemetery 3-J-11. Cemetery 3-J-10 was situated near the Christian church site in an area of alluvial deposits and was surrounded by rock outcrops (Ginns, 2010a; 2006). This cemetery was in use between approximately AD 1100 and AD 1400 which includes the time period of Nubia converting to Islam (Ginns, 2006; Vollner, 2016). An estimated 262 box-grave monuments were believed to be present at this site and by the end of the excavations, a total of 126 individuals were recovered (Ginns, 2010a). Cemetery 3-J-11 was located near the northern edge of the island in a terrain of alluvial formation and pebble deposits from the river, which was about 150 meters away (Ginns 2010b). Representing the largest burial site on Mis Island, this cemetery spanned AD 300 – AD 1400 (Soler, 2012; Vollner, 2016). A total of 288 sets of remains were excavated from cemetery 3-J-11 which was about half of the individuals likely interred at this site (Ginns, 2010b). The stone box-type monuments varied in size and style between graves and based on the variations in burial practices, this cemetery contained multiple phases (Ginns 2010b; 2007). The remains from cemeteries 3-J-10 and 3-J-11 comprise the Mis Island Nubian Bioarchaeological Collection that is currently on loan from the British Museum and housed at Michigan State University under the curation of Dr. Todd Fenton.

Generating the research sample

This study concentrated on adult remains and the accumulated effect of loading regimes experienced over their life courses. In older adults, endosteal resorption increases, particularly in

older females (Davies et al., 2014; Gosman et al., 2011). Because this study did not assess the endosteal contour of cross-sections, adults over fifty years at time of death were excluded from the sample to control for this age-related process. Individuals younger than approximately twenty years were also omitted, as their sex could not be reliably estimated. The sex and age of these individuals had been previously evaluated by Soler (2012), whose database with this information was utilized in this project to identify which individuals to sample and to group individuals into sex cohorts for analyses. To increase sub-sample sizes, probable males were grouped into the male series and probable females into the female group.

Based on literature suggesting the lower limb does not demonstrate significant lateralization, only the right side was sampled in this project when available (Sparacello et al., 2011). If the right femur or tibia was missing or incomplete, the left side was sampled instead. These long bones were included in the sample if they exhibited acceptable preservation to allow for the putty to adhere to the surface without damaging the bone. Femora and tibiae were also sampled if the majority of the bone was available and the appropriate features were present to locate sections. The number of sampled femora and tibiae varied between both the diaphyseal sections and each cross-sectional property. This change in sub-sample sizes was due to the differential states of preservation among the bones and along their diaphyses, as well as whether measurements could be taken that were necessary to calculate two of the cross-sectional properties. Tables 4.1 and 4.2 show the number of individuals included in the sex and cemetery sub-samples for each of the diaphyseal locations and cross-sectional variables. Although not shown, the number of individuals included in the analyses for the AP/ML ratio of the midshaft femur are the same as those for the I_{max}/I_{min} ratio.

Table 4.1: Number of total individuals, separated by sex, for each cross-sectional variable at the three diaphyseal locations. F50: femur midshaft, F80: subtrochanteric region of femur, T50: tibia midshaft.

	I_{max}/I_{min}			J			TA		
	Total	Males	Females	Total	Males	Females	Total	Males	Females
F50 n	79	41	38	51	27	24	65	32	33
F80 n	73	38	35	53	27	26	64	31	33
T50 n	74	42	32	48	27	21	54	30	24

Table 4.2: Number of males and females, separated by cemetery, for each cross-sectional variable at the three diaphyseal locations. F50: femur midshaft, F80: subtrochanteric region of femur, T50: tibia midshaft.

		I_{max}/I_{min}		J		TA	
		Males	Females	Males	Females	Males	Females
3-J-10	F50 n	23	13	16	5	19	9
	F80 n	20	11	16	6	18	9
	T50 n	23	10	16	5	17	7
3-J-11	F50 n	18	25	11	19	13	24
	F80 n	18	24	11	20	13	24
	T50 n	19	22	11	16	13	17

Methods

Obtaining cross-sections

Each femur and tibia was oriented according to the specifications outlined by Ruff and Hayes (1983). The bones were set up on an osteometric board and adjusted with plasticine clay to meet the following planes' dimensions. The femur was placed on an osteometric board perpendicular to its arms. Its proximal end was raised with clay until the points just distal to the lesser trochanter and just proximal to the femoral condyles were in the same plane and equidistant from the board's surface (Figure 4.1). For the tibia, a small piece of clay was placed

under the lateral condyle on the posterior surface until the anterior-most points of the articular surfaces were aligned (Figure 4.2). The tibia's proximal end was positioned against the stationary arm of the osteometric board and the distal end was adjusted so that the diaphysis was perpendicular to the board's stationary arm. After this orientation, the tibia's distal end was raised with clay until the following two points were in the same plane: the centerpoint of the talar surface and the centerpoints of the tibial plateau articular surfaces.

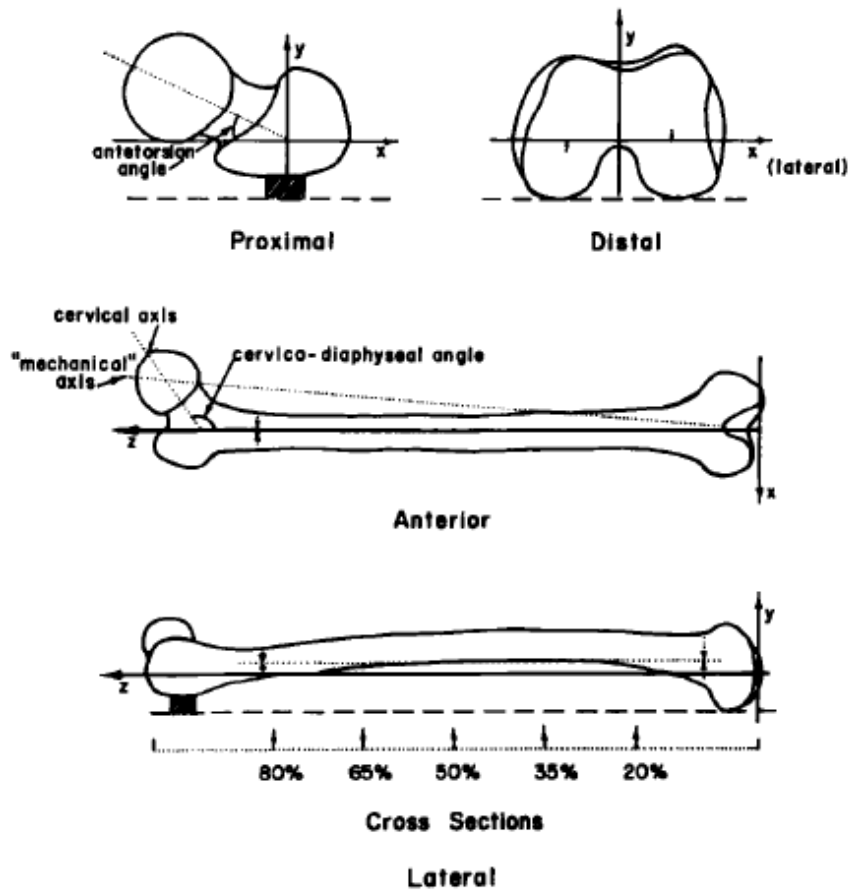


Figure 4.1: Proper orientation and reference planes of the femur (from Ruff and Hayes, 1983).

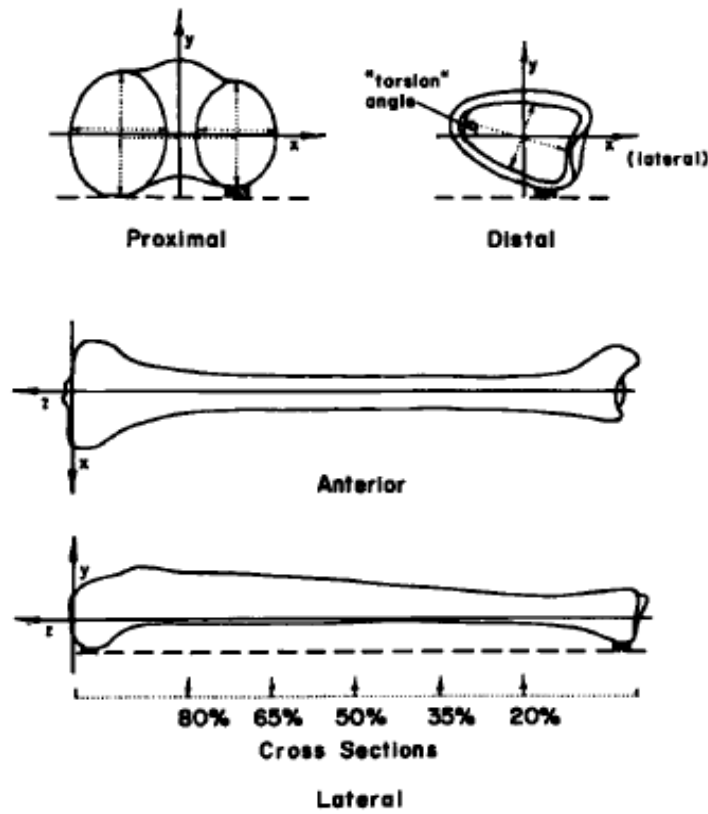


Figure 4.2: *Proper orientation and reference planes for the tibia (from Ruff and Hayes, 1983).*

After appropriately orienting the femora and tibiae, the diaphyseal sections were located based on biomechanical length. The biomechanical length of the femur was calculated as the average distance between the femoral condyles and the most-inferior point of the femoral neck (White et al., 2012) and measured with an Alvin® graduated beam compass. For the tibia, the biomechanical length was the average distance between the center of the talar articular surface and the centerpoints of the medial and lateral condyles (White et al., 2012), as measured with an osteometric board and triangular ruler. The section locations were calculated based on these lengths and found on the diaphyses with an osteometric board after they were properly oriented. In lower-limb CSG bioarchaeological studies, diaphyseal sections typically focus on midshaft regions of the femur and tibia, and may include the femoral subtrochanteric area. Therefore, the

cross-sections were collected at the midshaft of both the femur and tibia, calculated as 50% of the biomechanical length, and the subtrochanteric region of the femur, which was 80% of biomechanical length.

Each femur was situated with the distal-most part of the medial condyle against the stationary arm and the diaphysis both perpendicular to the stationary arm and parallel to the board's surface. The tibiae were placed with the proximal end touching the stationary arm and the diaphyses positioned as the femora were. As each bone was properly oriented on an osteometric board, the section sites were located using a straight ruler to find the exact section locations. In addition to the measurements taken to locate diaphyseal locations, several other measurements were made. The anteroposterior (AP) and mediolateral (ML) diameters at midshaft of the femora were measured with sliding calipers. These measurements were utilized in cross-sectional shape analyses. To arrive at the necessary estimated body size standardization factors, vertical femoral head diameter was found with sliding calipers and the maximum lengths of the femora and tibiae were measured with an osteometric board (White et al., 2012). Measurements that were recorded by the author and those taken by the much-appreciated help of Christiana Hench were averaged for the final measurement.

When a long bone was incomplete or fragmented, certain diaphyseal sections were approximated based on diaphyseal features and morphology, as described by Trinkaus and Ruff (2012). After orienting an incomplete femoral diaphyses with plasticine clay, 50% was located where the shaft was narrowest and the linea aspera was at its maximum extent, and 80% was found where the gluteal buttress ended and the linea aspera began. Midshaft of the tibia was where the soleal line met the posteromedial corner of the diaphysis. These techniques of

approximating diaphyseal sections were employed only when the necessary features were present and there was a sufficient amount of the bone present to visually assess these locations.

To obtain the cross-sectional outlines, an external mold was used that created a cast of the section's periosteal contour. Previous studies have validated this method of excluding the medullary cavity, and found that cross-sectional properties calculated solely on the outer boundaries are highly correlated with measures that account for the endosteal contour (Macintosh et al., 2013; Sparacello and Pearson, 2010; Stock and Shaw, 2007). At each of the section locations, a vinyl putty called Coltene Coltoflax® (produced by Whaledent) was shaped around the diaphysis at each section and hardened into a cast (Figures 4.3 and 4.4). Following placement of the molds at the sites, a triangle ruler and straight ruler were moved along the osteometric board to mark on the casts where the exact sections were located. The anatomical positions (i.e., anterior, medial, posterior, lateral) were also marked on the casts prior to removing them from the bones. The molds were detached with an X-acto® knife and wooden rod, and then trimmed with the knife at the marked section. The inner borders of the casts were traced onto computer paper with the superior side facing up and anatomical directions marked on the paper, as well as identifying information.



Figure 4.3: *Femur with molds at midshaft and the subtrochanteric region.*



Figure 4.4: *Tibia with cast at midshaft.*

Calculating cross-sectional geometric properties

The cross-sectional properties were calculated from the traced outlines with an image analysis computer program. After the tracings were scanned and saved as TIFF files, the images were altered using the image modification software GIMP[®] to create a solid outline. Each solid outline was then processed using the open-access program BoneJ[©] (Doube et al., 2010), which is a plugin for the software package ImageJ[©] (Schneider et al., 2012). In utilizing the “slice geometry” application within BoneJ[©], the cross-sectional properties were calculated from the image. This application provided a spreadsheet with data on the cross-section, as well as the principal axes drawn on the processed solid outline (Figure 4.5). These axes represent the minimum and maximum axes of bending rigidity (i.e., where it is hardest and easiest to bend the bone) about which the cross-sectional geometric properties analyzed in this project were calculated.

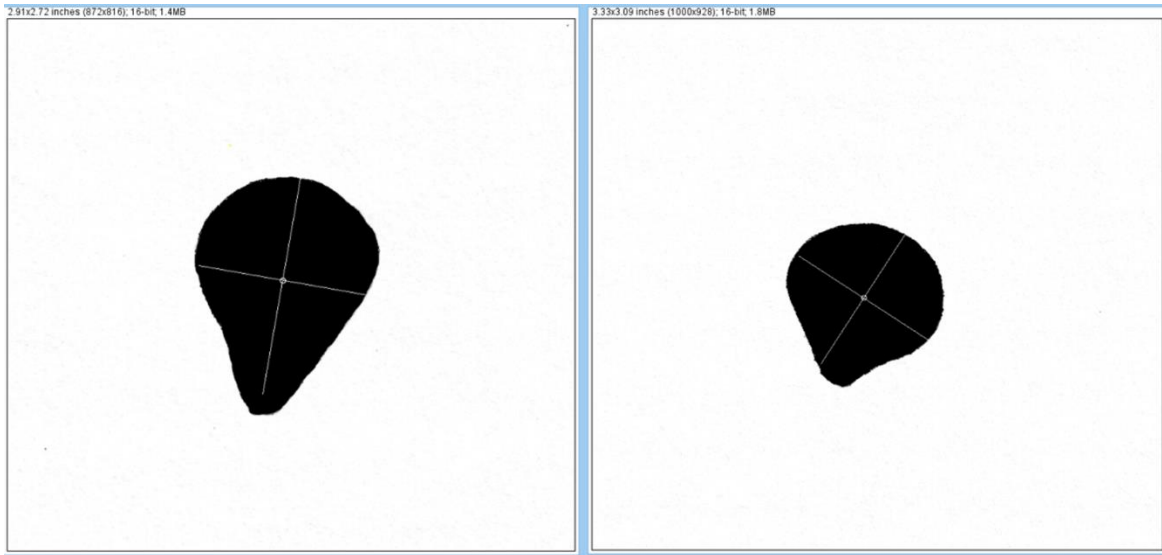


Figure 4.5: Two solid outlines processed in BoneJ with principal axes.

Cross-sectional geometric variables

Table 4.3: Cross-sectional geometric variables with descriptions.

CSG Variable	Formula	Description
Shape ratio: I_{max}/I_{min}	I_{max}/I_{min}	<ul style="list-style-type: none"> • Distribution of bone about major and minor axes of cross-section • Describes extent of cross-section's circularity
Polar second moment of area: J (mm ⁴)	$I_{max} + I_{min}$	<ul style="list-style-type: none"> • Strength of bone in torsion • Twice average bending and torsional rigidity • Measure of overall bone strength
Total subperiosteal area: TA (mm ²)	—	<ul style="list-style-type: none"> • Measure of compressional strength • High correlation with cortical area

Three cross-sectional geometric properties were calculated and analyzed in this project (Table 4.3)—a shape ratio between I_{max} and I_{min} (I_{max}/I_{min}), the polar second moment of area (J), and the total subperiosteal area (TA). When two second moments of area perpendicular to one another are represented as a ratio (e.g., I_{max} and I_{min}), the resulting value is a quantification of the cross-section's degree of circularity or non-circularity and is a representation of the distribution of cortical bone within the section with respect to the section centroid (Davies et al., 2014; Shaw and Stock, 2009). This cross-sectional property is based on the process of bone being deposited

in the diaphysis to comply with higher loads, and therefore indicates the direction of the greatest load the bone experiences (Davies et al., 2014). For example, the lower limbs of individuals who walk or run frequently are subjected to higher anteroposterior strains which contribute to a more anteroposteriorly elongated cross-sectional shape (Davies et al., 2014). In this project, the cross-sectional shape variable was derived from the ratio of the maximum second moment of area (I_{max}) and the minimum second moment of area (I_{min}), which reflect the maximum and minimum bending rigidity of the bone at the section's location, respectively. I_{max} and I_{min} are values that indicate the distribution and amount of bone relative to the principal axes, which are the empirically determined axes in Figure 4.5.

In this study, the shape variable was calculated using I_{max} and I_{min} rather than I_x and I_y , because these measures are less sensitive to error from orienting the bone while recording the cross-sections (Shaw and Stock, 2009). Although the anatomical axes were recorded on the casts in this study, their exact positioning was estimated and thus could not be taken as true axes with confidence. The ratio of I_{max} and I_{min} was also selected over I_x/I_y because these two principle moments of area are “determined by intrinsic distribution of mass in the cross-section rather than any superimposed set of perpendicular neutral planes” (Shaw and Stock, 2009:152). However, unlike I_x/I_y , the ratio between I_{max} and I_{min} does not express the orientation of the maximum and minimum bending rigidity of a cross-section—or in what direction a cross-section may be more elongated (Nikita et al., 2011). Given the common shape of the tibia, the I_{max} of the cross-sections are presumably situated more towards the anteroposterior axis rather than the mediolateral axis (Shaw and Stock, 2009). Therefore, this disadvantage of utilizing I_{max}/I_{min} does not affect the interpretation of this variable for the tibia. I_{max}/I_{min} is also appropriate for the subtrochanteric region, because its orientation is problematic in interpreting I_x/I_y (Ruff and

Larsen, 1990). For the midshaft of the femur, I_{max}/I_{min} expresses the relative distribution of bone about the major and minor axes of a cross-section, but the extent of an assumed AP elongation is not definitive. Therefore, the ratio between AP and ML femoral midshaft diameters was added to the analyses to achieve a better sense and quantification of diaphyseal shape.

The subperiosteal area (TA) and polar second moment of area (J) are indicators of a bone's rigidity with respect to different forces. The polar second moment of area, signified by J , is proportional to torsional rigidity and represents (twice) average bending rigidity (Davies et al., 2014; Ruff, 2008). This value is used as a measure of general rigidity and strength of a bone and represents overall levels of loading (Davies et al., 2014; Ruff, 2008). J is the sum of any two perpendicular second moments of area, and in this project, was calculated as the sum of I_{max} and I_{min} . The total subperiosteal area of a cross-section, or TA , is the area within the boundaries of the section's outer surface (Ruff, 2008). Total subperiosteal area is proportional to axial rigidity and resistance to compression (Davies et al., 2014). Greater values of TA indicate higher loads experienced by living bones (Davies et al., 2014). Before calculating J , I_{max} and I_{min} were standardized by estimated body size and TA was standardized by estimated body mass.

Size standardizing

Because an individual's body mass influences the mechanical loads experienced by the lower limbs, it is critical to control for variation in body size through standardizing cross-sectional geometric properties with appropriate estimates of body measures (Pomeroy, 2013). This study standardized cross-sectional properties by the factors that are considered the most influential, in that TA is primarily affected by body mass and J is proportional to a factor involving both body mass and beam length (Pomeroy, 2013). Therefore, both cross-sectional measures were adjusted by the accepted and appropriate estimates of body size (Macintosh et al.,

2014; Pomeroy, 2013): $TA/estimated\ body\ mass, J/(estimated\ body\ mass*(maximum\ bone\ length^2))$. Individual estimated body mass was calculated using the equations recommended by Ruff et al. (1997) and Auerbach and Ruff (2004) shown in Table 4.4 which require the individual's femoral head diameter in millimeters. The final values for estimated body mass were calculated as the mean of equations #1 and #2, and the appropriate sex-specific equation. Because the values of I_{max}/I_{min} and AP/ML represent a ratio, these properties did not require final standardization.

Table 4.4: *Body mass estimation formulae derived from Ruff et al. (1997)*. BM is body mass (kg) and FH is femoral head diameter(mm).

Male equation	$BM = (2.741*FH - 54.9)(0.9)$
Female equation	$BM = (2.426*FH - 35.1)(0.9)$
Equation #1	$BM = 2.239*FH - 39.9$
Equation #2	$BM = 2.268*FH - 36.5$

Statistical analyses

The statistical analyses in this project primarily involved independent t-tests for testing the hypotheses between sub-groups, as well as *k*-means cluster analysis to investigate the distribution of the cross-sectional properties and any emerging patterns inherent in the data. These analyses were performed with the statistical software Stata 14SE and RStudio 1.0.136.

Independent-samples t-tests

Independent-samples t-tests were selected to test hypotheses because the population parameters are unknown. Before performing the t-tests, two additional tests were conducted to determine whether the data met the assumptions of the test. The test of equality of standard

deviation was used to determine equality of variances. The Shapiro-Wilk test was used to test for normality. If the data did not meet these tests, the sub-group comparisons were further explored with exclusion of outliers, unequal variances t-tests, and Wilcoxon Rank Sum tests. Independent t-tests were carried out in Stata 14SE between cemetery and sex sub-groups as appropriate for this study's research questions.

The first research question is designed as a comparison between the two cemeteries that comprise the Mis Island collection. For this inter-cemetery comparison, the three cross-sectional properties (i.e., I_{max}/I_{min} , J , and TA) were included for each of the three locations on the diaphyses. The comparisons were carried out using independent t-tests between individuals from 3-J-10 and 3-J-11 to test whether there were significant differences in cross-sectional properties between the two cemeteries. However, these comparisons were separated by sex. The reason behind comparing males with males, and females with females, of the two cemeteries was to account for any significant differences in cross-sectional properties between the sexes. As demonstrated in the results section, there was no significant difference found between the cemetery groups and therefore, males and females from each cemetery were able to be combined into the two larger male and female groups for the second research question.

The second research question is an intra-site examination of potential trends of mechanical loading among individuals from Mis Island. Trends of cross-sectional geometric properties between individuals within a sample are interpreted as possible indications of distribution of labor and mobility. The cross-sectional data were compared between males and females through independent t-tests for each cross-sectional variable derived from the three diaphyseal sites to explore the possible variation between the groups.

Cluster analysis

Cluster analysis was utilized in this study to further explore and visualize the structure of the data through data mining. This approach is effective for determining whether a sample can be separated into sub-groups that are different from one another based on certain characteristics (Kachigan, 1982). The goal of this technique is to create clusters of objects that are more similar to each other based on the features of interest than objects in other clusters, so that there is less variation within clusters and large variation between (Kachigan, 1982; Zadora et al., 2014). The general process of cluster analysis first involves quantifying the amount of similarity, as distances, between each pair of objects that comprise the data set (Kachigan, 1982). In this project, measures of similarity between objects were found using the Euclidean distance, which is “a geometrical measure of distance between points in p -dimensional space” (Zadora et al., 2014:87). Following this step, an algorithm is used to group the objects into clusters of sub-groups based on the measures of similarity between the individual observations (Kachigan, 1982). The algorithm employed in this study was the k -means clustering method, which was performed in RStudio 1.0.136. K -means cluster analysis groups data into a specified number of clusters so that the sum of squares between the points in a cluster and the cluster’s assigned center are minimized (Han et al., 2011; R Documentation). A key component in cluster analyses is deciding the appropriate number of clusters to separate the sample into so that the goals of this approach are met. This is achieved by separating the data into different number of clusters and assessing the outcome (Kachigan, 1982).

Using the results of the cluster analysis, inherent patterns of the cross-sectional data were investigated without preconceived notions about gendered division of mobility or variation between cemeteries. K -means cluster analyses for each cross-sectional property of the three

diaphyseal locations assisted in evaluating the extent to which intrinsic clusters in the data were based on sex and cemetery. By visually inspecting the clusters in the data and their distribution, a better sense of the patterns between and within sub-groups (i.e., sex and cemetery) was achieved. This process began with two clusters and proceeded to three and four, after which the most effective number of logical clusters was determined. The results of these analyses are presented under the second research question after finding that there were no significant differences between cemetery sub-samples, therefore indicating that the clusters were unlikely to represent cemetery groupings.

Intra- and inter-observer error

Intra- and inter-observer error were assessed through the technical error of measurement (TEM) and intraclass correlation coefficient (ICC) methods. The intra-observer analysis involved the author resampling thirty femora, which were remeasured and casted at midshaft a second time to recalculate cross-sectional properties. The inter-observer error evaluation focused on the long bone dimension measurements taken by the author and Ms. Hench. The technical error of measurement was calculated with Microsoft Excel and the intraclass correlation coefficient was found in RStudio 1.0.136.

Technical error of measurement is a common technique of communicating the error margin in anthropometric data (Pernini et al., 2005). TEM is an index of standard deviation between measurements repeated by both a single observer and multiple evaluators (Pernini et al., 2005). This index expresses imprecision and reflects measurement quality control (Pernini et al., 2005; Ulijaszek and Kerr, 1999). Technical error of measurement is expressed as absolute TEM (TEM) and relative TEM (%TEM). Absolute TEM reflects the disagreements among measurements in the units that they were originally taken (e.g., mm) (Byrnes et al., 2017).

Relative TEM is error as it relates to the mean value of the variable and is expressed as a percentage which allows direct comparison of various measures with different units (Perini et al., 2005; Ulijaszek and Kerr, 1999).

Intraclass correlation coefficients are often utilized in measuring intra- and inter-observer correlation to assess reliability of numerical data produced by different observers (Johnson and Koch, 2011). An ICC is a measure of how similar units in the same group are in their values for a continuous variable (Elliot et al., 2016). In this study, two types of ICC were calculated, both of which used a two-way model. One of these types is the consistency ICC, which evaluates the reliability within each observer's set of values (McGraw and Wong, 1996). The other test is the agreement ICC, which reflects the consensus of measurements between observers or separate series of observations (Byrnes et al., 2017; McGraw and Wong, 1996).

CHAPTER 5: RESULTS

Research Question 1

Research Question 1—Inter-cemetery: Is there a difference in cross-sectional geometric properties between cemeteries 3-J-10 and 3-J-11?

H₀: There will not be a difference in cross-sectional properties between cemeteries 3-J-10 and 3-J-11.

H₁: There will be a difference in cross-sectional properties between cemeteries 3-J-10 and 3-J-11.

As exhibited in Table 5.1, all comparisons of cross-sectional variables between cemeteries 3-J-10 and 3-J-11 were not significant. Therefore, the null hypothesis fails to be rejected. Although there were no significant differences in the cross-sectional variables between cemeteries, further exploration of the data suggests the presence of trends between both cemeteries.

Table 5.1: *P-values from t-tests between males from 3-J-10 and males from 3-J-11, and females from 3-J-10 and females from 3-J-11 for each cross-sectional property at the three diaphyseal locations. (ns = not significant at $p < 0.05$).*

		I_{max}/I_{min}	J	TA
M 3-J-10 vs. M 3-J-11	Midshaft femur	ns	ns	ns
	Subtrochanteric femur	ns	ns	ns
	Midshaft tibia	ns	ns	ns
F 3-J-10 vs. F 3-J-11	Midshaft femur	ns	ns	ns
	Subtrochanteric femur	ns	ns	ns
	Midshaft tibia	ns	ns	ns

Midshaft femur

Table 5.2: Summary statistics for cross-sectional geometric properties at midshaft femur, separated by cemetery and sex. ($J = \text{mm}^4$, $TA = \text{mm}^2$)

		I_{max}/I_{min}		J		TA	
		M	F	M	F	M	F
3-J-10	n	23	13	16	5	19	9
	Mean \pm SD	1.52 (± 0.24)	1.39 (± 0.22)	374.35 (± 57.84)	297.49 (± 29.71)	8.84 (± 0.79)	8.28 (± 0.68)
3-J-11	n	18	25	11	19	13	24
	Mean \pm SD	1.51 (± 0.21)	1.41 (± 0.27)	356.66 (± 55.04)	284.45 (± 46.79)	8.61 (± 0.78)	7.84 (± 0.69)

There were no significant differences between males from 3-J-10 and males from 3-J-11, and between females from 3-J-10 and females from 3-J-11, for each of the cross-sectional variables at midshaft femur (Table 5.1). As shown in Table 5.2, mean values are relatively similar between males from both cemeteries and between females from both cemeteries. Upon visual inspection of the data's distribution separated by cemetery and sex in Figures 5.1, 5.3, and 5.4, there appears to be a wider range of data for all three cross-sectional variables in females from 3-J-11 compared to females from 3-J-10. There were no significant differences between males from 3-J-10 and males from 3-J-11; however, males from 3-J-10 had greater averages (Table 5.2) and medians (Figures 5.3 and 5.4) than males from 3-J-11 for J and TA . Regarding I_{max}/I_{min} , averages were practically the same between both groups and males from 3-J-11 had a higher median than males from 3-J-10, although the distribution for males from 3-J-10 extended into higher values (Figure 5.1). Figure 5.2 displays scatter plots between the ratios of I_{max}/I_{min} and AP/ML for males and females separated by cemetery. For cemetery 3-J-10, males exhibited a broader distribution with a few individuals demonstrating higher values of both variables,

whereas males from 3-J-11 did not extend as far into this range. Females from the two cemeteries were concentrated in the lower expanse of the distribution; however, females from cemetery 3-J-11 had a greater representation of individuals with higher values and shared a similar distribution with males from the same cemetery.

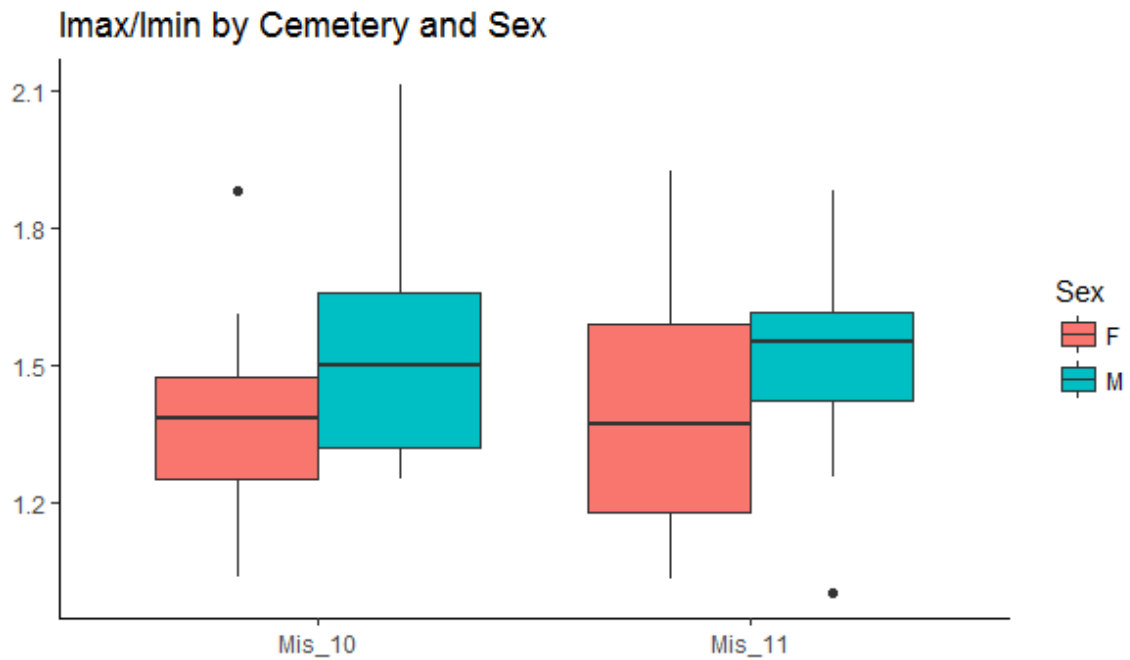


Figure 5.1: Boxplots for I_{max}/I_{min} at midshaft femur between cemeteries, separated by sex.

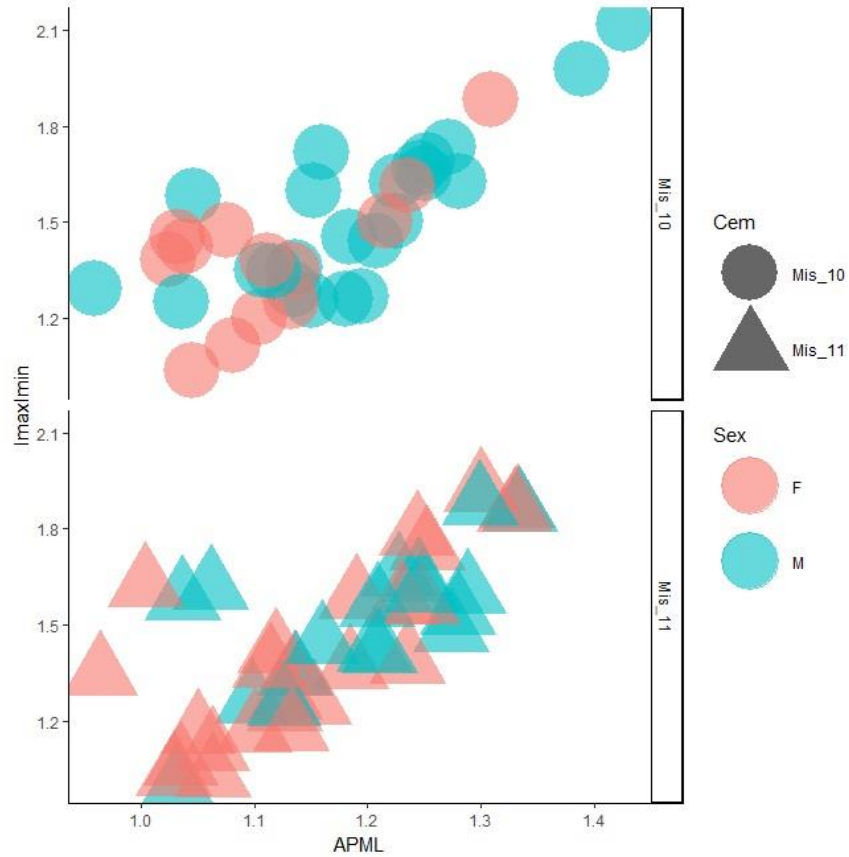


Figure 5.2: Scatter plots between I_{max}/I_{min} and AP/ML at midshaft femur, separated by cemetery.

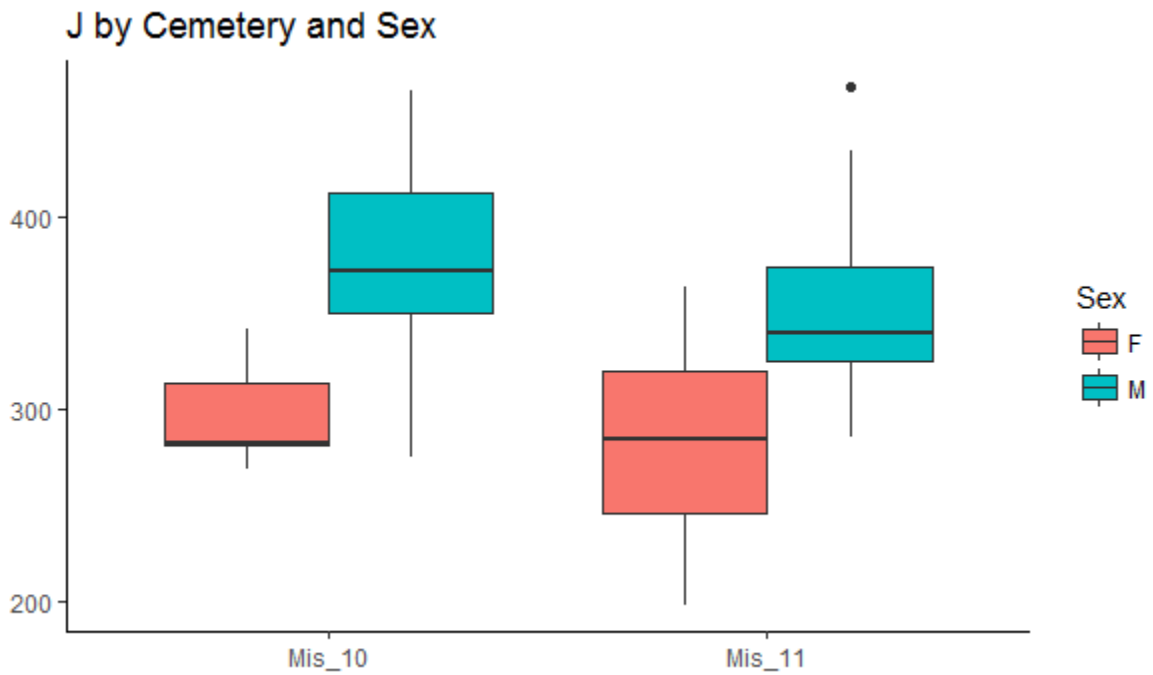


Figure 5.3: Boxplots for J at midshaft femur between cemeteries, separated by sex.

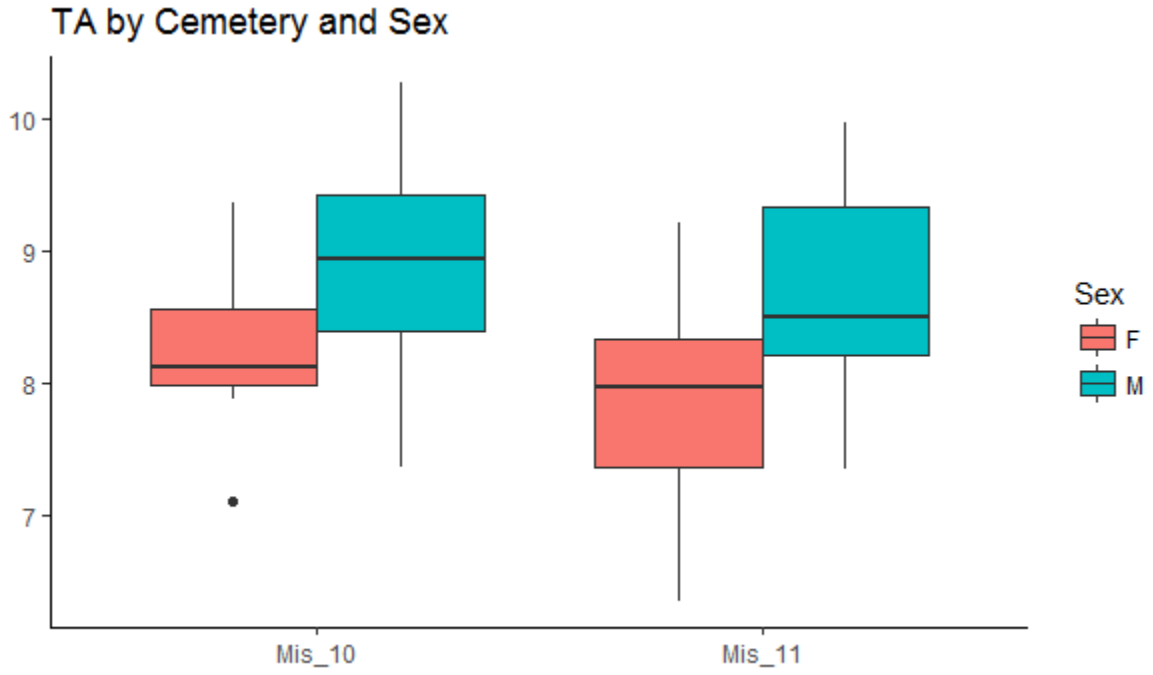


Figure 5.4: Boxplots for TA at midshaft femur between cemeteries, separated by sex.

Subtrochanteric region of femur

Table 5.3: Summary statistics for cross-sectional geometric properties at the subtrochanteric region of the femur, separated by cemetery and sex. ($J = \text{mm}^4$, $TA = \text{mm}^2$)

		I_{max}/I_{min}		J		TA	
		M	F	M	F	M	F
3-J-10	n	20	11	16	6	18	9
	Mean \pm SD	1.51 (± 0.24)	1.59 (± 0.23)	351.19 (± 60.66)	309.26 (± 24.31)	8.91 (± 0.80)	8.36 (± 0.60)
3-J-11	n	18	24	11	20	13	24
	Mean \pm SD	1.44 (± 0.22)	1.60 (± 0.33)	329.91 (± 38.48)	306.53 (± 37.34)	8.42 (± 0.56)	8.11 (± 0.54)

As communicated in Table 5.1, there were no significant differences between males from 3-J-10 and males from 3-J-11, and between females 3-J-10 and females from 3-J-11, for the three cross-sectional properties at the subtrochanteric region of the femur. Table 5.3 displays comparable mean values between males from the cemeteries and between females from both cemeteries. The distribution of I_{max}/I_{min} at the subtrochanteric femur, separated by cemetery and sex in Figure 5.5, shows a larger range of values in females from 3-J-11 compared to females from 3-J-10—similar to the pattern observed in the I_{max}/I_{min} data from the midshaft femur. This trend was not true for J and TA between females from both cemeteries, as both sub-samples were similar for J (Figure 5.6) and females from 3-J-10 exhibited a wider range of values than females from 3-J-11 for TA (Figure 5.7). Although no significant differences were found between males from cemetery 3-J-10 and males from cemetery 3-J-11, males from cemetery 3-J-10 had consistently higher averages (Table 5.3) and medians (Figures 5.5, 5.6, and 5.7) for all three cross-sectional variables.

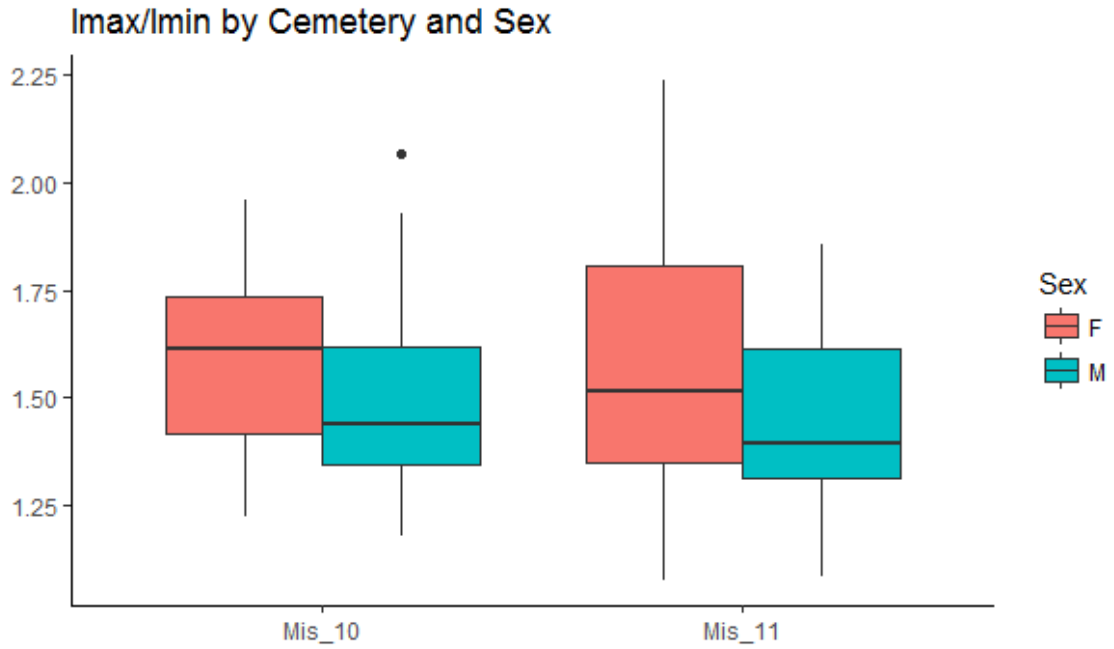


Figure 5.5: Boxplots for I_{max}/I_{min} at subtrochanteric femur between cemeteries, separated by sex.

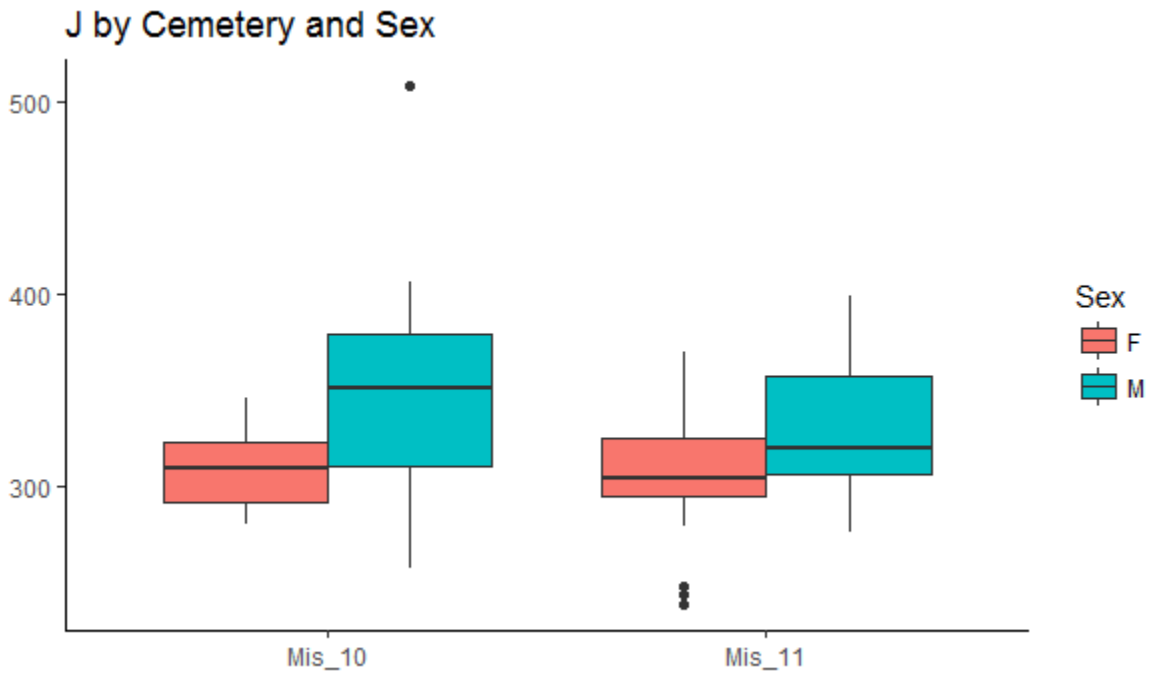


Figure 5.6: Boxplots for J at subtrochanteric femur between cemeteries, separated by sex.

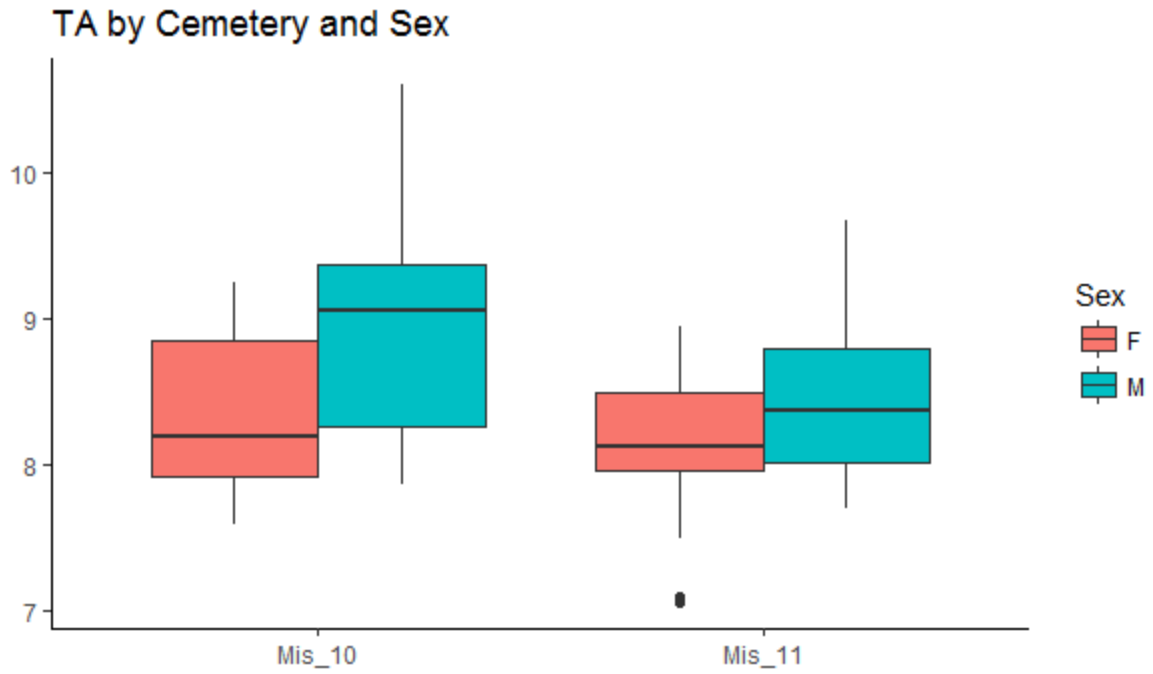


Figure 5.7: Boxplots for TA at subtrochanteric femur between cemeteries, separated by sex.

Midshaft tibia

Table 5.4: Summary statistics for cross-sectional geometric properties at midshaft tibia, separated by cemetery and sex. ($J = \text{mm}^4$, $TA = \text{mm}^2$)

		I_{max}/I_{min}		J		TA	
		M	F	M	F	M	F
3-J-10	n	23	10	16	5	17	7
	Mean \pm SD	2.13 (± 0.36)	2.05 (± 0.29)	337.20 (± 52.06)	293.97 (± 17.39)	7.04 (± 0.70)	6.73 (± 0.57)
3-J-11	n	19	22	11	16	13	17
	Mean \pm SD	2.14 (± 0.40)	2.18 (± 0.42)	351.63 (± 87.49)	274.67 (± 46.43)	7.08 (± 0.64)	6.36 (± 0.61)

There were no significant differences between males from the two cemeteries and between females from both cemeteries for the cross-sectional variables derived from midshaft tibia (Table 5.1). As displayed in Table 5.4, the means between males from 3-J-10 and males from 3-J-11, and females from 3-J-10 and females from 3-J-11, are relatively similar. Separating the midshaft tibia cross-sectional data by cemetery and sex in Figures 5.8, 5.9, and 5.10 reveals a trend previously displayed between females from both cemeteries. This observation is the greater range of data in the female group from 3-J-11 compared to the distribution of data in the female sub-sample from 3-J-10. The pattern observed from the previous diaphyseal sections between males from 3-J-10 and males from 3-J-11 is not as apparent in the data from the midshaft tibia. There were higher mean values for males from 3-J-11 than males from 3-J-10 for J and similar average values for I_{max}/I_{min} and TA (Table 5.4). Males from 3-J-11 had a higher median for I_{max}/I_{min} (Figure 5.8) and slightly higher median for J (Figure 5.9). Males from cemetery 3-J-10 had a higher median for TA than males from cemetery 3-J-11 (Figure 5.10), which is consistent with the pattern observed at the other diaphyseal locations.

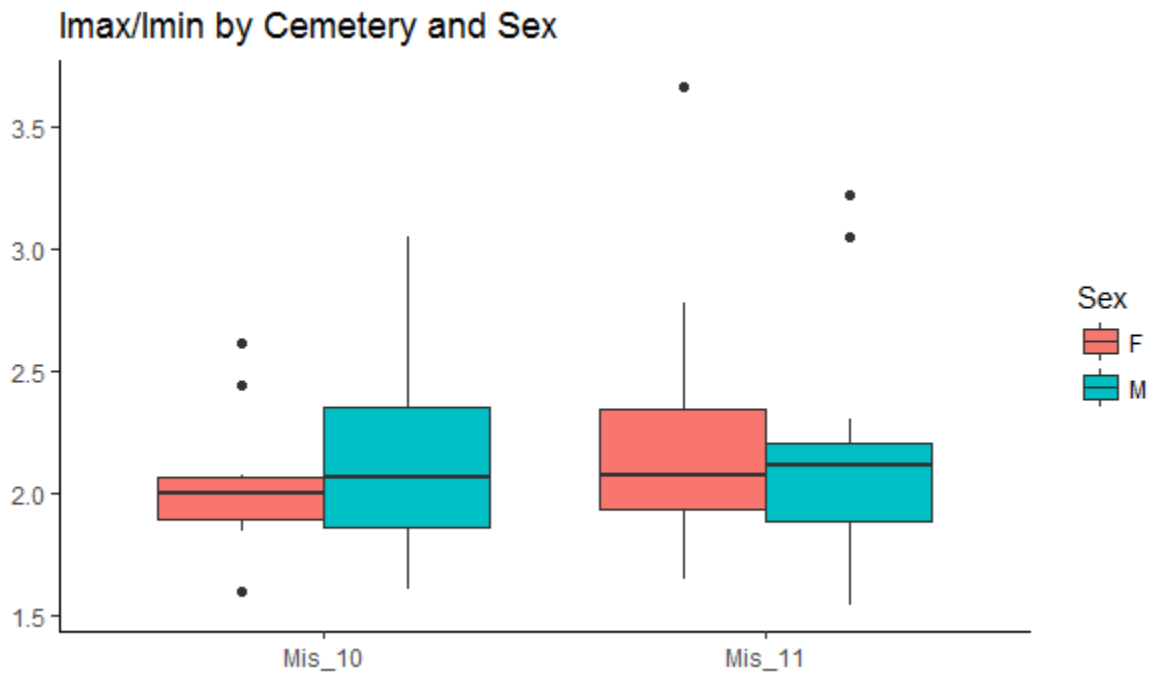


Figure 5.8: Boxplots for I_{max}/I_{min} at midshaft tibia between cemeteries, separated by sex.

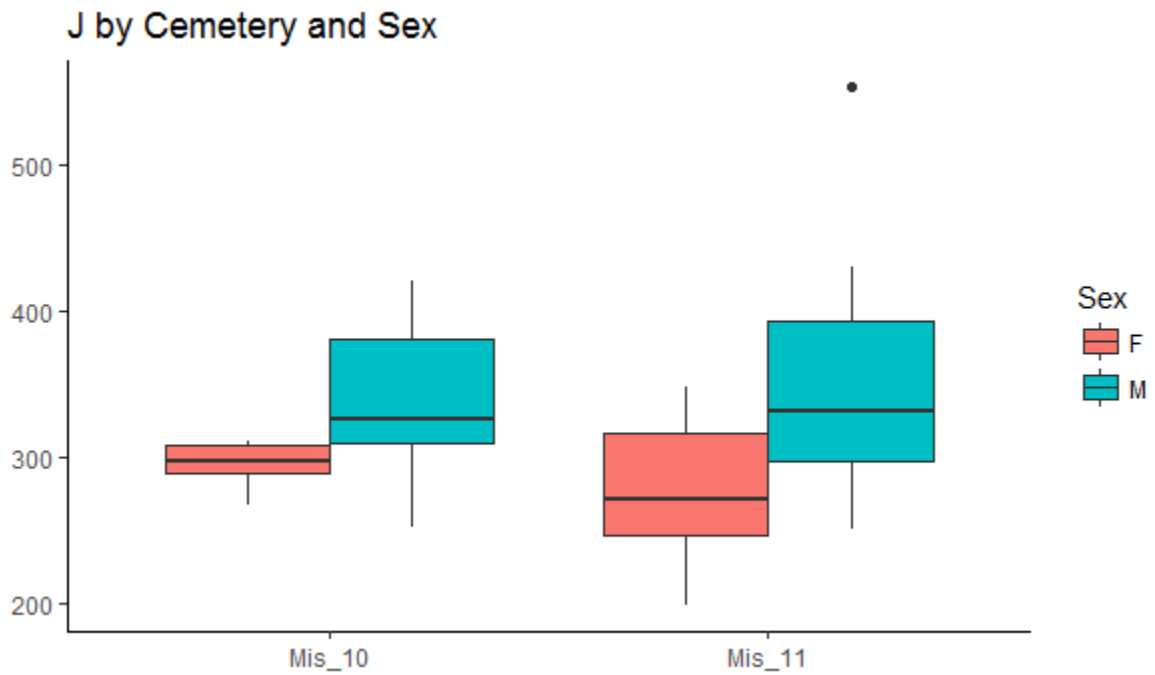


Figure 5.9: Boxplots for J at midshaft tibia between cemeteries, separated by sex.

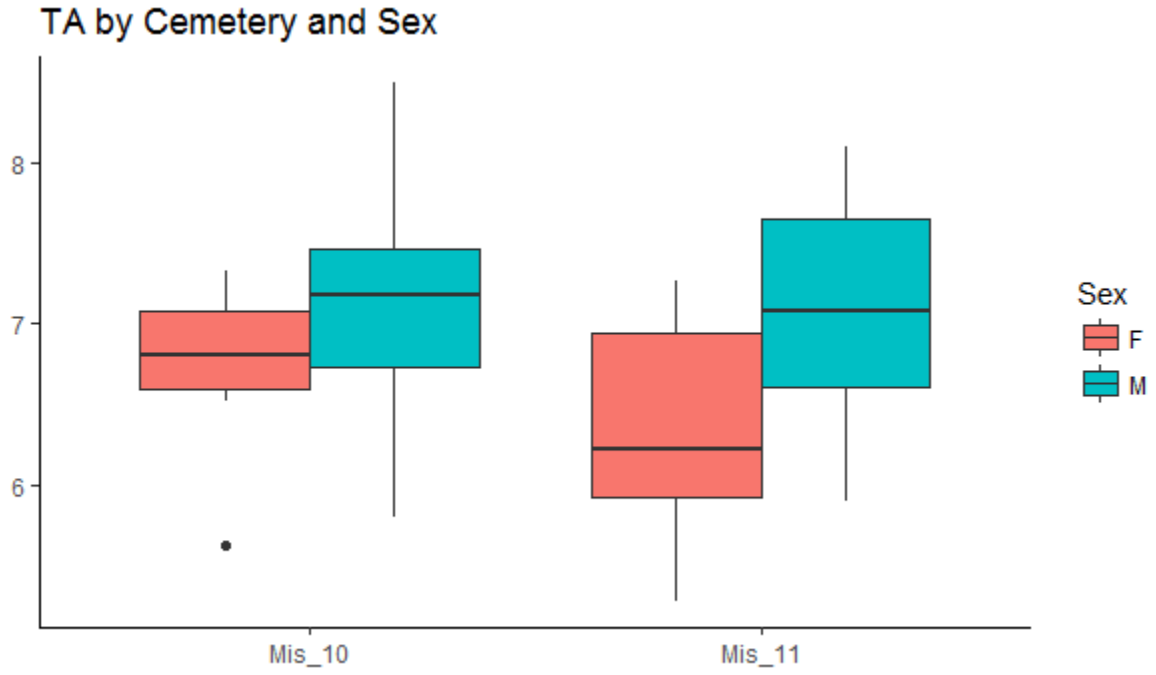


Figure 5.10: Boxplots for TA at midshaft tibia between cemeteries, separated by sex.

Research Question 2

Research Question 2—Intra-site: Are there patterns of cross-sectional geometric properties within the Mis Island collection that would suggest significantly different groups of individuals, primarily regarding males and females?

H₀: There will be no differences in cross-sectional properties between males and females.

H₁: There will be differences in cross-sectional properties between males and females.

As displayed in Table 5.5, the majority of comparisons of the cross-sectional geometric variables between males and females were significantly different. Therefore, the null hypothesis is rejected—there are significant differences in cross-sectional properties between males and females in the Mis Island collection.

Table 5.5: *P-values from comparisons between males and females for each cross-sectional property at the three diaphyseal locations.* (ns = not significant at $p < 0.05$)

	I_{max}/I_{min}	J	TA
Midshaft femur	0.038	<0.001	<0.001
Subtrochanteric femur	ns	0.01	0.0021
Midshaft tibia	ns	<0.001	0.0014

Midshaft femur

Table 5.6: Summary statistics for cross-sectional geometric properties at midshaft femur, separated by sex. ($J = \text{mm}^4$, $TA = \text{mm}^2$)

	I_{max}/I_{min}		J		TA	
	M	F	M	F	M	F
n	41	38	27	24	32	33
Mean	1.52	1.40	367.14	287.18	8.75	7.96
SD	0.22	0.25	56.34	43.55	0.78	0.70

Males had significantly higher values of the cross-sectional geometric variables at femoral midshaft than the female group. As displayed in Table 5.5, independent t-tests between males and females for the three cross-sectional variables resulted in significant differences for I_{max}/I_{min} ($t(77) = 2.11$, $p = 0.038$), J ($t(49) = 5.62$, $p < 0.001$), and TA ($t(63) = 4.30$, $p < 0.001$). Table 5.6 shows greater mean values of I_{max}/I_{min} for males (1.52 ± 0.22) than females (1.40 ± 0.25) and Figures 5.11 and 5.12 demonstrates this significant trend. To determine the relationship between I_{max}/I_{min} and AP/ML diameters, a Pearson's r correlation was calculated which suggested a strong positive correlation between the variables ($r = 0.75$). Therefore, it can be assumed that I_{max}/I_{min} essentially reflects the same information as AP/ML and that the results of I_{max}/I_{min} are comparable to those of the ratio between AP and ML diameters. Mean values of J were also significantly higher for males (367.14 ± 56.34) than females (287.18 ± 43.55) (Table 5.6). Figures 5.13 and 5.14 exhibit a distinct separation in values of J between males and females, with most males demonstrating higher values than females. Table 5.6 and Figures 5.15 and 5.16 present greater values of TA in males (8.75 ± 0.78) than females (7.96 ± 0.70), which as stated in Table 5.5, was a significant difference ($t(63) = 4.297$, $p < 0.001$).

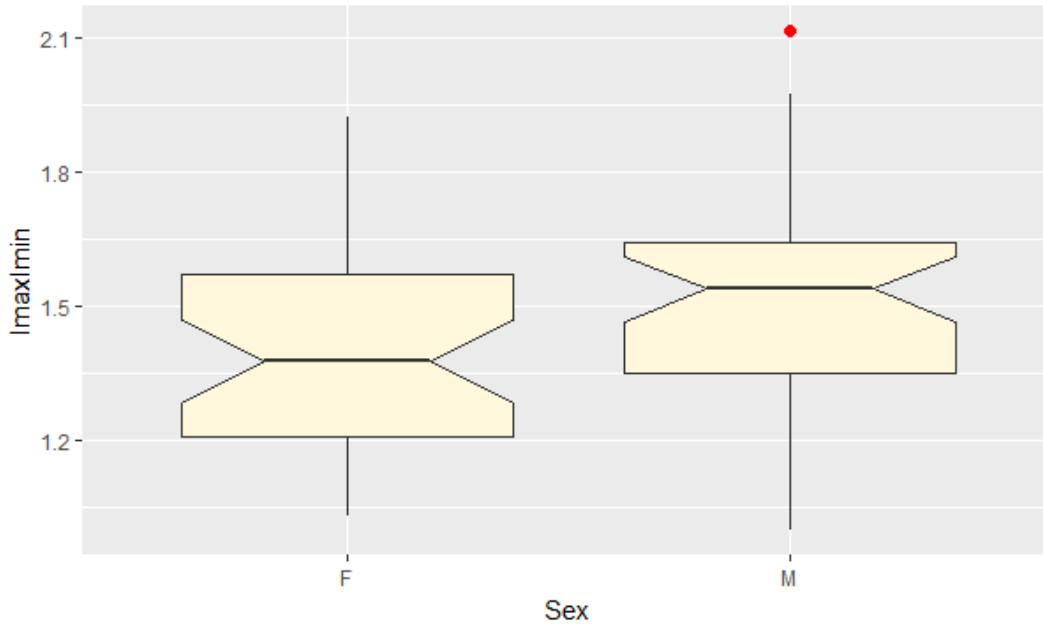


Figure 5.11: Violin plot of I_{max}/I_{min} values between males and females at midshaft femur (red dot denotes an outlier).

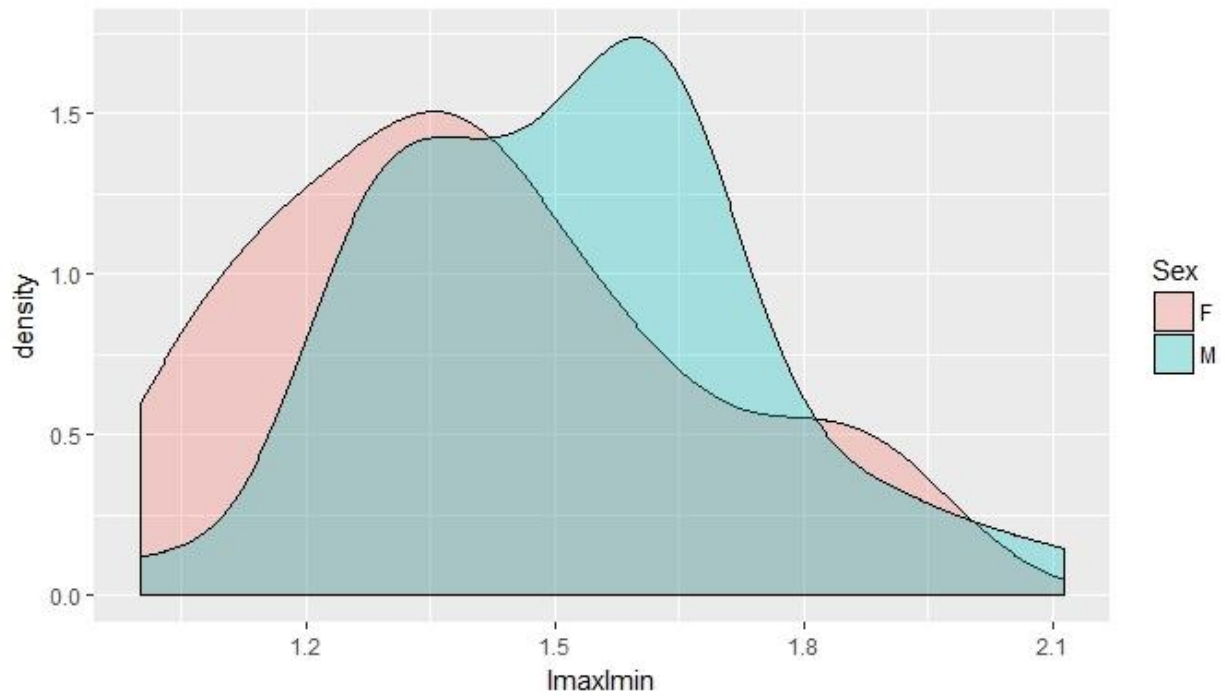


Figure 5.12: Density plot of I_{max}/I_{min} values between males (blue) and females (red) at midshaft femur.

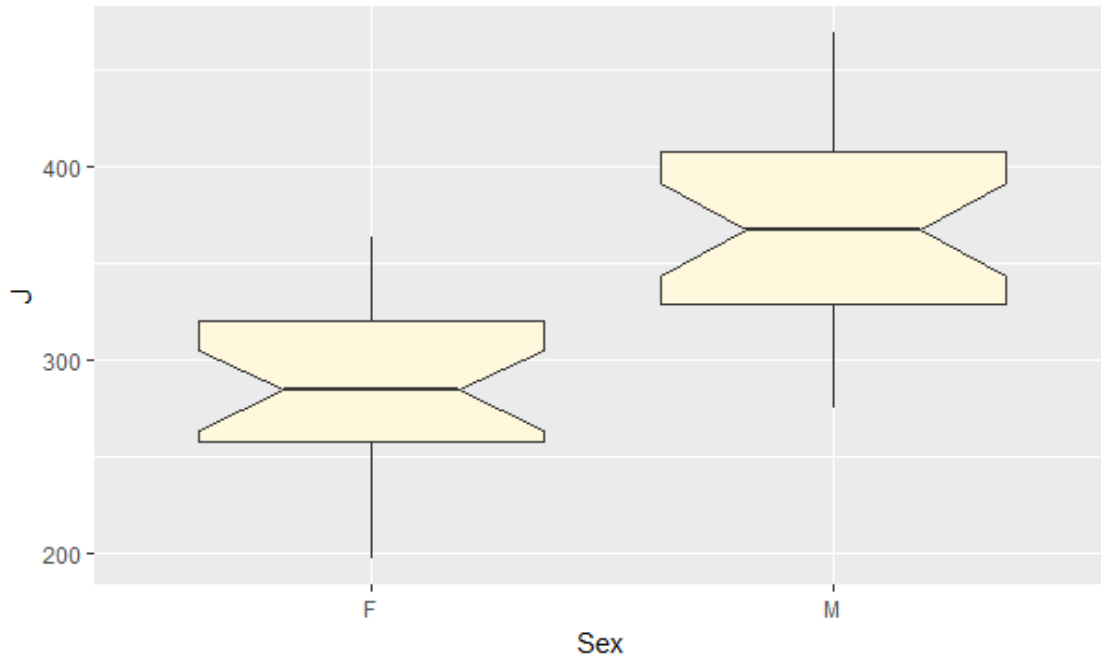


Figure 5.13: *Violin plot of J (mm^4) values between males and females at midshaft femur.*

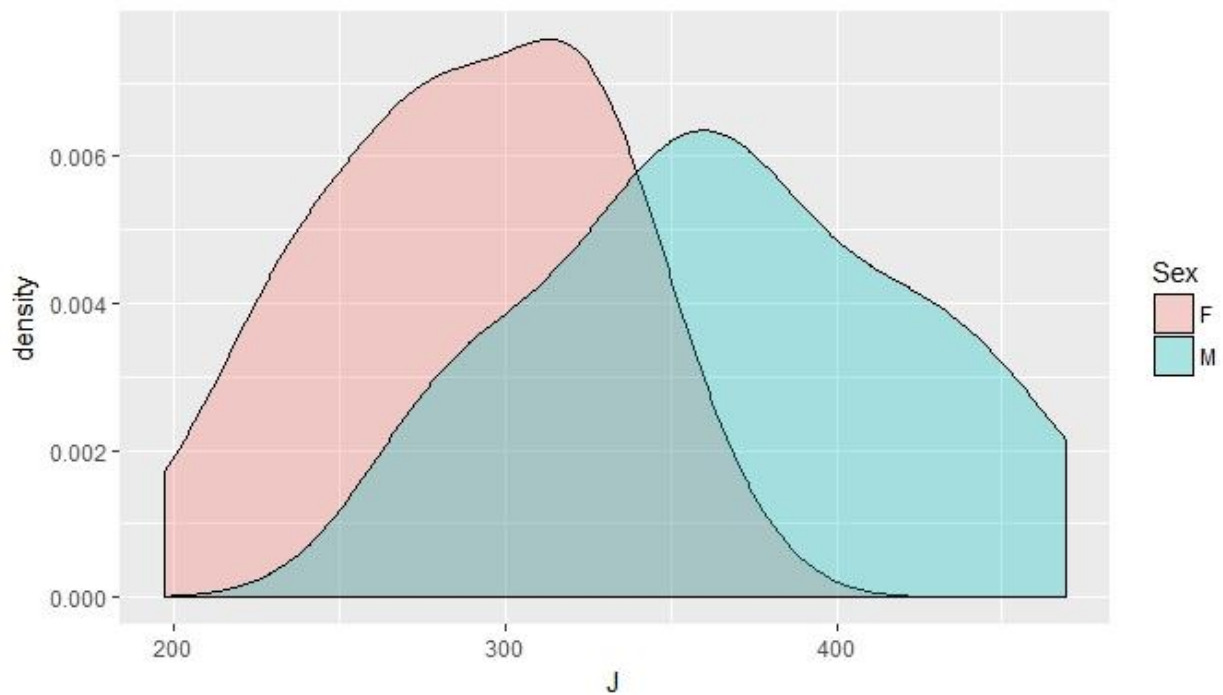


Figure 5.14: *Density plot of J (mm^4) values between males (blue) and females (red) at midshaft femur.*

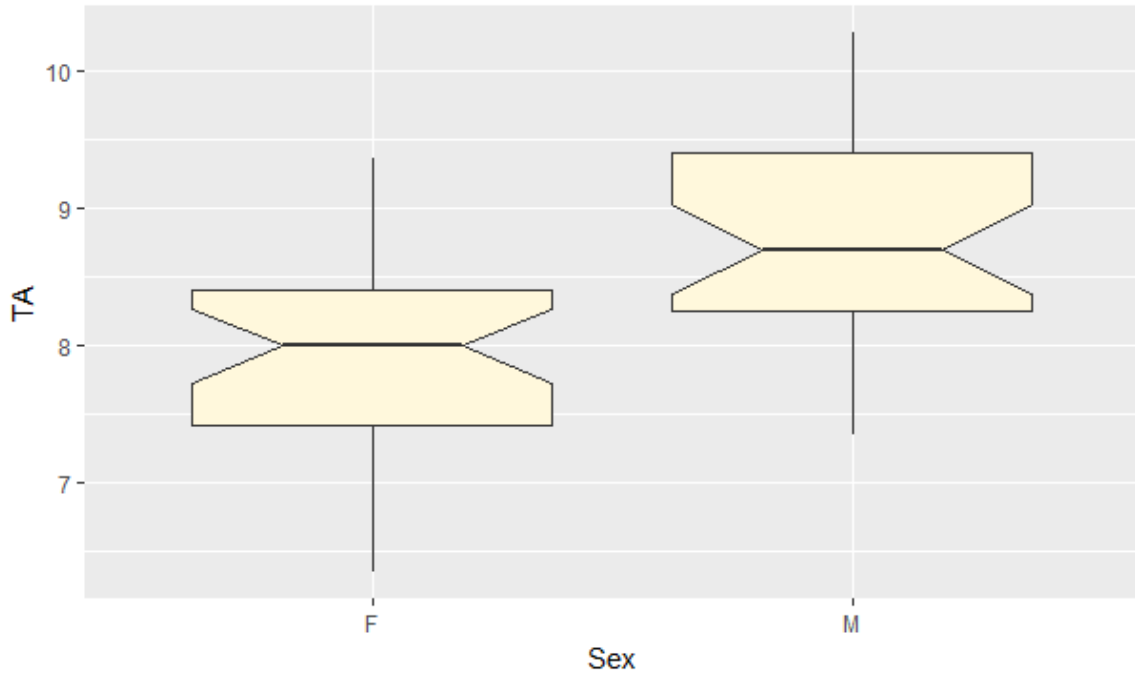


Figure 5.15: Violin plot of TA (mm^2) values between males and females at midshaft femur.

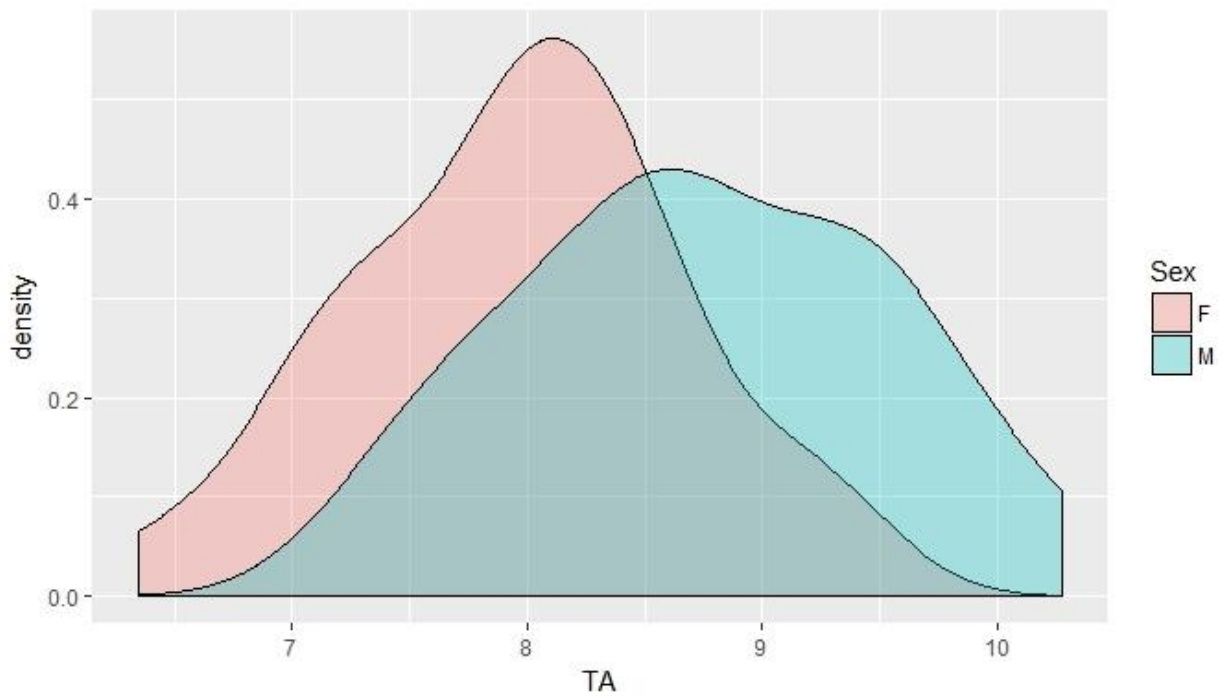


Figure 5.16: Density plot of TA (mm^2) values between males (blue) and females (red) at midshaft femur.

The cluster analyses of these cross-sectional properties at femoral midshaft demonstrate inherent groupings in the data primarily based on sex; however, there are varying degrees of overlap between males and females in the data's distribution. In Figure 5.17 of I_{max}/I_{min} , there are two clusters that display a greater number of females in the lower range of values (62% female vs. 38% male) and more males in the upper range (67% male vs. 33% female); however, the cluster with the highest values include an equal number of males and females (50% male and 50% female). The two clusters in Figure 5.18 represent a relatively clear separation between males and females in the data for J , with females on the lower end of the range (71% female vs. 29% male) and males on the higher (83% male vs. 17% female). This pattern is also evident in Figure 5.19, which displays two clusters in the data for TA that are primarily grouped by sex (cluster on the right: 69% female vs. 31% male; cluster on the right: 72% male vs. 28% female).

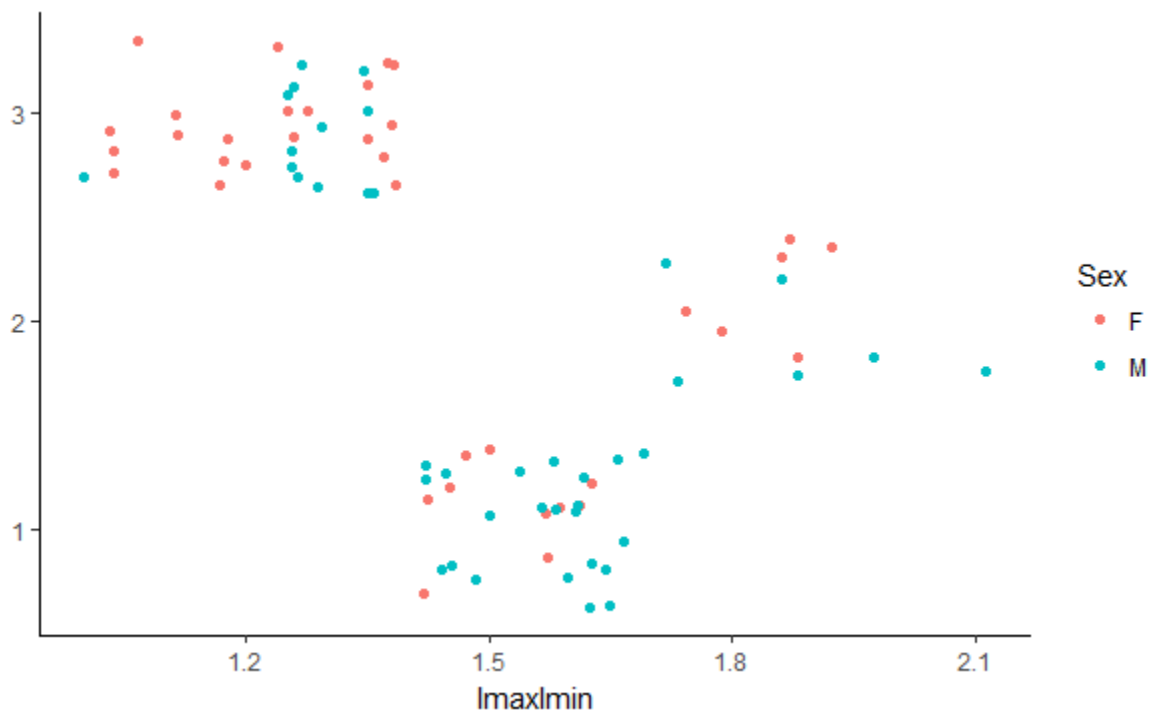


Figure 5.17: Scatter plot (with random jitter) of clusters after k-means cluster analysis of I_{max}/I_{min} at midshaft femur.

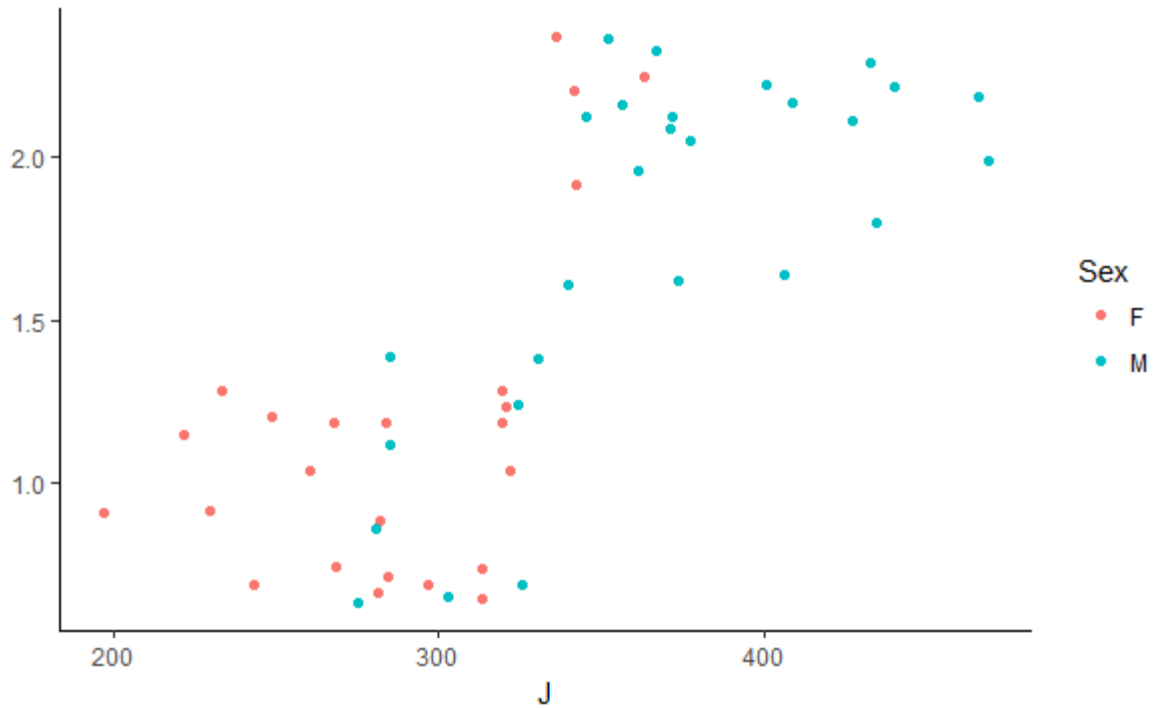


Figure 5.18: Scatter plot (with random jitter) of clusters after k-means cluster analysis of J at midshaft femur.

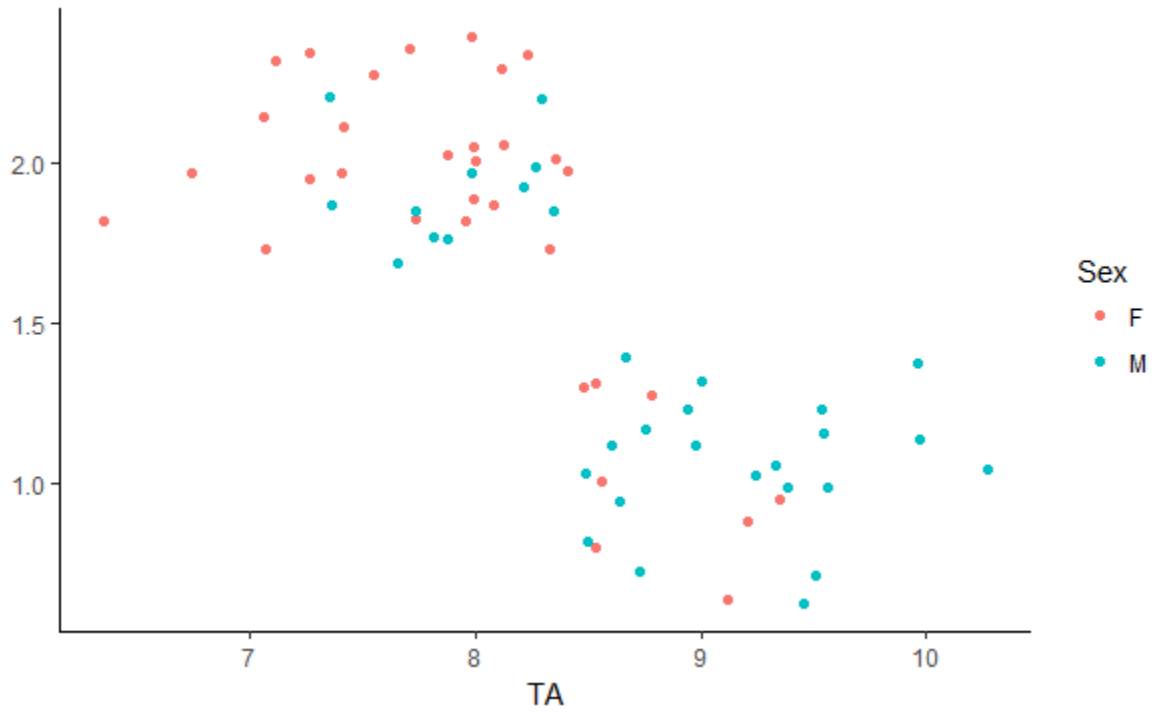


Figure 5.19: Scatter plot (with random jitter) of clusters after k-means cluster analysis of TA at midshaft femur.

Subtrochanteric region of femur

Table 5.7: Summary statistics for cross-sectional geometric properties at subtrochanteric region of femur, separated by sex. ($J = \text{mm}^4$, $TA = \text{mm}^2$)

	I_{max}/I_{min}		J		TA	
	M	F	M	F	M	F
n	38	35	27	26	31	33
Mean	1.47	1.60	342.52	307.16	8.70	8.18
SD	0.23	0.30	52.97	34.34	0.74	0.56

At the subtrochanteric region of the femur, males had significantly higher values for J and TA than females. The data for I_{max}/I_{min} at the subtrochanteric region of the femur were not normal, but because the sub-sample sizes for males and females were both over 30 individuals, an independent t-test was still utilized. This t-test yielded a nonsignificant difference between males and females (Table 5.5); however, the difference approached significance ($t(71) = -1.981$, $p = 0.052$) at the $\alpha = 0.05$ level. Although there was no significant difference between males and females for I_{max}/I_{min} , females had a higher average value (Table 5.7) and a distribution that extends into greater values (Figures 5.20 and 5.21) of I_{max}/I_{min} compared to males. Because the data for J were not normal, a Wilcoxon rank sum test was used to compare males and females. This test yielded a significant difference between males and females for J ($W = 208$, $p = 0.01$) (Table 5.5), with males exhibiting greater values of J than females (Table 5.7 and Figures 5.22 and 5.23). As shown in Table 5.5, there was a significant difference between males (342.52 ± 52.97) and females (307.16 ± 34.34) for TA at the subtrochanteric region of the femur ($t(62) = 3.21$, $p = 0.0021$). Table 5.7 displays a higher average value for males (342.52 ± 59.27) than females (307.16 ± 34.34) which is a trend illustrated in Figures 5.24 and 5.25.

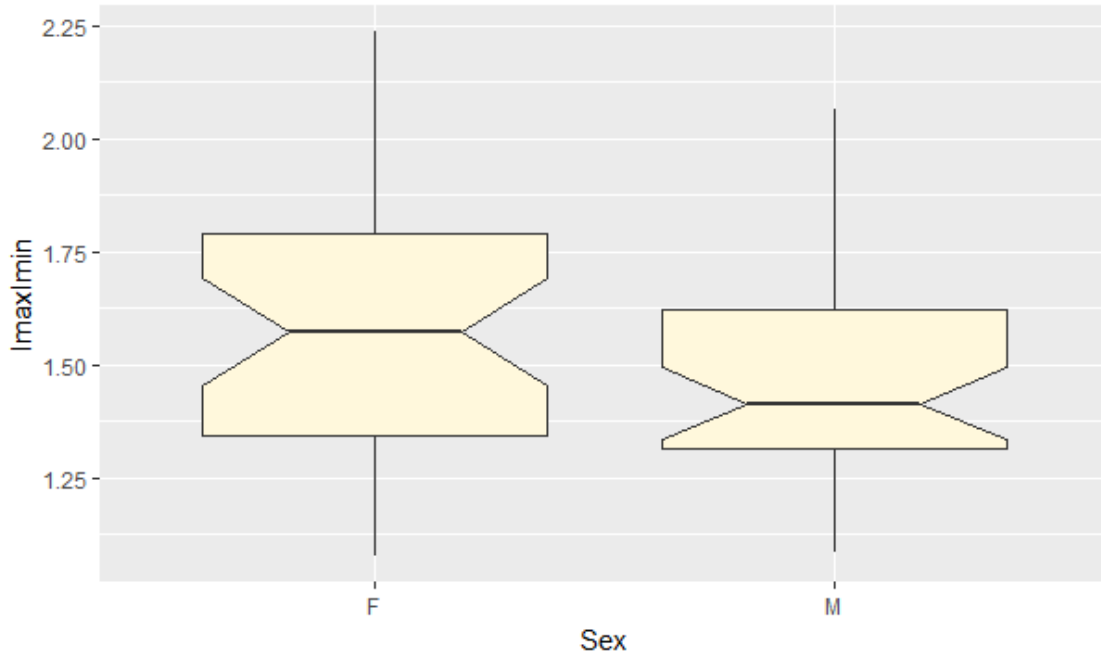


Figure 5.20: Violin plot of I_{max}/I_{min} values between males and females at subtrochanteric femur.

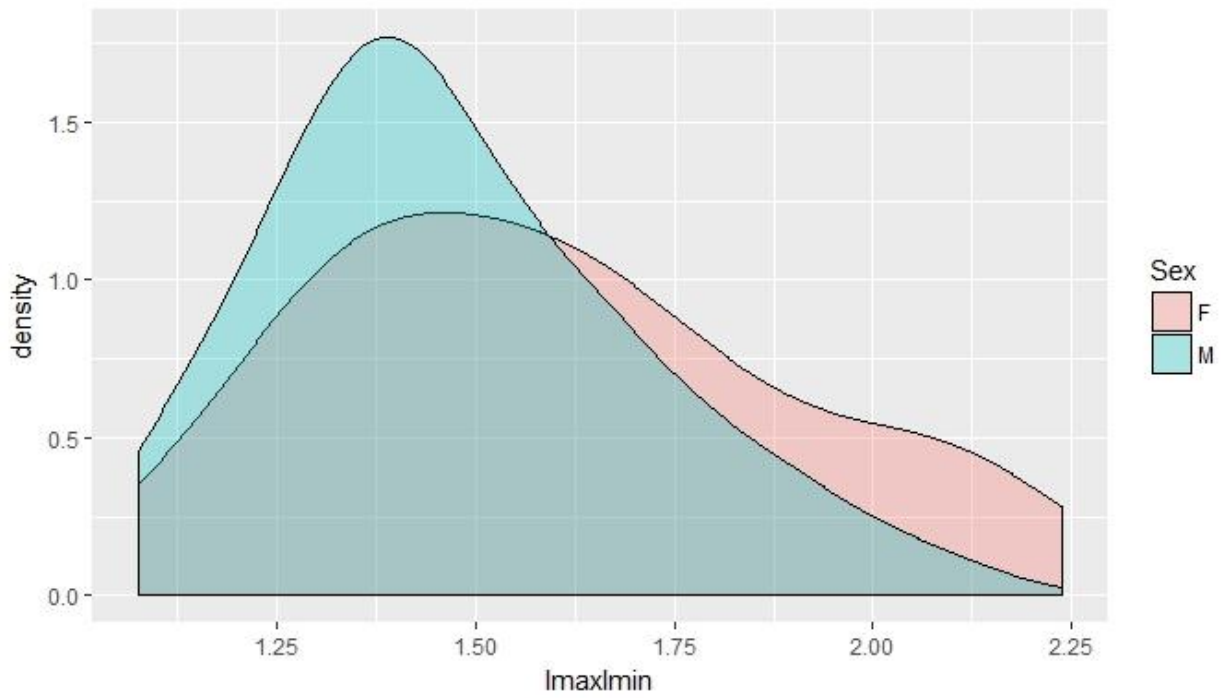


Figure 5.21: Density plot of I_{max}/I_{min} values between males (blue) and females (red) at subtrochanteric femur.

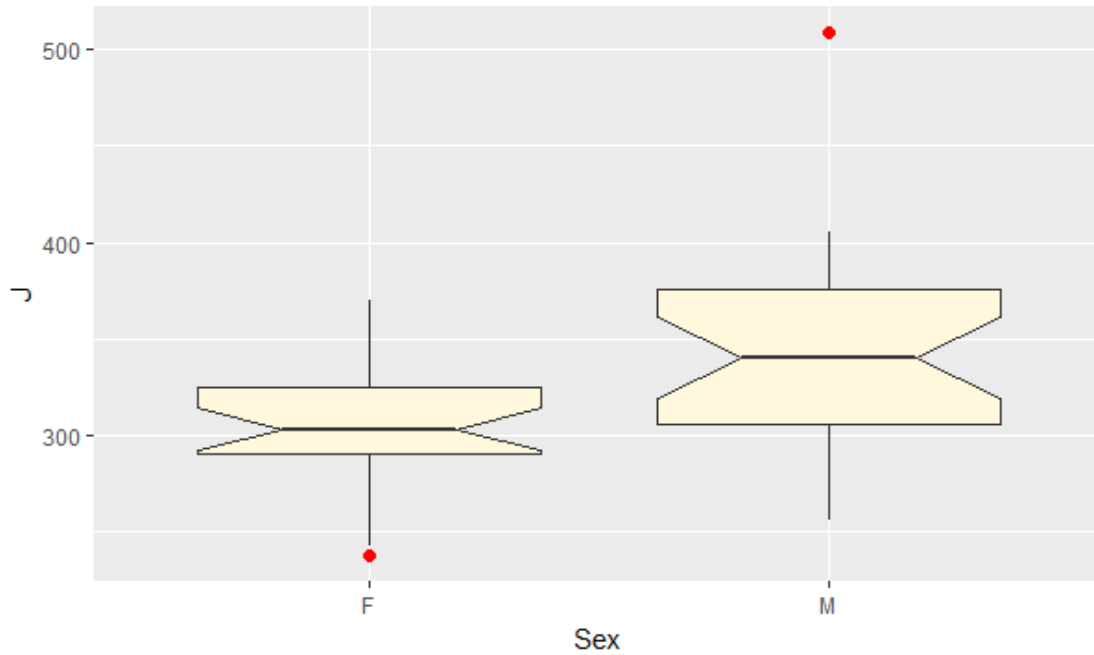


Figure 5.22: Violin plot of J (mm^4) values between males and females at subtrochanteric femur (red dot denotes an outlier).

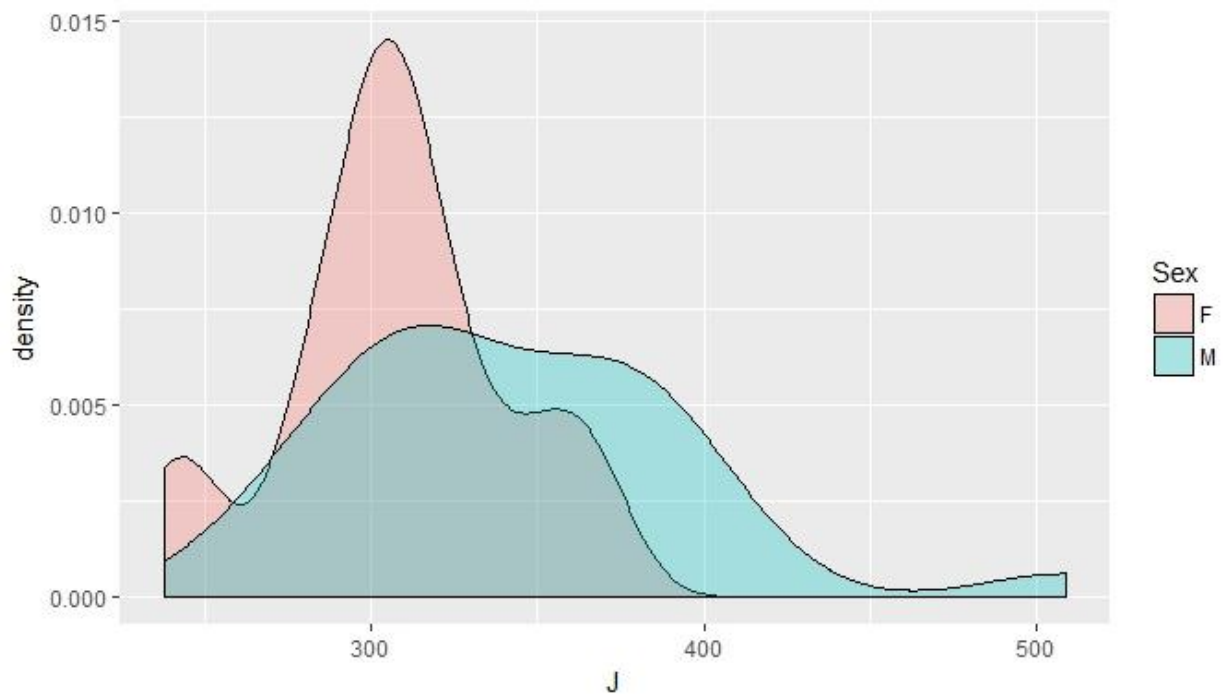


Figure 5.23: Density plot of J (mm^4) values between males (blue) and females (red) at subtrochanteric femur.

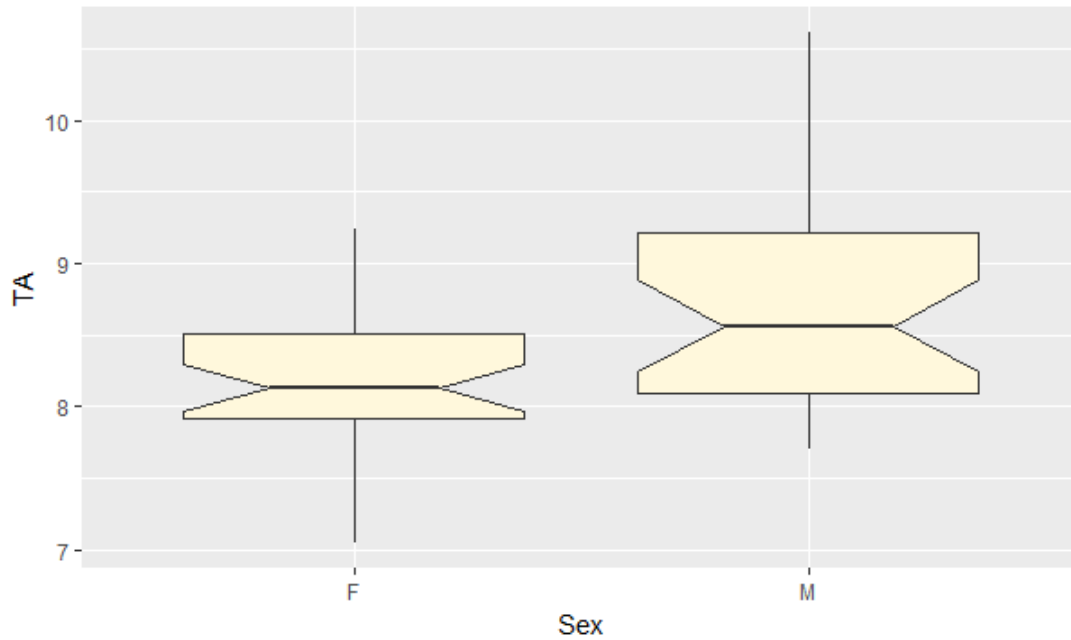


Figure 5.24: Violin plot of TA (mm^2) values between males and females at subtrochanteric femur.

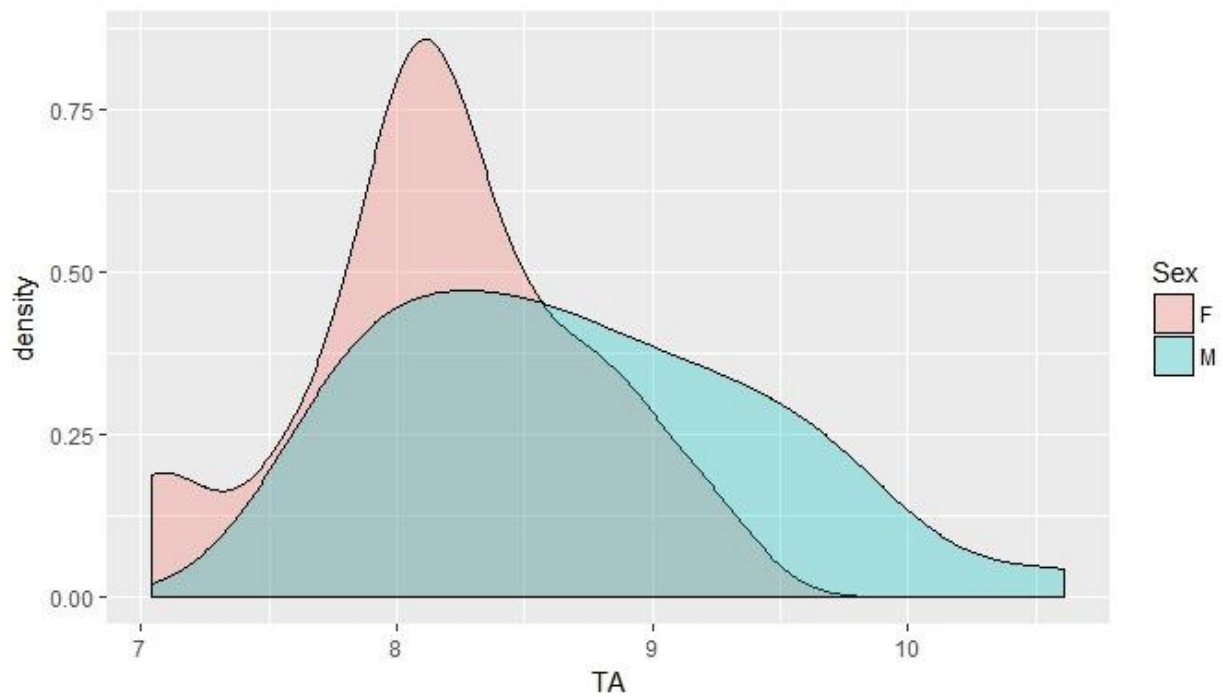


Figure 5.25: Density plot of TA (mm^2) values between males (blue) and females (red) at subtrochanteric femur.

The data derived from the subtrochanteric region of the femur assembled mainly based on sex through the cluster analyses. In Figure 5.26, the I_{max}/I_{min} data were grouped most logically into three clusters. The grouping with the lowest values included more males than females (64% male vs. 36% female), whereas a third cluster with the highest values was comprised of more females than males (69% female vs. 31% male). The second gathering of individuals in the intermediate range of values had a relatively equal representation of males and females (48% male and 52% female). Figure 5.27 displays two clusters of the data for J , with the lower cluster displaying both sexes but more females being represented (62% female vs. 38% male), and the cluster with higher values comprising primarily males (74% male vs. 26% female). The TA data were fitted to three clusters, as shown in Figure 5.28. The group on the lowest end included more females than males (68% female vs. 32% male) and the highest cluster was mostly males (85% male vs. 15% female). The intermediate cluster represented a relatively equal number of males and females (46% male and 54% female).

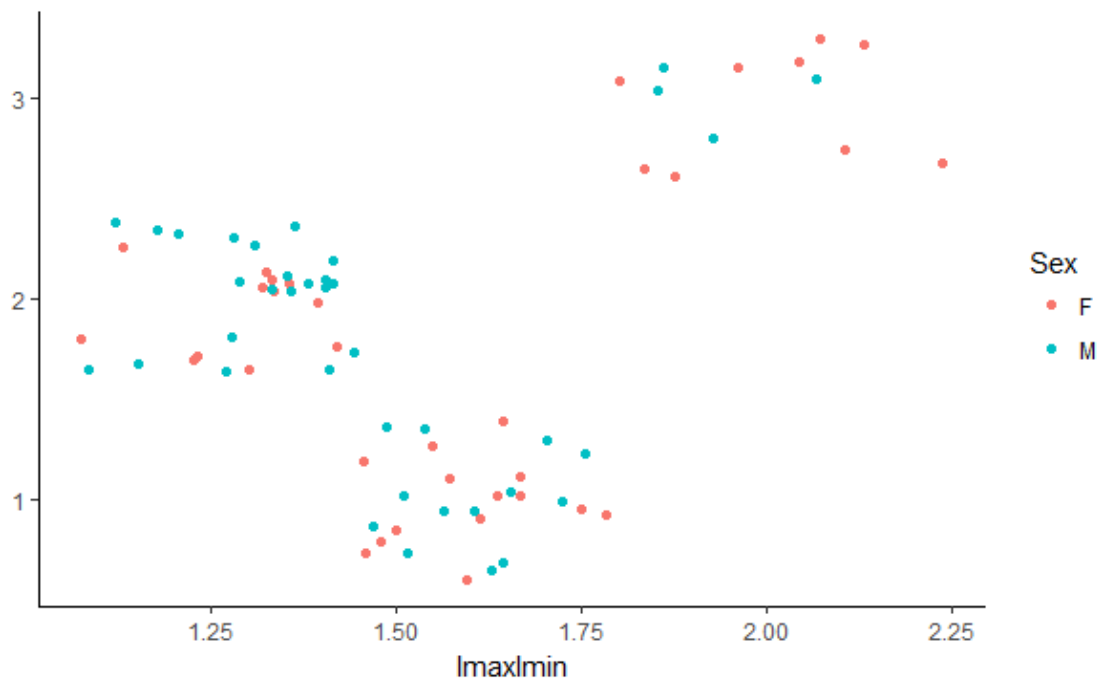


Figure 5.26: Scatter plot (with random jitter) of clusters after k -means cluster analysis of I_{max}/I_{min} at subtrochanteric femur.

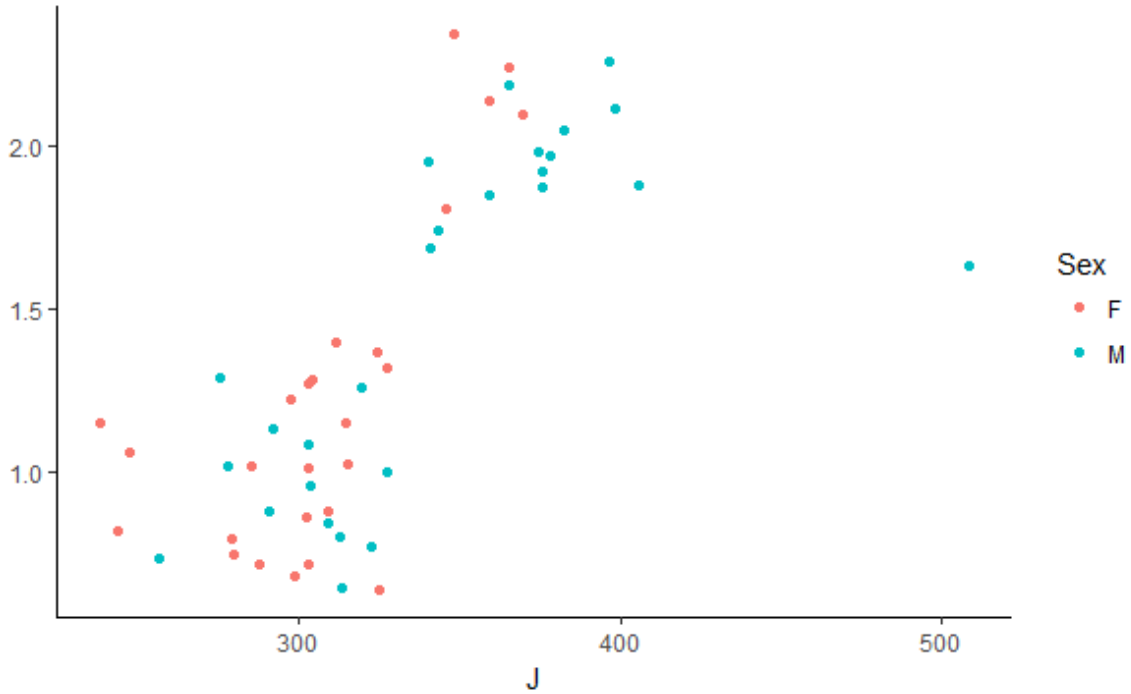


Figure 5.27: Scatter plot (with random jitter) of clusters after *k*-means cluster analysis of *J* at subtrochanteric femur.

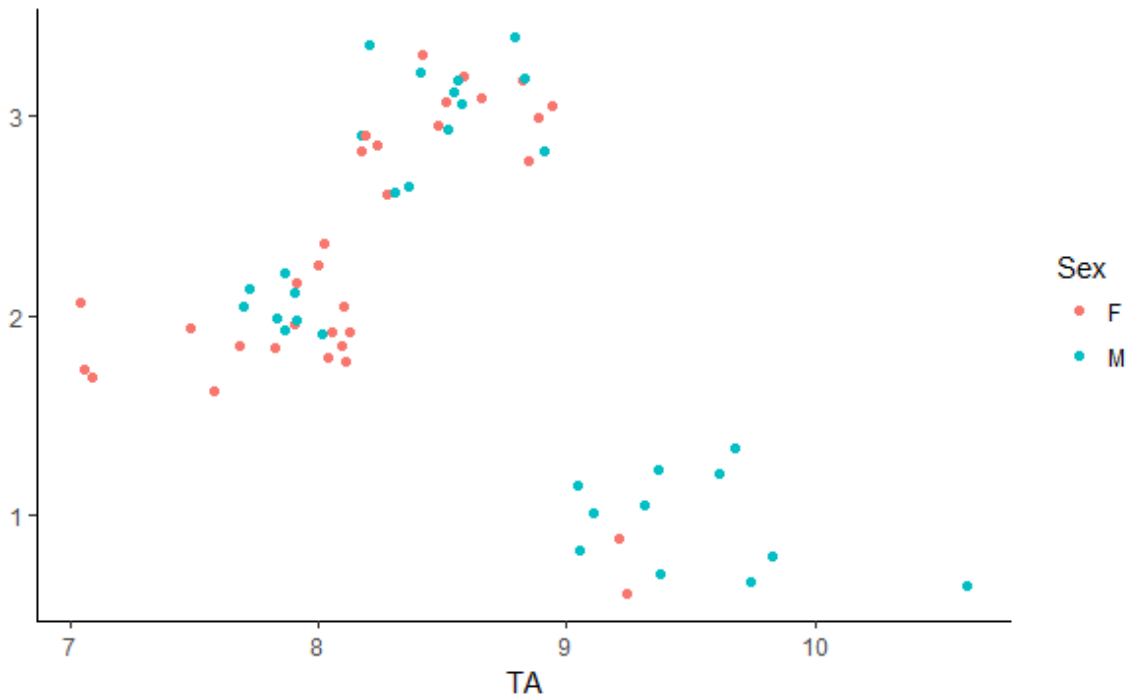


Figure 5.28: Scatter plot (with random jitter) of clusters after *k*-means cluster analysis of *TA* at subtrochanteric femur.

Midshaft tibia

Table 5.8: Summary statistics for cross-sectional geometric properties at midshaft tibia, separated by sex. ($J = \text{mm}^4$, $TA = \text{mm}^2$)

	I_{max}/I_{min}		J		TA	
	M	F	M	F	M	F
n	42	32	27	21	30	24
Mean	2.14	2.14	343.08	279.27	7.06	6.47
SD	0.37	0.38	67.53	41.81	0.66	0.61

Males had significantly greater values for J and TA than females at the tibial midshaft and there was no significant difference between the sub-groups for I_{max}/I_{min} . Although the data for I_{max}/I_{min} were not normal, an independent t-test was still performed because male and female sub-samples included over 30 individuals (Table 5.8). This test yielded a nonsignificant difference between males and females (Table 5.5), as the mean values are the same between males and females (Table 5.8) and the distribution of data is similar between sexes (Figures 5.29 and 5.30). The data for J were not normal, therefore a Wilcoxon rank sum test was utilized to compare males and females. There was a significant difference between males and females for J ($W = 115$, $p < 0.001$) (Table 5.5) and a higher mean value for J was calculated for males (343.08 ± 67.5) than females (279.27 ± 41.81) (Table 5.8). Figures 5.31 and 5.32 demonstrate the higher distribution of J for the male sub-group compared to the structure of data for females. A significant difference between males and females was found for TA ($t(52) = 3.38$, $p = 0.0014$) (Table 5.5). As illustrated in Table 5.8 and Figures 5.33 and 5.34, greater values of TA were exhibited in males compared to females with males having a higher mean value (7.06 ± 0.66) than females (6.47 ± 0.61).

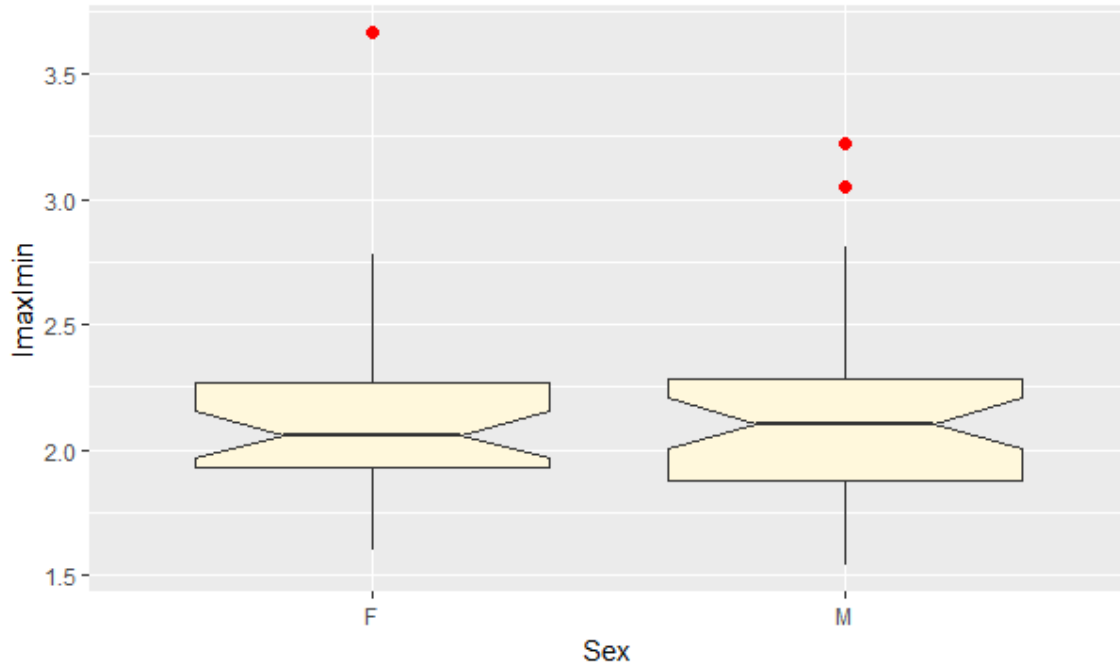


Figure 5.29: Violin plot of I_{max}/I_{min} values between males and females at midshaft tibia (red dot denotes an outlier).

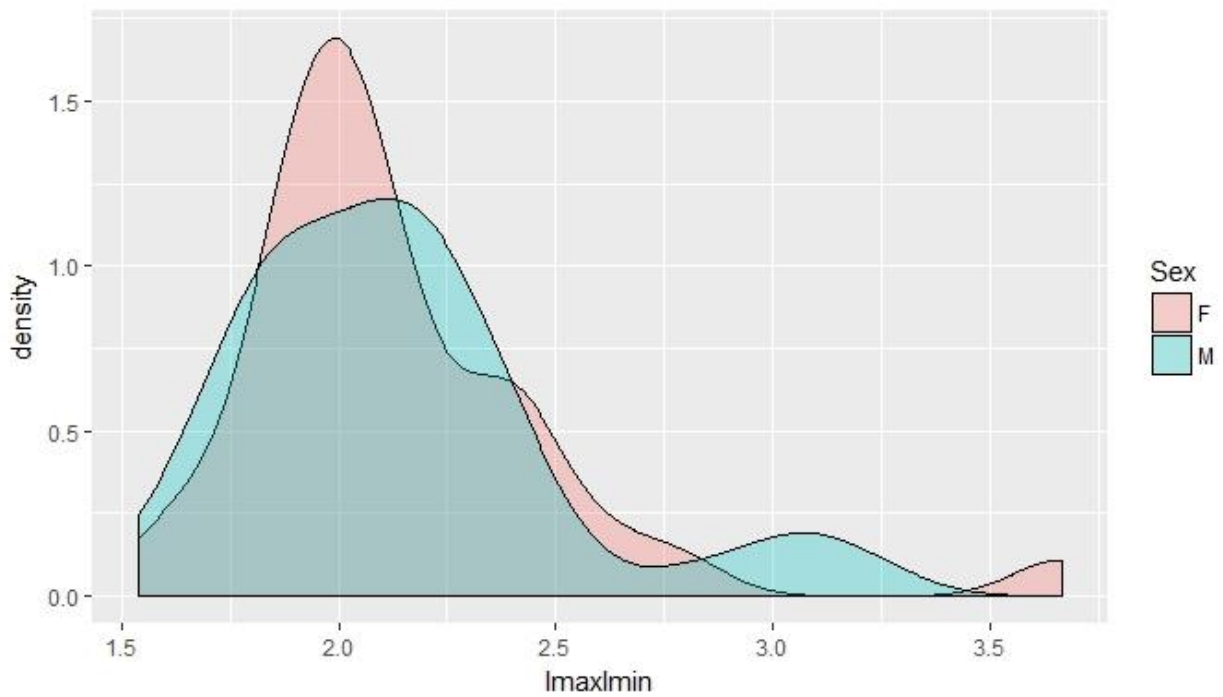


Figure 5.30: Density plot of I_{max}/I_{min} values between males (blue) and females (red) at midshaft tibia.

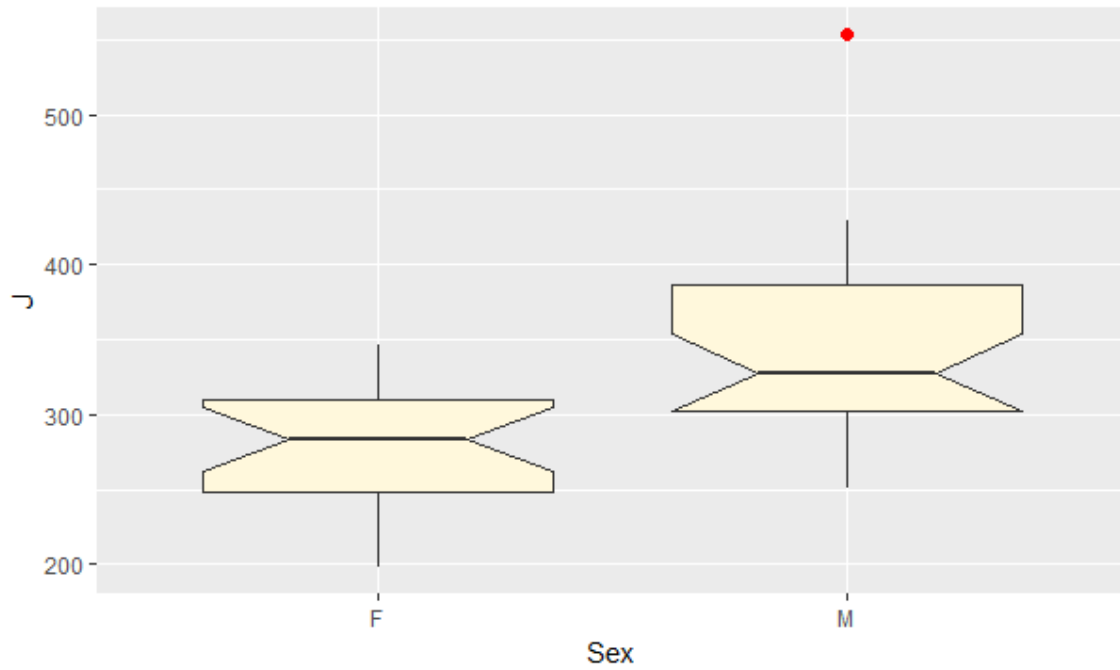


Figure 5.31: Violin plot of J (mm^4) values between males and females at midshaft tibia (red dot denotes an outlier).

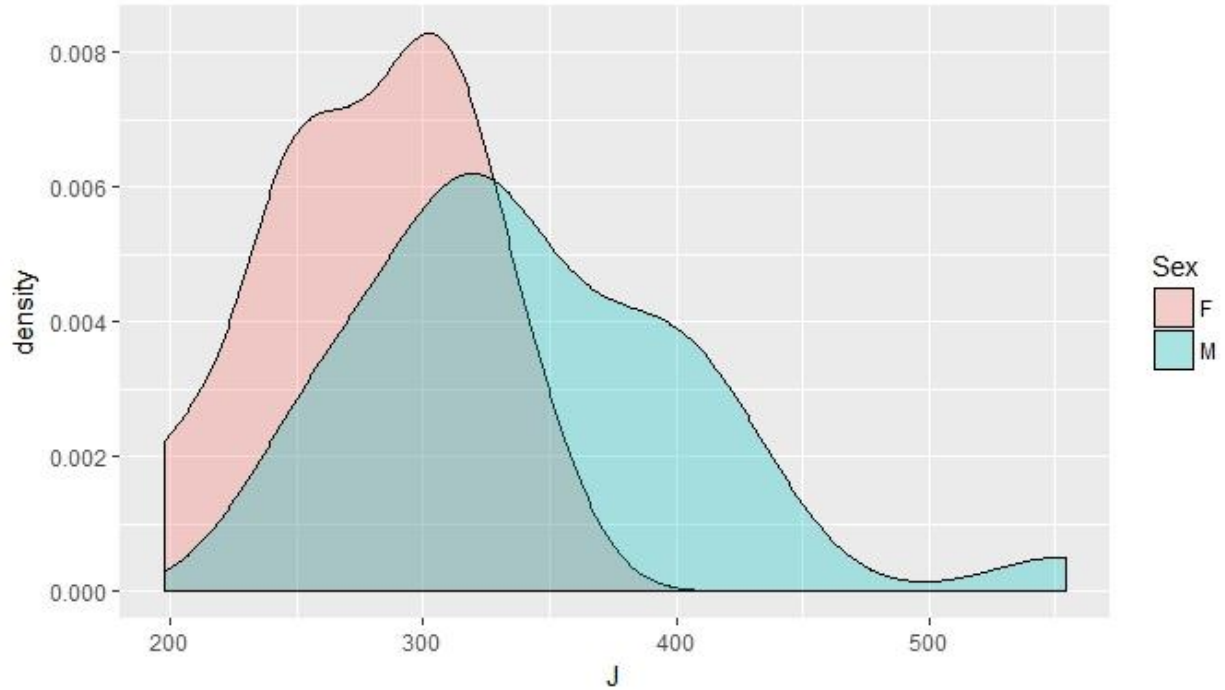


Figure 5.32: Density plot of J (mm^4) values between males (blue) and females (red) at midshaft tibia.



Figure 5.33: Violin plot of TA (mm^2) values between males and females at midshaft tibia.

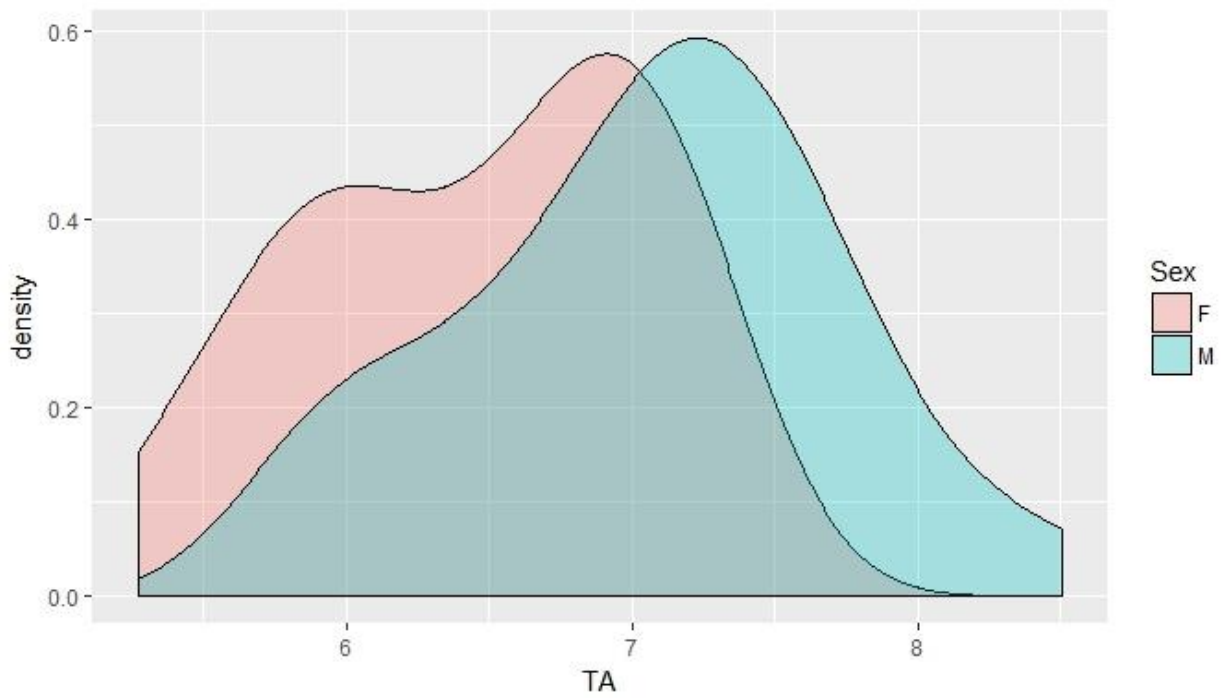


Figure 5.34: Density plot of TA (mm^2) values between males (blue) and females (red) at midshaft tibia.

Cluster analyses for the cross-sectional variables derived from the midshaft tibia revealed clusters for I_{max}/I_{min} that were not based on sex, and distinct sub-groups of males with the highest values of J and TA . As shown in Figure 5.35, males and females were relatively equally distributed within and between the two clusters (cluster on the left: 58% male and 42% female; cluster on the right: 53% male and 47% female). Therefore, the basis for groupings in the I_{max}/I_{min} data is not associated with sex. Regarding the two clusters for the data of J in Figure 5.36, the cluster with the lower values is comprised of males and females (45% male and 55% female) with more males than females on the higher end of the group. The cluster with the greatest values for J contained solely males (100% male vs. 0% female). A similar pattern is seen in Figure 5.37 for TA which displays the cluster with the highest values including only males (100% males vs. 0% females). The intermediate group involves an approximately equal number of males and females (52% male and 48% female), and the cluster with the lowest values has males and females with slightly more females (62.5% female and 37.5% male).

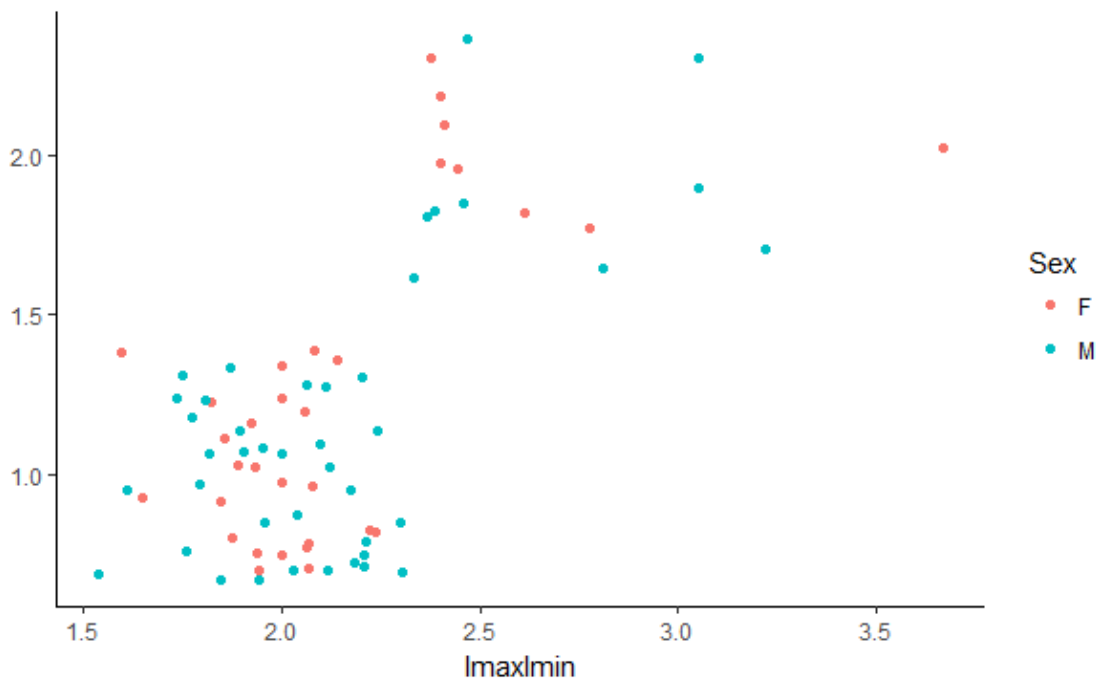


Figure 5.35: Scatter plot (with random jitter) of clusters after k -means cluster analysis of I_{max}/I_{min} at midshaft tibia.

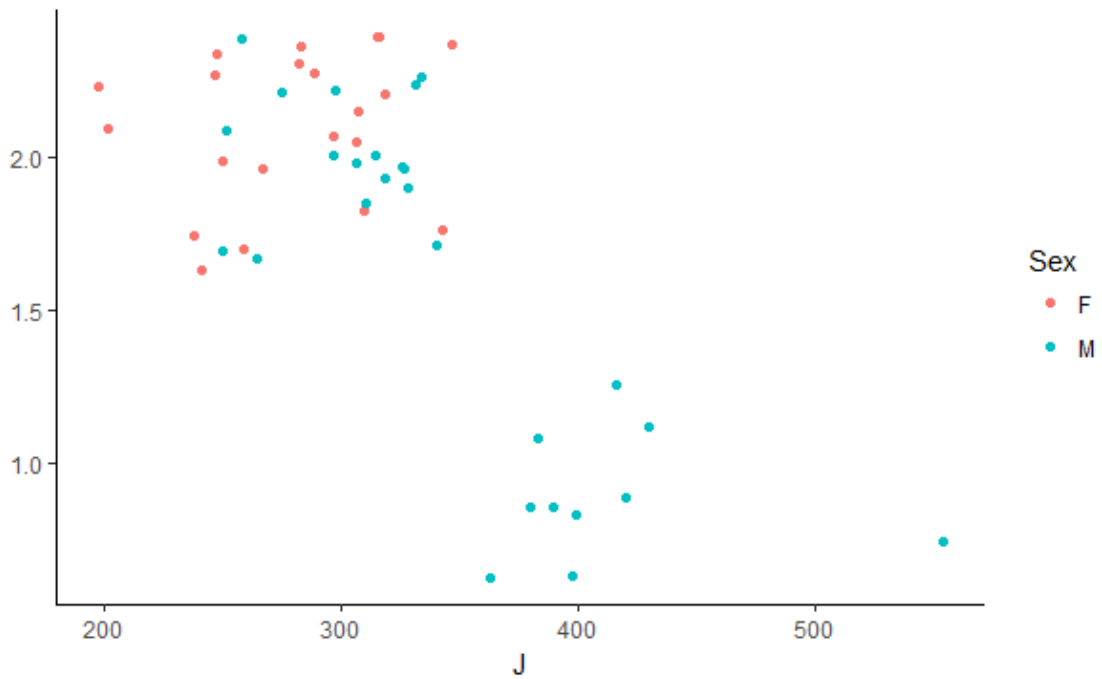


Figure 5.36: Scatter plot (with random jitter) of clusters after *k*-means cluster analysis of *J* at midshaft tibia.

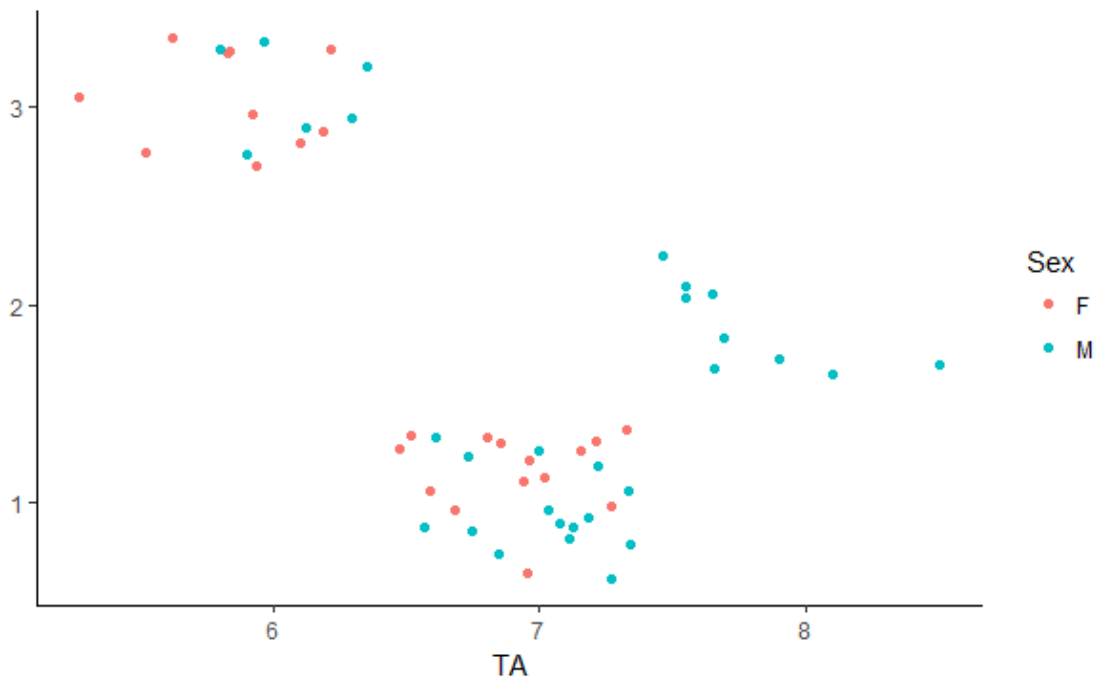


Figure 5.37: Scatter plot (with random jitter) of clusters after *k*-means cluster analysis of *TA* at midshaft tibia.

Comparisons within cemeteries

Table 5.9: *P-values from comparisons between males and females from cemetery 3-J-10 and males and females from 3-J-11 for each cross-sectional property at the three diaphyseal locations. (ns = not significant at $p < 0.05$)*

		I_{max}/I_{min}	J	TA
M 3-J-10 vs. F 3-J-10	Midshaft femur	ns	0.0016	ns (0.067)
	Subtrochanteric femur	ns	0.032	ns (0.06)
	Midshaft tibia	ns	0.01	ns
M 3-J-11 vs. F 3-J-11	Midshaft femur	ns	0.0018	0.0066
	Subtrochanteric femur	ns	ns	ns
	Midshaft tibia	ns	0.0093	0.004

The patterns of cross-sectional measures between males and females from Mis Island were also observed between males and females within each cemetery, although some levels of significance deviated from the Mis Island sample as a whole (Table 5.9). To corroborate how the previously demonstrated relationships between males and females were also present in each cemetery, the same analyses between males and females from cemetery 3-J-10 and males and females from cemetery 3-J-11 were carried out. The majority of comparisons between males and females in each cemetery matched the results of the combined sample (Tables 5.9, 5.10, and 5.11). This includes significantly higher values for males compared to females for J at all three diaphyseal sections in both cemeteries except for the subtrochanteric femur in the 3-J-11 subsample, as well as TA at the midshaft femur and tibia in cemetery 3-J-11. Additionally, the lack of significant differences for I_{max}/I_{min} at the subtrochanteric femur and midshaft tibia within both cemeteries paralleled the patterns between males and females in the Mis Island sample as a whole. However, some of the comparisons yielding significant differences in the combined

sample did not vary within each cemetery (Table 5.9), including: I_{max}/I_{min} at midshaft femur in both cemeteries; J at the subtrochanteric femur in 3-J-11; TA at the subtrochanteric femur in 3-J-11 and at all three diaphyseal locations in cemetery 3-J-10, although the midshaft and subtrochanteric femur approached significance. These discrepancies in statistical significance between males and females in the whole sample and males and females within each cemetery may be attributable to smaller sub-sample sizes. Despite some deviations in significance levels, the relative relationships in cross-sectional measures between males and females in each cemetery mirror those observed between males and females from both cemeteries combined, as indicated by the trends in mean values of cross-sectional measures at the three diaphyseal locations (Tables 5.10 and 5.11). Therefore, the patterns of diaphyseal cross-sectional measures between males and females within each cemetery are consistent with those found between males and females in the combined Mis Island sample.

Table 5.10: *Summary statistics for cross-sectional geometric properties at midshaft femur (F50), subtrochanteric femur (F80), and midshaft tibia (T50) separated by sex from cemetery 3-J-10. ($J = \text{mm}^4$, $TA = \text{mm}^2$)*

		I_{max}/I_{min}		J		TA	
		M	F	M	F	M	F
F50	n	23	13	16	5	17	7
	Mean	1.52	1.39	374.4	297.5	7.04	6.73
	SD	0.24	0.22	57.84	29.71	0.70	0.57
F80	n	20	11	16	6	18	9
	Mean	1.50	1.59	351.2	309.3	8.91	8.36
	SD	0.24	0.23	60.66	24.31	0.80	0.60
T50	n	23	10	16	5	17	7
	Mean	2.13	2.05	337.2	294.0	7.04	6.73
	SD	0.36	0.29	52.06	17.39	0.70	0.57

Table 5.11: Summary statistics for cross-sectional geometric properties at midshaft femur (F50), subtrochanteric femur (F80), and midshaft tibia (T50) separated by sex from cemetery 3-J-11. ($J = \text{mm}^4$, $TA = \text{mm}^2$)

		I_{max}/I_{min}		J		TA	
		M	F	M	F	M	F
F50	n	18	25	11	19	13	17
	Mean	1.51	1.41	356.66	284.45	7.08	6.36
	SD	0.21	0.27	55.04	46.80	0.64	0.60
F80	n	18	24	11	20	13	24
	Mean	1.44	1.60	329.91	306.53	8.42	8.11
	SD	0.22	0.33	38.48	37.34	0.56	0.54
T50	n	19	22	11	16	13	17
	Mean	2.14	2.18	351.6	274.7	7.08	6.36
	SD	0.40	0.42	87.50	46.43	0.64	0.60

Intra- and inter-observer error

Intra-observer error

Assessments of intra-observer error demonstrated a high degree of reliability in deriving cross-sectional variables and measuring dimensions. These intra-observer tests were performed on the midshaft femur for cross-sectional data and the series of measurements taken of the femur. In Table 5.12, all three cross-sectional variables had low values for absolute TEM (TEM) and relative TEM (% TEM), with *TA* resulting in the lowest values and *I_{min}* and *I_{max}* having higher values that were comparable to each other. A similar pattern was exhibited through both consistency and agreement intraclass correlation coefficients (ICC) for the cross-sectional properties. The two series of the cross-sectional variables derived by the author resulted in high values for ICC consistency and ICC agreement, with *TA* having higher correlation coefficients than *I_{min}* and *I_{max}* (Table 5.12). There was also a strong agreement between the repeated measurements of the femur (Table 5.13). As indicated by the TEM values, the discrepancy in the measurements did not exceed 1 mm, except for maximum length which was minimally above that level (Table 5.13). All measurements had low %TEM values and high ICC values, with ML midshaft diameter as the measurement showing the most disagreement.

Table 5.12: *TEM and %TEM, and ICC consistency and agreement values for CSG intra-observer error.*

Measurement	n	TEM	% TEM	ICC Consistency	ICC Agreement
<i>TA</i> (mm ²)	30	7.10	1.46	0.991	0.991
<i>I_{min}</i> (mm ⁴)	30	416	3.30	0.988	0.988
<i>I_{max}</i> (mm ⁴)	30	832	3.70	0.987	0.987

Table 5.13: *TEM and %TEM, and ICC consistency and agreement values for intra-observer error of measurements.*

Measurement	n	TEM	% TEM	ICC Consistency	ICC Agreement
Length to medial condyle (mm)	30	0.889	0.208	0.999	0.999
Length to lateral condyle (mm)	30	0.707	0.167	1	0.999
Biomechanical length (mm)	30	0.551	0.129	1	1
Femoral head diameter (mm)	30	0.221	0.524	0.992	0.993
Maximum length (mm)	30	1.10	0.245	0.998	0.998
AP midshaft diameter (mm)	30	0.261	0.923	0.992	0.992
ML midshaft diameter (mm)	30	0.371	1.55	0.967	0.968

Inter-observer error

There was low inter-observer error for both the femoral and tibial measurements, as indicated by the TEM and ICC values (Table 5.14 and Table 5.15). For the femoral measurements, disagreement between observers did not surpass 1 mm (Table 5.14). The measurements taken of the femur between observers were in agreement based on the %TEM, ICC consistency, and ICC agreement values (Table 5.14). However, similar to the intra-observer test of femoral measurements, the dimension with the most disagreement was the ML midshaft diameter, as it had the highest %TEM and lowest ICC values (Table 5.14). The tibial measurements also had low levels of inter-observer error. As displayed in Table 5.15, the absolute TEM values for the tibial measurements were slightly greater than those of the femoral measurements, but still did not exceed more than 1.6 mm. Additionally, the tibial measurements between observers had low %TEM values, and high ICC values (Table 5.15).

Table 5.14: *TEM and %TEM, and ICC consistency and agreement values for inter-observer error of femoral measurements.*

Measurement	n	TEM	% TEM	ICC Consistency	ICC Agreement
Length to medial condyle (mm)	21	0.806	0.192	0.999	0.999
Length to lateral condyle (mm)	21	0.877	0.211	0.999	0.999
Biomechanical length (mm)	21	0.610	0.146	1	1
Femoral head diameter (mm)	28	0.202	0.495	0.996	0.995
Maximum length (mm)	23	0.940	0.213	0.999	0.999
AP midshaft diameter (mm)	39	0.176	0.645	0.997	0.997
ML midshaft diameter (mm)	39	0.209	0.890	0.991	0.992

Table 5.15: *TEM and %TEM, and ICC consistency and agreement values for inter-observer error of tibial measurements.*

Measurement	n	TEM	% TEM	ICC Consistency	ICC Agreement
Length to medial condyle (mm)	18	1.51	0.426	0.998	0.997
Length to lateral condyle (mm)	18	1.36	0.380	0.998	0.998
Biomechanical length (mm)	18	1.35	0.380	0.998	0.998
Maximum length (mm)	18	1.58	0.415	0.997	0.997

CHAPTER 6: DISCUSSION

Research Question 1

The first research question is a comparison between the two cemeteries that comprise the Mis Island sample—cemetery 3-J-10 (AD 1100 – 1400) and cemetery 3-J-11 (AD 300 – 1400). This exploration was aimed at investigating whether the diachronic cultural change observed between the cemeteries involved changes in activity. To examine the relationship of mechanical loading between the cemeteries, independent-samples t-tests were conducted between males from cemetery 3-J-10 and males from cemetery 3-J-11, and between females from cemetery 3-J-10 and females from cemetery 3-J-11. The null hypothesis for this research question was that there would not be a difference in cross-sectional properties between cemeteries 3-J-10 and 3-J-11, whereas the alternative stated that differences would exist between cemeteries.

These comparisons did not result in significant differences of any cross-sectional property between the cemetery sub-groups, and thus the null hypothesis failed to be rejected. The lack of significant differences between the two cemeteries indicates that similar physical tasks and activities were carried out by the communities interred in the cemeteries. Additionally, this pattern suggests that activities involving the lower limb were relatively maintained throughout the period, as there was no significant departure in loading properties between the cemeteries that represent different time spans. Although there were no significant differences between cemeteries 3-J-10 and 3-J-11, two non-significant trends were observed between the male and female sub-groups of the cemeteries.

One of the non-significant patterns observed in the inter-cemetery comparisons was the wider range of data for females from 3-J-11 compared to females from 3-J-10 for all three cross-sectional variables at the femur and tibia midshaft, and I_{max}/I_{min} and J at the subtrochanteric

region of the femur. This pattern could be attributed to small sub-sample sizes, in that there were less female individuals in the 3-J-10 group than females from cemetery 3-J-11. Therefore, the wider distribution in values for females from 3-J-11 compared to 3-J-10 could be a function of more individuals in the dataset. This trend may also reflect the longer time period that cemetery 3-J-11 was occupied, and thus includes a greater diversity of individuals with more variable loading regimes.

The other non-significant trend in this facet of the project involved greater values of most cross-sectional properties (all three measures from both midshafts and subtrochanteric femur, and *TA* of midshaft tibia) in males from cemetery 3-J-10 compared to 3-J-11. Because cemetery 3-J-10 was occupied during the Late Medieval phase compared to cemetery 3-J-11, which represents the entirety of the medieval Nubian period, this non-significant pattern suggests the potential for a temporal shift in activity for males. During the Late Medieval phase, the kingdom of Makuria experience increased instability, as internal and external factors deteriorated the political body (Hurst, 2013; Soler, 2012; Trigger, 1965; Welsby, 2002). The unsteadiness in the Late Medieval period may have necessitated increased levels of activity involving the lower limb in males from cemetery 3-J-10, perhaps related to subsistence issues or fortification measures. This response may have occurred in late-phase males from cemetery 3-J-11 as well. However, the male individuals from 3-J-11 are representative of the whole medieval period, which included times of stability that may have involved lower activity levels. The trend observed in this comparison therefore illustrates a possible increase in male activities involving the lower limb in the Late Medieval period, as expressed by higher values of cross-sectional properties in males from 3-J-10 than 3-J-11, that may correspond to the political instabilities at this time.

Research Question 2

The second research question is an intra-site investigation of cross-sectional geometric properties in the Mis Island sample exploring patterns of significant differences among groups of individuals. This analysis focused on comparing males and females to evaluate the extent of sexual division of tasks involving the lower limb in this population. However, this examination also delved deeper into the data to assess their structure and distribution. The null hypothesis for this research question was that cross-sectional variables between males and females would not differ. Conversely, the alternative hypothesis posits that differences in cross-sectional properties exist between males and females.

Through independent-samples t-tests, significant differences were found between males and females for the cross-sectional variables (I_{max}/I_{min} , J , and TA) at the three diaphyseal locations, except for I_{max}/I_{min} at the subtrochanteric region of the femur and midshaft tibia. Therefore, the null hypothesis was rejected. The following discussion contextualizes the results of diaphyseal robusticity and shape as they relate to the Mis Island population and to research from other sites. This deliberation also considers the roles of non-mechanical factors behind the observed patterns.

Diaphyseal robusticity (J and TA)

The significantly higher values of J and TA in males compared to females in this sample at all three diaphyseal locations indicate a sexual division of tasks that resulted in increased lower-limb rigidity in males. Both J and TA reflect diaphyseal robusticity, in that J represents bending and torsional rigidity and TA is a measure of compressional strength (Davies et al., 2014; Macintosh et al., 2014; Ruff, 2008). Because males had significantly greater standardized values of femoral and tibial J and TA than females, and thus greater lower limb strength and

rigidity, these individuals from Mis Island appeared to have a sexual division of labor with males more involved in tasks that consistently placed greater mechanical loads on the lower limbs. Given the recurrent higher loading needed to induce diaphyseal expansion, such a division in habitual activities is likely to be primarily associated with subsistence responsibilities. The t-tests of these cross-sectional variables between males and females resulted in significant differences; however, the scatterplots of the variables' cluster analyses demonstrate varying degrees of overlap between males and females for lower limb robusticity. While a sexual division of tasks can be inferred from the significant differences in lower limb rigidity, there may have been some shared roles and responsibilities between the sexes that resulted in similar levels of mechanical loading on the lower limbs among some men and women. A pattern of sexual dimorphism in lower limb robusticity has been observed in other studies from the region with presumably similar subsistence practices.

Related research on archaeological Nubian skeletal material supports the sexual division of tasks inferred from the greater lower limb strength in males compared to females from medieval Mis Island. In a sample from Dynastic Kerma (2100 – 1500 BC), male femora displayed higher strength at midshaft, indicated by *J*, compared to female femora (Stock et al., 2011). An additional Kerma sample (2000 – 1550 BC) exhibited greater values of *TA* in males than females at femoral and tibial midshafts (Nikita et al., 2011). Males from a medieval sample at Kulubnarti also demonstrated greater femoral torsional and bending rigidity than females (Kyle, 2008). Additionally, in another sample from medieval Kulubnarti, significant differences in histomorphometric remodeling variables (e.g., osteon number and size) between males and females were attributed to different mechanical strains associated with separate physical roles between the sexes (Mulhern and Van Gerven, 1997). Taken together, these studies convey a

separation of physical activities involving the lower limbs between males and females in these past Nubian agricultural societies, one of which is contemporary with the population at Mis Island. Based on the Mis Island data for lower limb rigidity, there appeared to be a sexual division of tasks in this society, with males involved in habitual activities that placed greater mechanical loads on the legs compared to those carried out by females. This pattern has been observed in samples from Kerma and Kulubnarti, both of which implemented an agricultural economy (Mulhern and Van Gerven, 1997; Stock et al., 2011). Despite spatial and temporal differences between Mis Island and these archaeological samples, there may be some underlying cultural similarities between these sites regarding sexual division of labor with an agricultural subsistence strategy.

Although comparisons with modern ethnographies must be considered with caution, it is worth noting the roles between men and women in the region with an agricultural subsistence economy. Recent ethnographic observations of this region express sexual division of activity relating to subsistence practices that are compatible with the patterns of biomechanical stresses seen in the present study and others focused on ancient Nubia (Kilgore, 1984; Mulhern and Van Gerven, 1997). In this pattern of sexual division of tasks, men tend to be responsible for more physically intense labor associated with clearing fields, whereas women typically perform less physically-demanding roles such as maintaining fields, helping to harvest crops, and attending to livestock (Kilgore, 1984; Mulhern and Van Gerven, 1997). If this recent pattern of division of labor is similar to that in place in medieval Nubia, perhaps the roles and responsibilities of these individuals from Mis Island were similar to those practiced recently.

The patterns in diaphyseal rigidity observed in this study between male and female adults are likely driven primarily from differences in mechanical loading; however, it is important to

consider other non-mechanical factors that could affect these processes. One facet in the inferred sexual division of tasks may involve the role of ontogeny, as the responses of cortical bone to mechanical loads are greater during growth before adulthood (Carlson and Marchi, 2014; Davies et al., 2014; Sparacello et al., 2011; Wescott, 2014; Wescott and Cunningham, 2006). It is therefore a plausible implication that male individuals typically engaged in greater levels of physical activity that enacted greater mechanical loads on the lower limbs prior to maturity compared to females. Consequently, it is reasonable to infer that this sexual division of tasks in the Mis Island society was put into place before adulthood.

The individuals in the medieval settlement of Mis Island experienced poor health, as evidenced by high frequencies of skeletal indicators of stress (Soler, 2012). There were no significant differences in these stress indicators between adult males and females though, suggesting that both sexes were equally affected by stressors arising from the environment and culture (Soler, 2012). The lack of differences in these stress indicators between adult males and females proposes that these disease processes manifested in the skeleton are unlikely to be a factor behind the differences in diaphyseal robusticity between the sexes. However, if other health ailments unobserved in skeletal remains differentially affected males and females, then these conditions may have influenced an individual's ability to engage in activity.

Indications of nutritional deficiencies in subadult individuals in the Mis Island sample (Hurst, 2013) illustrated systemic stress during a developmental period that is critical for bone mechanical properties. Because mechanical loads have a greater impact on bone during growth than during adulthood, the nutritional stress experienced prior to adulthood in this sample likely affected cortical bone modeling and remodeling. Although it is not known whether the nutritional difficulties experienced by the subadults on Mis Island affected one sex more than the

other, that stress is unlikely to have played a role in the sexual dimorphic pattern of diaphyseal robusticity. A sample of subadults from medieval Kulubnarti exhibited endosteal resorption in the tibia during later juvenile years that was attributed to extensive nutritional stress (Hummert, 1983; Van Gerven et al., 1985). Despite the loss of bone on the endosteal surface, the outer dimensions and quantifications of bone strength were not affected and increased at a rate “consistent with the increased mechanical demands of advancing age and physical activity” (Van Gerven et al., 1985:279). It is possible that the limited nutrition experienced by subadults at Mis Island resulted in the similar endosteal response as the subadults at Kulubnarti. However, this nutritional distress did not seem to impact periosteal growth and mechanical response in the Kulubnarti sample, suggesting that relatively normal modeling and remodeling in the periosteal surface occurred in Mis Island subadults.

Diaphyseal shape (I_{max}/I_{min})

The significant difference between the sexes for I_{max}/I_{min} at the femoral midshaft, with males expressing higher values than females, indicates that male individuals were more mobile than females; however, the lack of difference in I_{max}/I_{min} values at the tibial midshaft between males and females suggests that they were involved in similar tasks regarding mobility (i.e., experienced relatively equal mobility). The analyses of the data for femoral midshaft I_{max}/I_{min} illustrate that female femora at midshaft tended to be more circular whereas male femora at midshaft were more elongated in the anteroposterior plane. While there was a significant difference in femur midshaft shape between males and females, the cluster analysis demonstrated some degree of overlap between the sexes—suggesting that this division is not so distinct. For I_{max}/I_{min} at midshaft tibia, there was no significance difference between males and females, as they had the same means for I_{max}/I_{min} and the associated cluster analysis did not reveal groupings

related to sex. As I_{max}/I_{min} in the lower limb is primarily interpreted in terms of mobility, the contrasting information between these two elements necessitates a comprehensive deliberation about the possible causes behind this trend and how they relate to the mobility of these individuals. Before further interpreting the results from the current study, it is important to explain how the shapes of the femoral and tibial midshafts are not necessarily associated with one another.

Because activities related to mobility are anticipated to generate anteroposterior mechanical loads in both the femoral and tibial midshaft, it would be expected that I_{max}/I_{min} values from both locations would be related to each other and follow a similar trend. During flexion and extension of the knee in activity, the greatest effect of mechanical loading occurs in the knee region, which has been observed in experimental studies that found localized responses to changes in mechanical loads (Ruff, 2005). It would be predicted then that the segment between midshaft femur and midshaft tibia that experiences these anteroposterior stresses would result in femoral and tibial midshafts that could both be generally connected to mobility. However, research suggests that diaphyseal shape between femoral and tibial midshafts are not strongly associated. In comparing AP/ML diameters and ratios of I_{max}/I_{min} between midshaft femur and tibia in a large sample, Pearson et al. (2014) found only weak correlations between the midshaft shape for the femur and tibia. In the present study, midshaft femur and tibia I_{max}/I_{min} were not correlated ($p = 0.58$, $r = 0.074$). Pearson and colleagues (2014) also assessed the relationship of I_{max} between femoral and tibial midshafts and observed inconsistent variation between population samples, as well as between males and females. These results suggest that instead of any widespread patterns based on sex or body shape, “group-specific patterns of sexual division of labor” is a primary influence on the relationship between midshaft femur and

tibia shapes (143). Given the disassociation between midshaft femur and tibia shapes, the results from the present study are substantiated and are also supported by other studies on Nubian sites taking this approach.

Differences in femoral midshaft shape between males and females have also been found at the sites of Kerma and Kulubnarti, with females demonstrating more circular cross-sections and males exhibiting more anteroposteriorly elongated cross-sections. From the Dynastic site of Kerma, researchers have observed more circular diaphyseal shapes at femoral midshaft in females compared to males (Nikita et al., 2011; Stock et al., 2011). In a medieval sample from Kulubnarti, Kyle (2008) saw slightly higher values of I_{max}/I_{min} at femoral midshaft in males compared to females that was not significant and perhaps not as pronounced due to smaller sample sizes. The results of femoral midshaft shape from these two sites indicate greater mobility in male individuals than females. In the present study, a similar conclusion could be drawn based solely on the sexually dimorphic pattern in midshaft femoral shape; however, the similarities between the sexes in tibial midshaft shape offer an opposing interpretation. Although not elaborated upon, I_{max}/I_{min} of the tibial midshaft in a sample from Dynastic Kerma was not significantly different between males and females (Nikita et al, 2011), which is also observed in the Mis Island sample.

Given the contrasting information from the femur midshaft and tibia midshaft, it is difficult to determine a basis for interpretations on mobility between males and females; however, research suggests that tibial midshaft shape may be a better indicator of mobility. Results from bioarchaeological samples suggest a higher association between biomechanical indications of mobility and diaphyseal cross-sectional geometry of the tibia compared to the femur (Macintosh et al., 2014; Ruff et al., 2006a). Additionally, Stock (2006) studied the

interaction between climate, or ecogeographic variation in body shape, as it relates to lower limb cross-sectional geometry and found that climate affected the femoral midshaft, whereas midshaft tibia was more influenced by activity. Although the effects of ecogeographic variation on the midshaft femur is not of consequence in the relatively homogeneous sample analyzed in the present study, it is interesting to note that activity appeared to have a greater impact on tibial midshaft compared to femoral midshaft. At the tibial midshaft, research suggests that diaphyseal shape is not affected by body breadth like femoral midshaft shape, or possible responses to body shape are superseded by other factors (Davies and Stock, 2014; Ruff et al., 2006a; Sládek et al. 2006; Sparracello et al., 2011; Wescott, 2014).

Investigations on the effect of body shape on diaphyseal morphology suggest that body shape, reflected as bi-iliac breadth alone or in a ratio with femoral length, may have a slight influence on femoral midshaft shape (Davies and Stock, 2014; Pearson et al., 2014; Shaw and Stock, 2011). The relationship between body shape and femoral midshaft shape, albeit it minimal and weak, seems to follow that greater bi-iliac breadth is slightly associated with relative mediolateral strengthening of the femoral midshaft (Davies and Stock, 2014; Shaw and Stock, 2011). The extent to which body shape affects the shape of femoral midshaft is generally uncertain, but Pearson et al. (2014) found that the influence of body shape was variable across sexes and population samples and accounted for only 0% – 25% of the variation observed in femoral midshaft shape. In the present study, therefore, it is possible that sexual dimorphism of bi-iliac breadth between males and females in the Mis Island sample offers some explanation behind the significant differences in I_{max}/I_{min} at femoral midshaft between the sexes. While the role of body shape on femoral midshaft shape is a valid consideration, this interaction does not seem to be a primary factor behind the diversity and patterns observed in femoral midshaft

shapes observed across populations (Pearson et al., 2014). Therefore, other possible explanations applicable to this study's results on femoral and tibial midshaft must be explored further.

There are several proposed processes behind conflicting patterns of femoral and tibial midshaft shape, in addition to the potential effect of body shape, that could be involved in the results of midshaft shapes in the current study. While the activities inferred from diaphyseal midshaft shape are often ascribed to some variation of walking and/or running, Wescott (2014) recommends considering non-mobile habitual activities that result in higher mechanical loads. The pattern of males displaying more anteroposteriorly elongated femoral midshafts than females in the Mis Island sample is seen in samples from Kerma and Kulubnarti—indicating that there is differential loading placed on the femur between males and females in these societies. However, because a similar tibial midshaft shape was displayed between males and females from Mis Island, and thus males and females might have shared similar patterns of mobility, the loading regimes enacted on the femora may have been associated with non-ambulatory activities.

Pearson and colleagues (2014) also propose alternative explanations behind conflicting trends in femoral and tibial cross-sections. One of these hypotheses is the idea that the midshaft femur and tibia “record different types of activity” (146). More experimental work is needed to understand how activity affects skeletal elements, but this concept suggests the femur and tibia midshafts do not react in the same way to varying kinds of loading and thus provide different information regarding activity. Pearson et al. (2014) also suggest that activity involving walking and/or running generate different systems of bending stress in the femoral and tibial midshafts rather than in the same anteroposterior plane. To illustrate this point, Pauwels' (1980) biomechanical model of the midshaft femoral cross-section demonstrated that this location is “best-adapted to resist bending along an axis from anterolateral to posteromedial” (Pearson et al.,

2014:147). This notion implies that bone may be deposited and distributed differently at these diaphyseal locations during activities associated with mobility.

Finally, the difference in diaphyseal shape of femoral and tibial midshafts may be influenced by the age at which individuals participated in physical activities. Because mechanical loading has a greater influence on bone during growth before skeletal maturity compared to adulthood (Pearson and Lieberman, 2004; Wescott, 2014), it is important to consider the role of ontogeny. Preliminary research conducted by Sparacello and colleagues (2010) on Gravettian subadult remains suggests that tibial midshaft shape develops more gradually than femoral midshaft shape, with adult femoral shape appearing by 11.5 years but only 80 – 90% of adult midshaft tibial shape values being obtained by 14 – 16 years. Based on this initial study, Pearson et al. (2014) posit the theory that greater mobility earlier on generates changes at the femoral midshaft, where later activity does not induce as much of a response at this location. It is also possible that the tibia is a better indicator of mobility closer to adulthood (Pearson et al., 2014). Regarding the current research then, perhaps the differences in midshaft femoral shape reflect early sexual division of tasks, with males participating in activities that involved more mobility and/or greater mechanical loads on the femoral midshaft compared to females. This hypothetical early sexual division of activities however, appeared to not significantly affect tibial midshaft shape. If the processes that induce change in tibial midshaft shape are more delayed, then perhaps both males and females had comparable mobility activities particularly closer to adulthood.

Taken together, the significant differences between males and females in diaphyseal robusticity and in femoral midshaft I_{max}/I_{min} indicate that there was sexual division of tasks in this society during the medieval period. However, the lack of significant differences in tibial

midshaft I_{max}/I_{min} suggest that there may not have been a substantial sexual division in mobility. Based on the discussion above, there are multiple factors that could have influenced this contrasting relationship between femoral and tibial midshaft shape, including body shape, biomechanical considerations, and ontogeny. Additionally, multiple studies suggest that the shape of the tibia at midshaft may be a better indicator of mobility than diaphyseal shape at femoral midshaft, which may be influenced by factors not related to activity in addition to mechanical loads. Therefore, the most parsimonious explanatory model for the pattern observed in this study is a relatively equal mobility between males and females in this society, with males perhaps being slightly more mobile based on femoral midshaft shape and diaphyseal robusticity.

This conclusion of overall equal mobility between males and females in the Mis Island sample is consistent with other research on past agricultural populations. Studies that have investigated transitions to agricultural subsistence economies demonstrate that differences in relative mobility between males and females tend to decrease in changing from mobile subsistence strategies (e.g., hunter-gatherer), with higher mobility in males, to agricultural practices that are associated with greater sedentism for the whole population (Carlson et al., 2007; Macintosh et al., 2014; Ruff, 1987). Medieval Nubia is associated with sedentism and agricultural subsistence practices (Adams, 1977; Welsby, 2002; Żurawski, 2014), and while there is an absence of archaeological evidence on subsistence at Mis Island, it is likely to have been some form of agriculture. Individuals from sedentary agricultural populations tend to exhibit less sexual dimorphism in femoral midshaft shape compared to those from populations with more mobile subsistence strategies (Ruff and Larsen, 1990; Ruff, 1987). Although interpretations of equal mobility between the sexes have been made from femoral midshaft shape, the same inference based on the similar tibial midshaft shape between the males and

females in this study is consistent with the model of a sedentary agricultural population. The patterns of femoral and tibial midshaft diaphyseal shape within this comparative context suggest relatively equal mobility, or perhaps sedentism, between males and females at Mis Island.

Although not significant, the trend of higher values of I_{max}/I_{min} at the subtrochanteric femur in females compared to males is likely attributable to differences in body shape. The t-test between males and females for I_{max}/I_{min} at the subtrochanteric femur did not yield a significant difference; however, the p-value approached significance with females exhibiting greater values than males. This pattern of higher subtrochanteric I_{max}/I_{min} values in females compared to males is consistent with findings from other studies that associate this result with sexual dimorphism in pelvic structure (Ruff, 2005, 2008; Ruff and Larsen, 1990). With generally wider hips in females from obstetric demands, there is more mediolateral distance between joints that likely generates greater mediolateral bending loads in the proximal femur—resulting in females having slightly more mediolaterally strengthened proximal femoral shafts (Davies and Stock, 2014; Ruff, 2005, 2008).

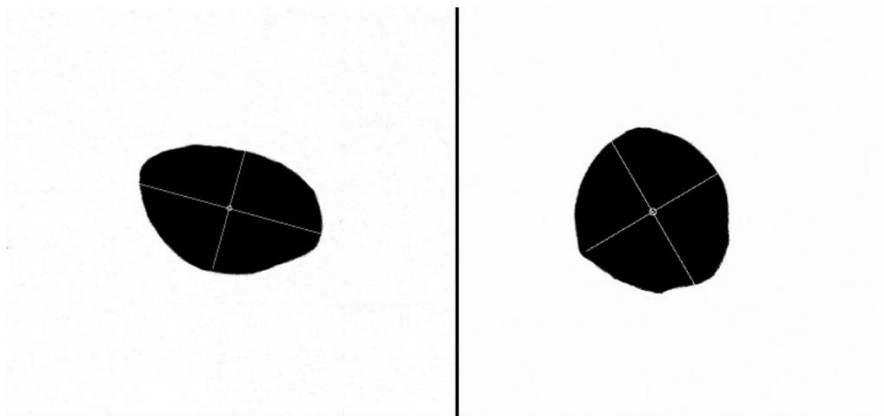


Figure 6.1: Two subtrochanteric cross-sections from a female (left) and male (right) from Mis Island.

Whereas the axes that I_{max} typically aligns with in cross-sections of midshaft femur and tibia are essentially anteroposteriorly oriented, a more mediolaterally elongated shape of the

subtrochanteric area of the femur results in I_{max} falling closer to the mediolateral plane. Upon visual inspection of the subtrochanteric cross-sections in this study (Figure 6.1), females tended to display subtrochanteric cross-sectional shapes that were more mediolaterally extended, creating higher values of I_{max}/I_{min} . In males, the subtrochanteric cross-sections generally did not deviate as much from circularity which yielded lower I_{max}/I_{min} values. The sexual dimorphism in proximal femur cross-sectional shape observed in other samples is not related to subsistence strategy and there is no consistent temporal pattern, suggesting that sexual dimorphism in pelvic structure is the primary factor behind proximal femur shape (Ruff, 1987, 2005). Therefore, the probable explanation behind the trend in the present study is based on sexual dimorphism in body breadth that affects proximal femur shape.

Intra- and inter-observer error

Through analyzing intra-observer error, it is evident that both generating cross-sectional properties and measuring dimensions were reliably conducted by the author. Intra-observer error was assessed by resampling thirty femora which involved deriving midshaft cross-sectional properties a second time and remeasuring the series of femoral dimensions. The low intra-observer error observed in the cross-sectional data demonstrates that the data obtained from the casting method were repeatable. Among the cross-sectional properties, I_{min} and I_{max} had slightly more disagreement, perhaps from minimal changes in axis orientation between cross-sections. The femoral measurements were also consistent and reliable. The measurement with the most error was the mediolateral diameter at midshaft, which may have resulted from greater dimensional variation in the mediolateral plane along the diaphysis. Additionally, this measurement may have been more difficult to replicate due to positioning error of the calipers.

Femoral and tibial measurements between the two observers were also in agreement, demonstrating reliable data collected by the author and Ms. Hench. Similar to the evaluation of intra-observer error, the femoral midshaft mediolateral diameter was less reliable, likely because of the aforementioned reasons. The tibial measurements between observers demonstrated higher discrepancy than those of the femur, but were still reliable and repeatable. The slightly greater disagreement in tibial measurements may be attributed to difficulties in maneuvering around the intercondylar eminence.

Limitations

This study aimed to control for as many variables as possible; however, there are limitations inherent in the project that should be considered. Accurately locating the cross-sections of interest is crucial in comparing cross-sectional properties. This need for precision was demonstrated by Sládek et al. (2010), who concluded that if the tibial midshaft cannot be estimated within a 14 – 20mm interval, then a researcher should consider excluding the individual's skeletal element. Therefore, estimating section locations on incomplete bones can be difficult (Jurmain et al., 2012). While the skeletal material in the Mis Island collection was well-preserved, there were fragmentary femora and tibiae within the sample. Proper protocols were carried out regarding approximating section locations and orientating fragmented diaphyses (Trinkaus and Ruff, 2012), but these close estimations may not have been taken at the exact cross-sectional locations. This limitation was considered during data collection and only mostly complete fragments were used while erring on the side of caution.

As is often an obstacle in research on archaeological remains, some comparisons between individuals in this study involved small sub-sample sizes. The tests between males from both cemeteries and females from the two cemeteries included sub-groups as low as five, six, or seven

individuals. The small sub-samples in some of these comparisons therefore may not be representative of their respective sub-population. The small samples present here however, do not necessarily nullify the trends observed within this sample.

The method of obtaining cross-sectional properties in this research quantified the periosteal contour of the cross-sections while excluding the medullary cavity, and thus, the cross-sectional properties are estimates of “true” values. This validated technique has demonstrated high correlations with true cross-sectional properties and is also supported by the observation that the periosteal contour alone is the most important in determining diaphyseal rigidity (Davies et al., 2012; Macintosh et al., 2013; Stock and Shaw, 2007; Sparacello and Pearson, 2010; Wescott, 2001). In utilizing this method, the endosteal contour was not considered in this study and potential variation in quantifications of cortical area was not investigated.

These limitations should be taken into account when interpreting the results from this research. However, this sample provided valuable data and insight that attempted to utilize the full potential of the data. The inferences drawn from this project serve to fill a gap in the lower-limb biomechanical information for this region.

CHAPTER 7: CONCLUSION

This research investigated relative levels of mobility and activity involving the lower limbs between groups of individuals in a medieval sample from Mis Island. Analyzing cross-sectional geometric properties of the femoral and tibial midshafts and subtrochanteric region of the femur, this study sought to discern significant patterns between cemetery groups, and between males and females. The results were interpreted in terms of division of labor within this society and potential temporal changes in activity.

The first facet of this study investigated whether the groups of individuals from the two cemeteries in the sample—cemetery 3-J-10 (AD 1100 – 1400) and cemetery 3-J-11 (AD 300 – 1400)—exhibited different mechanical loading patterns that would suggest a diachronic change or communal separation in physical behavior. This comparison did not yield significant results, indicating that the individuals from both cemeteries likely engaged in similar levels of activity involving the lower limbs throughout the medieval period. Results however, demonstrated two non-significant trends, both of which may be to some degree a consequence of small sub-sample sizes. One of these patterns was a wider range of data for females from 3-J-11 compared to females from 3-J-10 for the cross-sectional properties at femoral and tibial midshaft, and I_{max}/I_{min} and J at the subtrochanteric region of the femur. As cemetery 3-J-11 was occupied for a longer duration, this pattern may reflect a group with more diverse loading regimes caused by more variation in physical activity. The second trend in this inter-cemetery comparison demonstrated higher values for cross-sectional variables in males from 3-J-10 than males from 3-J-11. This pattern may represent an increase in activity involving the lower limbs during the Late Medieval phase, which was a time of instability in the kingdom of Makuria.

In the comparison between males and females in this Mis Island sample, sexual division of tasks was likely in place in this society. The significant sexual dimorphism in the measures of diaphyseal robusticity at all three diaphyseal locations indicate a separation of physical behavior involving the lower limb between men and women. As males had higher values of these cross-sectional properties than females, it appears that they were engaged in more physically demanding roles involving the lower limb.

While this study's results convey a sexual division of labor, they also suggest males and females may have been performing similar roles regarding mobility. Measures of femoral midshaft shape were significantly higher in males than females; however, cross-sectional shape at tibial midshaft did not significantly differ between males and females. As diaphyseal shape at midshaft of the femur and tibia are typically interpreted in terms of mobility levels, these results would seem to yield conflicting inferences. However, several lines of evidence contribute to a conclusion on mobility based more on the results of tibial midshaft. Although the males had significantly more anteroposteriorly elongated femoral midshafts than females, the distribution of data indicate that this difference was not as severe. Additionally, femoral midshaft shape may be slightly influenced by body shape. Therefore, sexual dimorphism in pelvic breadth may have been a contributing factor in the difference between males and females in femoral midshaft shape. The midshaft of the tibia does not seem to be influenced by body shape and may also be more associated with mobility than femoral midshaft shape. In addition to differences in body shape, other factors contributing to femoral midshaft shape have been posited, such as mechanical loading associated with non-mobility activities, differential loading responses, and ontogenetic factors. Given these aspects, greater weight was given to the tibial midshaft findings than those of the femoral midshafts. This study's results therefore indicate a similar degree of

mobility between males and females in this farming community, with males perhaps being slightly more mobile. A relatively similar level of mobility between males and females is congruous with a population practicing agriculture (Carlson et al., 2007; Macintosh et al., 2014; Ruff, 1987).

The outcomes of this study contribute to other research conducted on the life experiences of individuals in this Mis Island sample, as well as that on medieval Nubia. Further insight of division of labor would be gained by investigating the cross-sectional geometry of the upper limbs of these individuals. Additionally, changes in activity and mobility could be observable by comparing the mechanical loading to other populations from this region.

LITERATURE CITED

LITERATURE CITED

- Adams WY. 1977. Nubia: corridor to Africa. Princeton: Princeton University Press.
- Agarwal SC. 2016. Bone morphologies and histories: life course approaches in bioarchaeology. *Yearbook of physical anthropology* 159:130 – 49.
- Auerbach BM, Ruff CB. 2004. Human body mass estimation: a comparison of “morphometric” and “mechanical” methods. *American journal of physical anthropology* 125:331 – 42.
- Bice G. 2003. Reconstructing behavior from archaeological skeletal remains: a critical analysis of the biomechanical model, PhD dissertation. East Lansing: Michigan State University.
- Byrnes JF, Kenyhercz MW, Berg GE. 2017. Technical note: examining interobserver reliability of metric and morphoscopic characteristics of the mandible. *Journal of forensic sciences* 1 – 5.
- Carlson KJ, Grine FE, Pearson OM. 2007. Robusticity and sexual dimorphism in the postcranium of modern hunter-gatherers from Australia. *American journal of physical anthropology* 134:9 – 23.
- Carlson KJ, Marchi D. Towards Refining the Concept of Mobility. In: Carlson KJ, Marchi D, editors. *Reconstructing mobility: environmental, behavioral, and morphological determinants*. New York, NY: Springer, 2014;1 – 9.
- Cowgill LW. 2010. The ontogeny of Holocene and Late Pleistocene human postcranial strength. *American journal of physical anthropology* 141:16 – 37.
- Davies TG, Shaw CN, Stock JT. 2012. A test of a new method and software for the rapid estimation of cross-sectional geometric properties of long bone diaphyses from 3D laser surface scans. *Archaeological and anthropological sciences* 4:277 – 90.
- Davies TG, Stock JT. 2014. The influence of relative body breadth on the diaphyseal morphology of the human lower limb. *American journal of human biology* 26:822 – 35.
- Davies TG, Pomeroy E, Shaw CN, Stock JT. Mobility and the skeleton: a biomechanical view. In: Leary J, editor. *Past mobilities*. Surrey, England: Ashgate, 2014;129 – 53.
- Doube M, Kłosowski MM, Arganda-Carreras I, Cordelières F, Dougherty RP, Jackson J, Schmid B, Hutchinson JR, Shefelbine SJ. (2010) BoneJ: free and extensible bone image analysis in ImageJ. *Bone* 47:1076-9. doi: 10.1016/j.bone.2010.08.023
- Edwards DN. 2007. The archaeology of Sudan and Nubia. *Annual review of anthropology* 36:211 – 28.

Elliot M, Fairweather I, Olsen W, Pampaka M. A dictionary of social research methods. Oxford University Press. 2016.

Frankel VH, Nordin M. Biomechanics of bone. In: Nordin M, Frankel VH, editors. Basic biomechanics of the musculoskeletal system. Philadelphia, PA: Lippincott Williams & Wilkins, 2012;24 – 59.

Ginns A. 2006. Preliminary report on the excavations conducted on Mis Island (AKSC), 2005 – 2006. Sudan & Nubia, 10, 13 – 19.

Ginns A. 2007. Preliminary report on the second season of excavations conducted on Mis Island (AKSC). Sudan & Nubia, 11, 20 – 26.

Ginns A. 2010a. Medieval cemetery 3-J-10 draft report.

Ginns A. 2010b. Medieval cemetery 3-J-11 draft site report.

Godlewski W. The kingdom of Makuria. In: Anderson JR, Welsby DA, editors. The Fourth Cataract and beyond: proceedings of the 12th international conference for Nubian studies. Leuven: Peeters, 2014;155 – 69.

Gosman JH, Stout SD, Larsen CS. 2011. Skeletal biology over the life span: a view from the surfaces. Yearbook of physical anthropology 54:86 – 98.

Han J, Kamber M, Pei J. Cluster analysis: basic concepts and methods. In: Han J, Kamber M, Pei J, editors. Data Mining: concepts and techniques. Waltham, MA: Morgan Kaufmann, 2011;43 – 95.

Hummert JR. 1983. Cortical bone growth and dietary stress among subadults from Nubia's Batn El Hajar. American journal of physical anthropology 62:167 – 76.

Hurst CV. 2013. Growing up in Medieval Nubia: health, disease, and death of a medieval juvenile sample from Mis Island, PhD dissertation. East Lansing: Michigan State University.

Johnson WD, Koch GG. Intraclass correlation coefficient. In: International encyclopedia of statistical science. Editor: Lovric M. Springer-Verlag Berlin Heidelberg 2011;685 – 87.

Jurmain R. Studies of bone geometry: the shape of things to come? In: Jurmain R, editor. Stories from the skeleton: behavioral reconstruction in human osteology. Amsterdam, The Netherlands: Overseas Publishers Association, 1999;231 – 59.

Jurmain R, Cardoso FA, Henderson C, Villotte S. Bioarchaeology's holy grail: the reconstruction of activity. In: Grauer AL, editor. A companion to paleopathology. Chichester, West Sussex; Malden, MA: Wiley-Blackwell. 2012;531 – 52.

- Kachigan SK. 1982. Cluster analysis. In: *Multivariate statistical analysis: a conceptual introduction*. Radius Press, New York. 261 – 70.
- Kilgore L 1984. Degenerative joint disease in a medieval Nubian population, PhD dissertation. Boulder: University of Colorado, Boulder.
- Kyle BR. 2008. Lifestyle and activity in medieval Nubia: inferences from osteoarthritis and femoral morphology, Master's thesis. Columbus: Ohio State University.
- Lieberman DE, Polk JD, Demes B. 2004. Predicting long bone loading from cross-sectional geometry. *American journal of physical anthropology* 123:156 – 71.
- Macdonald HM, Cooper DML, McKay HA. 2009. Anterior-posterior bending strength at the tibial shaft increases with physical activity in boys: evidence for non-uniform geometric adaptation. *Osteoporosis international* 20:61 – 70.
- Macintosh AA, Davies TG, Ryan TM, Shaw CN, Stock JT. 2013. Periosteal versus true cross-sectional geometry: a comparison along humeral, femoral, and tibial diaphyses. *American journal of physical anthropology* 150:442 – 52.
- Macintosh AA, Pinhasi R, Stock JT. 2014. Lower limb skeletal biomechanics track long-term decline in mobility across ~6150 years of agriculture in Central Europe. *Journal of archaeological science* 52:376 – 90.
- Maggiano IS, Schultz M, Kierdorf H, Sosa TS, Maggiano CM, Blos VT. 2008. Cross-sectional analysis of long bones, occupational activities and long-distance trade of the Classic Maya from Xcambó—archaeological and osteological evidence. *American journal of physical anthropology* 136:470 – 77.
- Marchi D, Sparacello VS, Holt BM, Formicola V. 2006. Biomechanical approach to the reconstruction of activity patterns in Neolithic Western Liguria, Italy. *American journal of physical anthropology* 31:447 – 55.
- Marchi D. 2008. Relationships between lower limb cross-sectional geometry and mobility: the case of a Neolithic sample from Italy. *American journal of physical anthropology* 137:188 – 200.
- Martin DL 1983. Paleophysiological aspects of bone remodeling in the Meroitic, X-Group and Christian populations from Sudanese Nubia, PhD dissertation. Amherst: University of Massachusetts.
- McGraw KO, Wong SP. 1996. Forming inferences about some intraclass correlation coefficients. *Psychological methods* 1(1):30 – 46.
- Meyer C, Nicklisch N, Held P, Fritsch B, Alt KW. 2011. Tracing patterns of activity in the human skeleton: an overview of methods, problems, and limits of interpretation. *Journal of comparative human biology* 62:202 – 17.

- Mulhern DM, Van Gerven DP. 1997. Patterns of femoral bone remodeling dynamics in a medieval Nubian population. *American journal of physical anthropology* 104:133 – 146.
- Näser C. 2007. The Humboldt University Nubian expedition 2005: Works on Sherari and Us. In: Näser C, Lange M, editors. *Proceedings of the Second International Conference on the Archaeology of the Fourth Nile Cataract*. *Meroitica* 23:118- 133.
- Nikander R, Sievänen H, Uusi-Rasi K, Heinonen A, Kannus P. 2006. Loading modalities and bone structures at nonweight-bearing upper extremity and weight-bearing lower extremity: A pQCT study of adult female athletes. *Bone* 39:886 – 94.
- Nikita E, Siew YY, Stock J, Mattingly D, Lahr MM. 2011. Activity patterns in the Sahara Desert: an interpretation based on cross-sectional geometric properties. *American journal of physical anthropology* 146:423 – 34.
- Noldner LK. 2013. Spanish missionization and Maya social structure: skeletal evidence for labor distribution at Tipu, Belize, PhD dissertation. Albuquerque: The University of New Mexico.
- O’Neil MC, Ruff CB. 2004. Estimating human long bone cross-sectional geometric properties: a comparison of noninvasive methods. *Journal of human evolution* 47:221 – 35.
- Pearson OM. 2000. Activity, climate, and postcranial robusticity: implications for modern human origins and scenarios of adaptive change. *Current anthropology* 41:569 – 607.
- Pearson OM, Lieberman DE. 2004. The aging of Wolff’s “Law”: ontogeny and responses to mechanical loading in cortical bone. *American journal of physical anthropology*. 47:63 – 99.
- Pearson OM, Peterson TR, Sparacello VS, Daneshvari SR, Grine FE. Activity, “body shape,” and cross-sectional geometry of the femur and tibia. In: Carlson KJ, Marchi D, editors. *Reconstructing mobility: environmental, behavioral, and morphological determinants*. New York, NY: Springer, 2014;133 – 51.
- Perini TA, de Oliveira GL, dos Santos Ornellas J, de Oliveira FP. 2005. Technical error of measurement in anthropometry. *Rev Bras Med Esporte* 11(1):86 – 90.
- Pomeroy E. 2013. Biomechanical insights into activity and long distance trade in the south-central Andes (AD 500 – 1450). *Journal of archaeological science* 40:3129 – 40.
- RStudio Team (2015). *RStudio: Integrated Development for R*. RStudio, Inc., Boston, MA URL <http://www.rstudio.com/>.
- Ruff CB. 2005. Mechanical determinants of bone form: insights from skeletal remains. *Journal of musculoskeletal and neuronal interactions* 5(3):202 – 12.

Ruff CB. Biomechanical analyses of archaeological human skeletons. In: Katzenberg MA, Saunders SR, editors. *Biological anthropology of the human skeleton*. Hoboken, NJ: John Wiley & Sons, Inc., 2008;183 – 206.

Ruff CB, Hayes WC. 1983. Cross-sectional geometry of Pecos Pueblo femora and tibiae—a biomechanical investigation: I. Method and general patterns of variation. *American journal of physical anthropology* 60:359 – 381.

Ruff CB. 1987. Sexual dimorphism in human lower limb bone structure: relationship to subsistence strategy and sexual division of labor. *Journal of human evolution* 16:391 – 416.

Ruff CB, Larsen CS. 1990 Postcranial biomechanical adaptations to subsistence strategy changes on the Georgia Coast. In: Larsen CS, editor. *The archaeology of Mission Santa Catalina de Guale, Part 2: biocultural interpretations of a population in transition*. *Anthropological papers American Museum of Natural History* 68:94–120.

Ruff CB, Trinkaus E, Walker A, Larsen CS. 1993. Postcranial robusticity in Homo. I: Temporal trends and mechanical interpretation. *American journal of physical anthropology* 91:21 – 53.

Ruff CB, Trinkaus E, Holliday TW. 1997. Body mass and encephalization in Pleistocene Homo. *Nature*. 387:173 – 176.

Ruff CB, Holt BM, Sládek V, Berner M, Murphy Jr. WA, zur Nedden D, Seidler H, Recheis W. 2006a. Body size, body proportions, and mobility in the Tyrolean “Iceman”. *Journal of human evolution* 51:91 – 101.

Ruff CB, Holt B, Trinkaus E. 2006b. Who’s afraid of the big bad Wolff?: “Wolff’s Law” and bone functional adaptation. *American journal of physical anthropology* 129:484 – 98.

Ruff CB, Garofalo E, Holmes MA. 2013. Interpreting skeletal growth in the past from a functional and physiological perspective. *American journal of physical anthropology* 150:29 – 37.

Ruff CB, Larsen CS. Long bone structural analyses and the reconstruction of past mobility: a historical review. In: Carlson KJ, Marchi D, editors. *Reconstructing mobility: environmental, behavioral, and morphological determinants*. New York, NY: Springer, 2014;13 – 29.

Ruff CB, Holt B, Niskanen M, Sladek V, Berner M, Garofalo E, Garvin HM, Hora M, Junno JA, Schuplerova E, Vilka R, Whitley E. 2015. Gradual decline in mobility with the adoption of food production in Europe. *Proceedings of the national academy of sciences* 112(23):7147 – 52.

Schneider CA, Rasband WS, Eliceiri KW. 2012. NIH Image to ImageJ: 25 years of image analysis. *Nature methods* 9(7):671 – 75.

Shaw CN, Stock JT. 2009. Intensity, repetitiveness, and directionality of habitual adolescent mobility patterns influence the tibial diaphysis morphology of athletes. *American journal of physical anthropology* 140:149 – 59.

Shaw CN, Stock JT. 2011. The influence of body proportions on femoral and tibial midshaft shape in hunter-gatherers. *American journal of physical anthropology* 144:22 – 29.

Sládek V, Berner M, Sailer R. 2006. Mobility in Central European Late Eneolithic and Early Bronze Age: tibial cross-sectional geometry. *Journal of archaeological science* 33:470 – 82.

Sládek V, Berner M, Galeta P, Friedl L, Kudrnová S. 2010. Technical note: the effect of midshaft location on the error ranges of femoral and tibial cross-sectional parameters. *American journal of physical anthropology* 141:325 – 32.

Soler A. 2012. Life and death in a Medieval Nubian farming community: the experience at Mis Island, PhD dissertation. East Lansing: Michigan State University.

Sparacello VS, Pearson OM. 2010. The importance of accounting for the area of the medullary cavity in cross-sectional geometry: A test based on the femoral midshaft. *American journal of physical anthropology* 143:612 – 24.

Sparacello VS, Pearson OM, Cowgill L. 2010. Growing up in the Gravettian: ontogeny of cross-sectional geometry in the lower limb (abstract). *American journal of physical anthropology supplementary* 50:S221.

Sparacello VS, Pearson OM, Coppa A, Marchi D. 2011. Changes in skeletal robusticity in an Iron Age agropastoral group: The Samnites from the Alfedena necropolis (Abruzzo, Central Italy). *American journal of physical anthropology* 144:119 – 30.

StataCorp. 2015. *Stata Statistical Software: Release 14*. College Station, TX: StataCorp LP.

Stock JT. 2002. A test of two methods of radiographically deriving long bone cross-sectional properties compared to direct sectioning of the diaphysis. *International journal of osteoarchaeology* 12:335 – 42.

Stock JT. 2006. Hunter-gatherer postcranial robusticity relative to patterns of mobility, climatic adaptation, and selection for tissue economy. *American journal of physical anthropology* 131:194 – 204.

Stock JT, Shaw CN. 2007. Which measures of diaphyseal robusticity are robust? A comparison of external methods of quantifying the strength of long bone diaphyses to cross-sectional geometric properties. *American journal of physical anthropology* 134:412 – 23.

Stock JT, O’Neil MC, Ruff CB, Zabecki M, Shackelford L, Rose JC. Body size, skeletal biomechanics, mobility and habitual activity from the Late Paleolithic to the Mid-Dynastic Nile

Valley. In: Pinhasi R, Stock JT, editors. Human bioarchaeology of the transition to agriculture. Hoboken, NJ: Wiley Blackwell, 2011;347 – 67.

Stock JT, Macintosh AA. 2015. Lower limb biomechanics and habitual mobility among mid-Holocene populations of the Cis-Baikal. *Quaternary international* 1 – 10.

Trigger BG. 1965. History and settlement in Lower Nubia. New Haven: Yale University Publications in Anthropology no. 69.

Trinkaus E, Ruff CB. 2012. Femoral and tibial diaphyseal cross-sectional geometry in Pleistocene *Homo*. *PaleoAnthropology* 13 – 62.

Ulijaszek SJ, Kerr DA. 1999. Anthropometric measurement error and the assessment of nutritional status. *British journal of nutrition* 82:165 – 77.

Van Gerven DP, Hummert JR, Burr DB. 1985. Cortical bone maintenance and geometry of the tibia in prehistoric children from Nubia's Batn el Hajar. *American journal of physical anthropology* 66:275 – 80.

Vollner JM 2016. Examining the population history of three medieval Nubian sites through craniometric analyses, PhD dissertation. East Lansing: Michigan State University.

Welsby DA. 2002. The medieval kingdoms of Nubia. London: The British Museum Press.

Welsby DA. 2006. The Merowe Dam Archaeological Salvage Project: excavations in the vicinity of ed-Doma (AKSE), 2005 – 2006. *Sudan & Nubia*, 10, 8 – 13.

Wescott DJ. 2001. Structural variation in the humerus and femur in the American Great Plains and adjacent regions: differences in subsistence strategy and physical terrain, PhD dissertation. Knoxville: University of Tennessee.

Wescott DJ, Cunningham DL. 2006. Temporal changes in Arikara humeral and femoral cross-sectional geometry associated with horticultural intensification. *Journal of archaeological science* 33:1022 – 36.

Wescott DJ. The relationship between femur shape and terrestrial mobility patterns. In: Carlson KJ, Marchi D, editors. *Reconstructing mobility: environmental, behavioral, and morphological determinants*. New York, NY: Springer, 2014;111 – 32.

White TD, Black MT, Folkens PA. *Human osteology*. San Diego, CA: Academic Press, 2012.

Zadora G, Martyna A, Ramos D, Aitken C. 2014. Continuous data. In: *Statistical analysis in forensic science: evidential value of multivariate physicochemical data*, first edition. John Wiley & Sons, Ltd. 35 – 106.

Żurawski B. The Fourth Cataract in the medieval period. In: Anderson JR, Welsby DA, editors. The Fourth Cataract and beyond: proceedings of the 12th international conference for Nubian studies. Leuven: Peeters, 2014;135 – 53.